DESIGN AND CHARACTERIZATION OF ALL-IN-ONE ARTIFICIAL PROTEIN PLATFORM TOWARD NOVEL ANTIMICROBIAL MATERIALS

by

Christopher Patrick Camp

A Dissertation Submitted to the Faculty of the

DEPARTMENT OF BIOMEDICAL ENGINEERING

In Partial Fulfillment of the Requirements

For the Degree of

DOCTOR OF PHILOSOPHY

In the Graduate College

THE UNIVERSITY OF ARIZONA

2023

THE UNIVERSITY OF ARIZONA
GRADUATE COLLEGE

As members of the Dissertation Committee, we certify that we have read the dissertation prepared by: *Chris Camp*, titled: *Design and Characterization of All-in-One Artificial Protein Platform Toward Novel Antimicrobial Materials* and recommend that it be accepted as fulfilling the dissertation requirement for the Degree of Doctor of Philosophy.

Minkyu Kim, PhD Date: 4/26/2023

Kaveh Laksari, PhD Date: 4/25/2023

Terry O Matsunaga, PhD Date: 4/25/2023

Anne M Wertheimer, PhD Date: 4/26/2023

Jeong-Yeol Yoon, PhD Date: 4/25/2023

Final approval and acceptance of this dissertation is contingent upon the candidate's submission of the final copies of the dissertation to the Graduate College.

I hereby certify that I have read this dissertation prepared under my direction and recommend that it be accepted as fulfilling the dissertation requirement.

Minkyu Kim, PhD Dissertation Committee Chair Date: 4/26/2023

Department of Biomedical Engineering

Department of Materials Science & Engineering

Bio5 Institute

ACKNOWLEDGEMENTS

First, I would like to acknowledge my dissertation committee, Professors Minkyu Kim, Kaveh Laksari, Terry Matsunaga, Anne Wertheimer, and Jeong-Yeol Yoon for their mentorship and guidance through this process. Next, I would like to acknowledge members of the biopolymer materials lab, Wertheimer lab, and colleagues throughout the Biomedical Engineering department for their collaboration, knowledge, and support, especially Professor Minkyu Kim, Professor Anne Wertheimer, David Knoff, Taehee Lee, Fathima Doole, Samuel Kim, Haley Szczublewski, Suyoung Lee, Bumjoon Kim, Tiffany Ulep, Ingrid Peterson, Lauren Melcher, and Peter Dawson, as well as undergraduate mentees Audrey Cohen, Connor Maxwell, Vy Nguyen, Miguel Peña, and Nick Bai. The nature of this work required a team effort, and these results truly belong to everyone involved in making it happen.

Finally, I would also like to thank friends and family who have supported me throughout these studies, especially Tim Liu, Chet Preston, Andres Nuncio, Dustin Tran, Zaynab Hourani, Ashley Thrower, and Tyler Larson. I'll always remember these years for the great friends that were made and the good times that were had along the way, and I look forward to more good times that are yet to come.

TABLE OF CONTENTS

LIST OF TABLES

LIST OF FIGURES

ABSTRACT

Antimicrobial resistance is a crisis affecting millions of people each year around the globe and is progressively getting worse, but there are too few promising solutions in the pipeline. Antimicrobial peptides (AMPs) are an exciting alternative to antibiotics due to their broad-spectrum activity, but *in vivo* instability, such as proteolysis, has largely prevented their clinical approval. AMP drug delivery systems have made gains in stabilizing AMPs, but their complexity and high expense have been barriers to large-scale clinical translation. Here, we present an all-in-one artificial protein platform that simplified synthesis and processing and has the functionality to form micelle structures and hydrogels. We utilize genetic engineering and artificial proteins to form a single polymer strand that contains the material forming component, spacer component, and antimicrobial peptide such that conjugation steps are unnecessary. The use of elastin-like polypeptides as the representative artificial protein exploits an inexpensive protein purification strategy that avoids expensive chromatography. We showed that the all-in-one artificial protein platform can target the mechanical properties of natural tissues by manipulating the crosslinking formulations, we evaluated the biocompatibility of the material against fibroblasts, and we demonstrated the protein can form micelles at body temperature. Furthermore, we devised a method to improve the elastic moduli of hydrogels when self-assembled structures disrupted the efficiency of crosslinking. Altogether, these data provide the foundation toward utilizing the all-in-one artificial protein platform to stabilize AMPs and enhance AMP efficacy for clinical applications, such as tissue engineering and drug delivery.

Antimicrobial Resistance Crisis

Antimicrobial resistant pathogens affect around 2.8 million people and cause 32,000 deaths each year in the United States as well as roughly 700,000 deaths worldwide[1, 2]. Estimates suggest that number could increase to ten million deaths every year by 2050[1]. In addition to being a primary cause for hospitalization, antimicrobial-resistant infections are common as secondary infections that complicate treatment or recovery from other infections or emergencies, such as the 2009 H1N1 influenza pandemic, the SARS-CoV-2 pandemic, post-operation infections, chronic conditions such as diabetes, and nosocomial infections[2, 3].

Antimicrobial therapies, including antibiotics, are used in a variety of applications, including as treatments for acute or chronic infections, as a sterilization tool during surgical procedures, and in agriculture to protect farm-raised animals from infections[4]. The heavy use of antimicrobials creates a high selective pressure on microbes to acquire resistance through gene transfer, and the practice enables bacteria with antimicrobial resistance genes to outcompete existing native strains. Furthermore, animal and human waste has led to substantial concentrations of antibiotics in the environment including in soil, rivers and oceans, adding more opportunities for microbes to evolve resistance to antimicrobials[4]. In addition, antibiotic overuse, prescribing or taking antibiotics when it is inappropriate to do so, continues to accelerate the crisis more than necessary[5].

Efforts to mitigate the antimicrobial resistance crisis include reducing antibiotic consumption and producing novel antimicrobial drugs[6]. Reducing antibiotic consumption diminishes opportunities for microbes to develop resistance and lowers the concentrations of antimicrobials in the environment. However, antimicrobial consumption in healthcare has been largely unchanged as alternatives are limited, and the health of each individual patient is

consistently prioritized over the antimicrobial resistance crisis at large[6]. Furthermore, a low quantity of innovative solutions in the pipeline of new antibiotics, particularly as it pertains to pathogens designated by the World Health Organization as critical-priority, highlights the need for alternative solutions for the treatment of antibiotic resistant infections[7].

Antimicrobial Peptides

Antimicrobial peptides (AMPs) are a diverse group of small peptides that are naturally produced by animals, plants, and microorganisms as a first line of immunological defense against pathogens. AMPs generally have a broad spectrum of activity, are selective against microorganisms compared to mammalian cells, and though there are some mechanisms whereby pathogens have evolved resistance to AMPs[8], the broad-spread potency of AMPs have slowed the development of resistance against them relative to antibiotics. AMPs often have an amphipathic structure with a cationic side and a hydrophobic side (Figure 1A). This property facilitates electrostatic attraction and integration with bacterial cell membranes, which typically have a negative charge (Figure 1B), compared to a mostly neutral charge for mammalian cell membranes (Figure 1C). There are seven AMPs that are currently used or have been used, and four more are considered under development (Figure 1D), but these represent a small fraction of the over 3,700 antimicrobial peptides[9]. More efforts are underway to better understand the AMP mechanisms of antimicrobial action and to develop ways to improve their efficacy for translation to the clinic. Such as discovering new natural AMPs, designing synthetic AMPs[10], producing precursor proteins that are able to be cleaved, conjugations, and synergistic combinations with other AMPs and antibiotics[11].

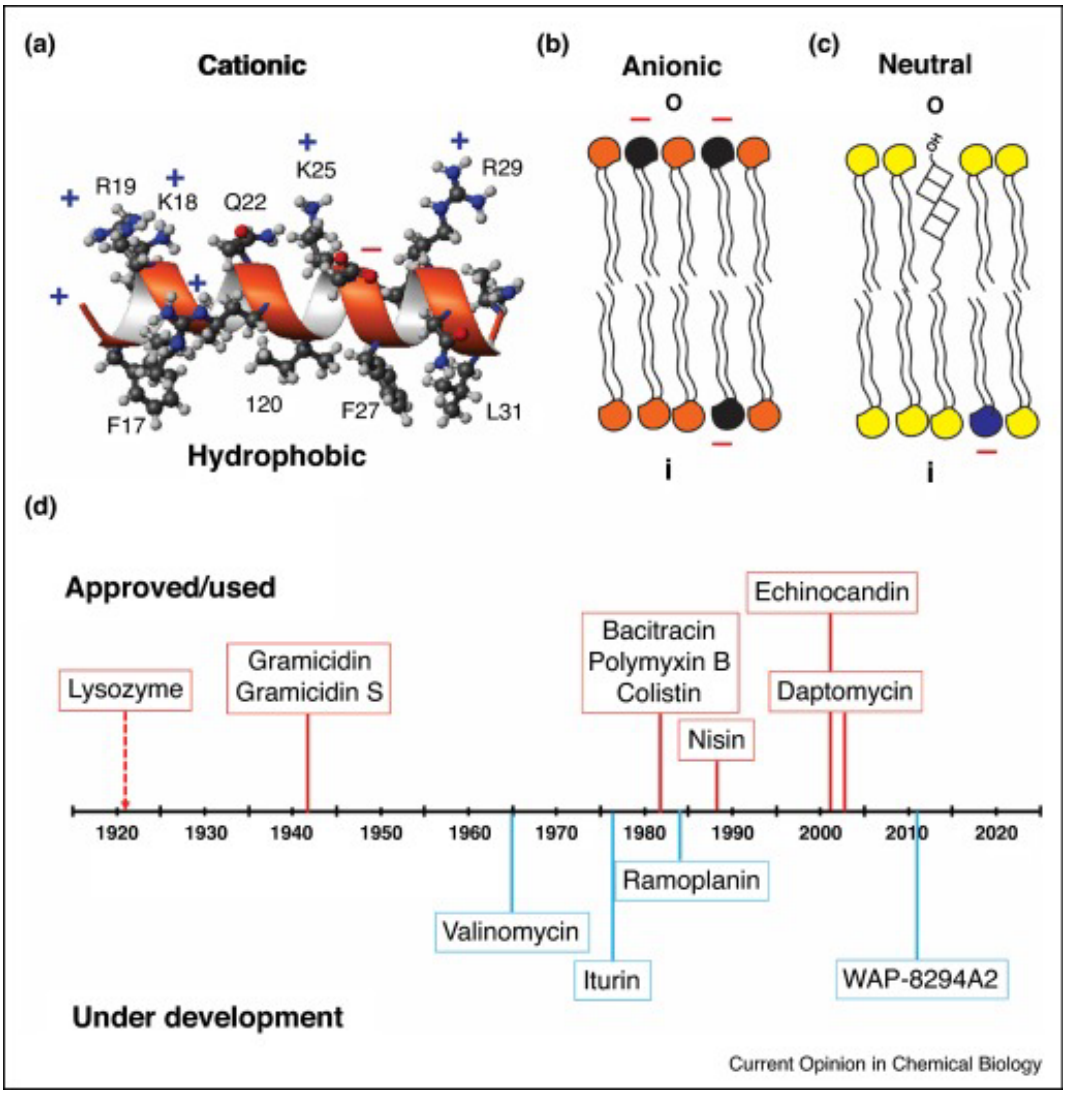

Figure 1. A) Amphipathic structure of a representative antimicrobial peptide, LL-37, **B)** Schematic of *Escherichia coli* cell membrane, representative gram-negative bacteria, consisting of anionic phosphatidylglycerols (black) and phosphatidylethanolamines (orange) for the inner (i) and outer (o) bilayer. **C)** Representative mammalian cell consisting of phosphatidylcholines (yellow), cholesterol (square) and anionic lipid on the inside bilayer (black). Reprinted with permission from Mishra, B.; Reiling, S.; Zarena, D.; Wang, G. Host defense antimicrobial peptides as antibiotics: design and application strategies. *Current Opinion in Chemical Biology* **2017**, *38*, 87-96. DOI: 10.1016/j.cbpa.2017.03.014. Copyright 2017, Elsevier.

There are two main categories of mechanisms of action to kill or inhibit the growth of bacteria. First, they can target and destabilize cell membranes using one of three widely accepted mechanistic models, such as barrel-stave pore, carpet, toroidal, or detergent (Figure 2)[12, 13]. Pores in the bacterial cell membrane will cause deionization of the cell and will often lead to cell death. Alternatively, they can target intracellular components such as enzymes or nucleic acids that are critical to survival[14]. Some AMPs are also able to increase the immune response, such as promoting the response of immunocytes[15, 16].

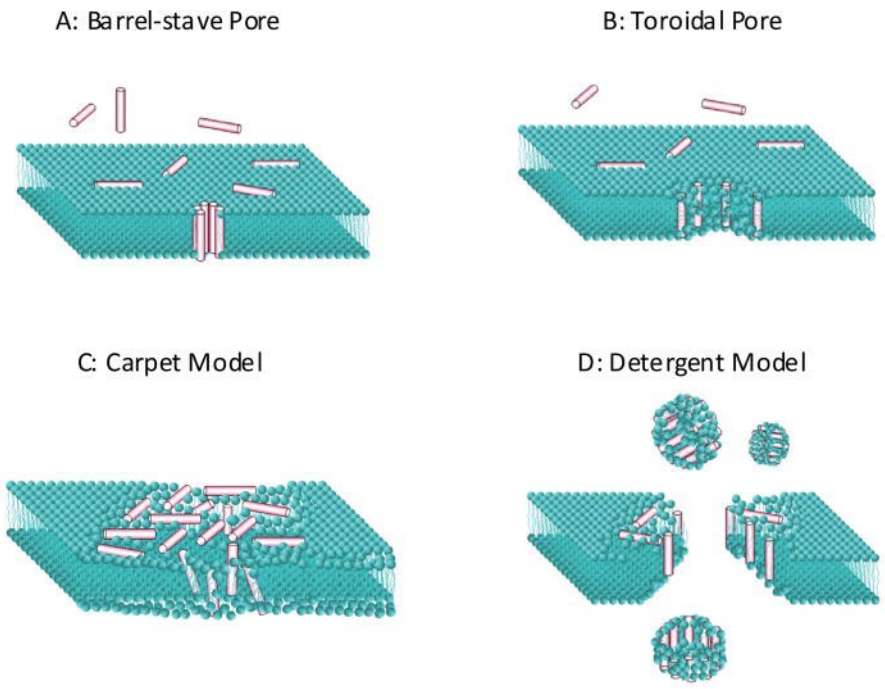

Figure 2. Schematic demonstrating antimicrobial peptide membrane-disruption mechanisms. Reprinted with permission from Wimley, W. C. Describing the Mechanism of Antimicrobial Peptide Action with the Interfacial Activity Model. ACS Chemical Biology 2010, 5 (10), 905-917. Copyright 2010, American Chemical Society.

Despite their exciting promise as a new category of antimicrobial therapeutics, AMPs often have poor stability when injected into tissue or the bloodstream due to protease degradation and

filtration by organs[9]. These limitations have prevented the widespread implementation of AMPs as clinical therapeutic tools[9, 17]. Therefore, much current AMP research focuses on improving the half-life and overall efficacy to translate the promising properties of AMPs to the clinic.

Conjugation of Antimicrobial Peptides to Materials

The attachment of AMPs onto material surfaces has been shown to enhance their stability, which is an important hurdle for translation of many AMPs to clinical use. Many strategies exist for immobilizing AMPs, such as attaching AMPs to polymers (e.g., polyethylene glycol (PEG)[18], Pluronic F127[19]) or to a modified material surface (Figure 3)[20]. Regarding binding an AMP to a modified material surface, either the AMP needs to be modified to contain the functional groups used for the conjugation or the AMP would need to contain those groups naturally, limiting the available AMPs that can be utilized via that chemistry. Attaching the AMPs to polymers often will enhance the half-life and solubility of AMPs, yet many challenges remain[21]. It can be difficult to calculate the concentrations of conjugated AMPs, for polymers and for surfaces, to compare to soluble AMPs because the conjugation yields are often unknown. Purifying polymers, such as PEG, from the AMP-conjugated polymers can be difficult because the conjugated polymers and free polymers are often similar sizes[22]. Adding functional groups to AMPs may affect their antimicrobial activity, and if they are conjugated in random locations that can be critical for structure formation or binding, the uncontrolled conjugation can result in the reduction of AMP activity[23].

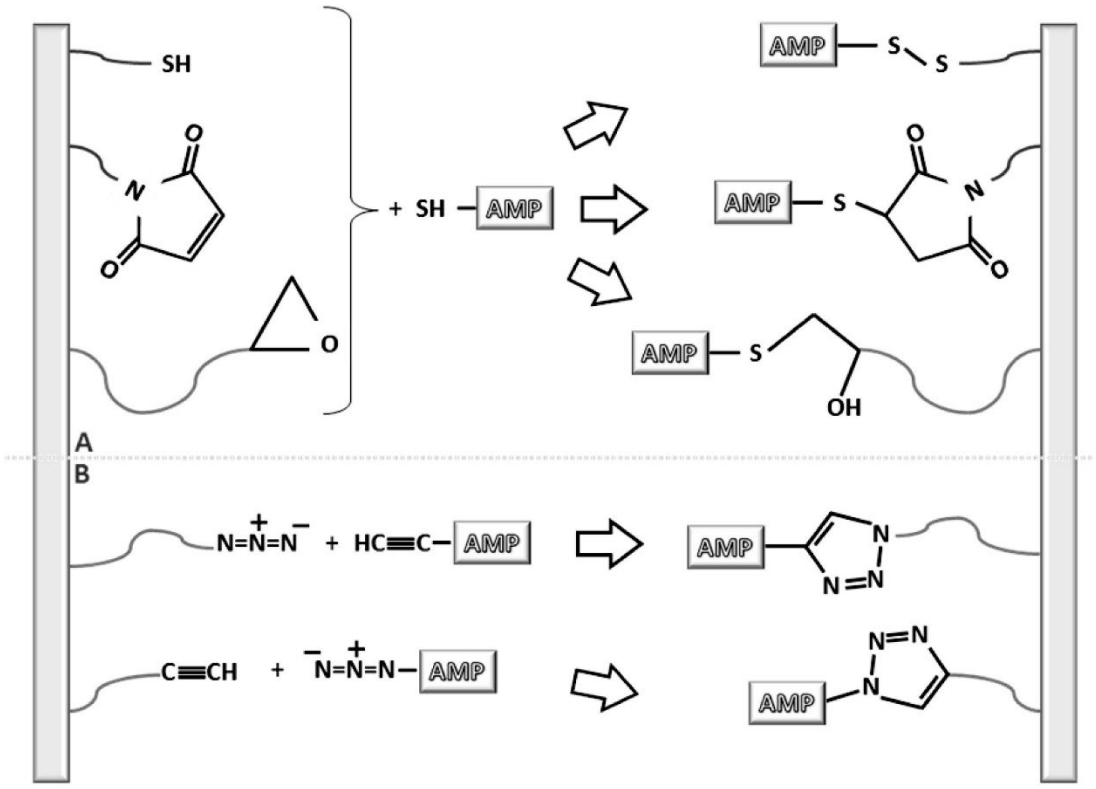

Figure 3. Strategies to covalently immobilize AMPs onto material surfaces. **A)** AMPs containing a cysteine residue can be chemically attached to thiol-, maleimide-, or epoxide-modified surfaces. **B)** AMPs containing residues with alkyne groups can be attached to azide-modified surfaces or residues with azide groups can be immobilized onto alkyne-modified surfaces. Reprinted with permission from Costa, F.; Carvalho, I. F.; Montelaro, R. C.; Gomes, P.; Martins, M. C. L. Covalent immobilization of antimicrobial peptides (AMPs) onto biomaterial surfaces. *Acta Biomaterialia* **2011**, *7* (4), 1431-1440. DOI: 10.1016/j.actbio.2010.11.005. Copyright 2011, Elsevier.

An additional major factor influencing the efficacy and stability of AMPs is if a tether is used to separate the AMP from the surface[24]. A tether can increase the efficacy of AMPs because they can separate the AMP from chemical or physical interference from the material, allowing the AMP to have more freedom to move and form structures in the bacterial cell membrane. The

physical and chemical properties of the tether, such as the polarity and stiffness, will affect the efficacy of AMPs[23], as well as the special orientation of the AMP[25]. However, even if those parameters are well controlled and optimized, attaching the AMP to a tether and a tether to the material surface also provides another complex step and expense, as well as an additional source of error or inconsistency in material processing. In addition, despite the promise of AMP materials, conjugating AMPs onto material surfaces can be cost-prohibitive because a large portion of AMPs can be lost in the conjugation process, and synthesis of small peptides is often expensive. Many methods will also allow AMPs to attach randomly to material surfaces, such as attaching AMPs using the polypeptide backbone. However, these methods can have lower efficacy if the spatial orientation of the AMPs is not controlled. More research is needed in AMP materials to stabilize and increase the efficacy of AMPs while reducing costs and optimizing consistency. Thus, the material format and composition need to be carefully considered to maximize AMP efficacy and consistency while reducing costs.

Polymeric Hydrogels With Incorporated Antimicrobial Peptides

Polymeric hydrogels are an excellent class of materials to incorporate AMPs to treat resistant infections because hydrogels can mimic the composition of natural tissues, composed of one to several polymer networks that swell to hold many times its weight in water[26]. However, hydrogels designed for therapeutic use need to be carefully targeted to match the mechanical strength of the tissue with which they are designed to interact, because the proliferation and differentiation of cells are directed by the mechanics of the surrounding tissues (Figure 4)[27-29]. To achieve the desired mechanical strength, hydrogel polymer networks can be formed using physical or chemical crosslinking. Physical crosslinking utilizes noncovalent interactions, such as electrostatic interactions, hydrogen bonding, and hydrophobic interactions. Physical

crosslinking can often offer self-repair functionalities because bonds can reform after they are dissociated. However, physically crosslinked hydrogels are often weaker than chemically crosslinked hydrogels, which are crosslinked using covalent bonds[30].

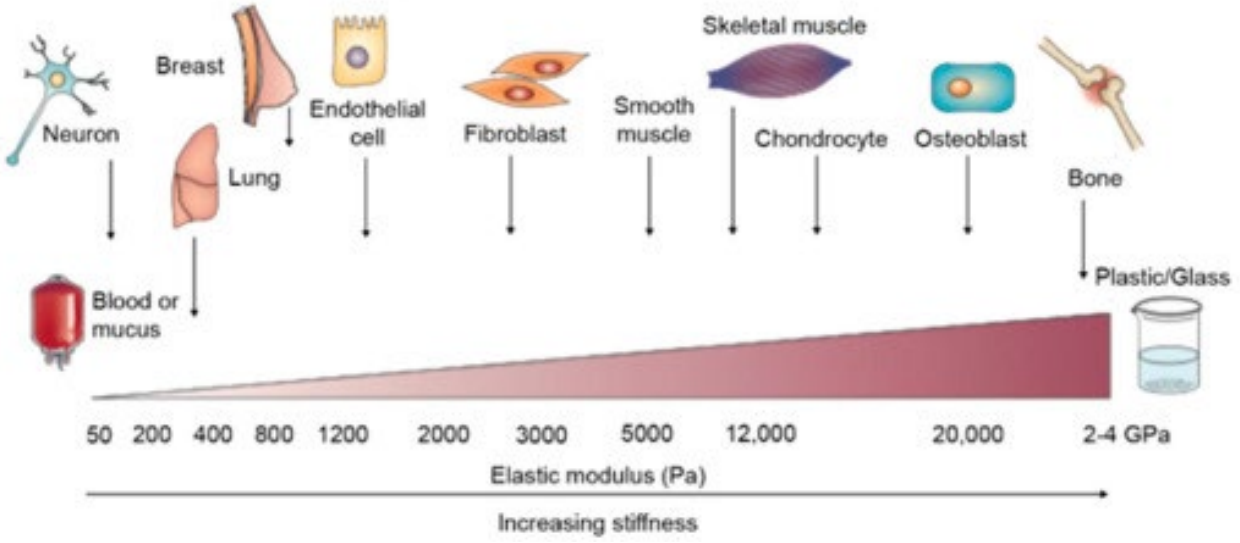

Figure 4. Cell behaviors, such as proliferation and differentiation, are tuned to the elastic modulus of their respective natural tissues. Reprinted with permission from Huerta-López, C.; Alegre-Cebollada, J. Protein Hydrogels: The Swiss Army Knife for Enhanced Mechanical and Bioactive Properties of Biomaterials. *Nanomaterials (Basel)* **2021**, *11* (7). DOI: 10.3390/nano11071656. This figure was reprinted from an open access article distributed under the terms and conditions of the Creative Commons Attribution (CC BY) license (https://creativecommons.org/licenses/by/4.0/).

While attaching AMPs to hydrogel polymer networks to stabilize AMPs, the attachment of AMPs onto surfaces can reduce their activities because their movement in space becomes restricted and they cannot form the complex structures that are necessary to carry out the microbe killing mechanism[31]. Adding tethers or spacers between the AMP and the material

surface can enhance the AMP efficacy but connecting the tether to the surface and the AMP to the tether involves more preparation steps that can lead to irreproducible materials and inconsistent efficacy results. Furthermore, the concentration of AMPs in the hydrogel must be carefully controlled because the selectivity of AMPs for microbes relative to human cells can break down for higher concentrations, increasing toxicity of AMPs[23]. Therefore, the dosages of AMPs must be carefully controlled in AMP therapies, but current strategies to attach AMPs onto materials often lead to inconsistent dosages. These obstacles have thus far mitigated the use of AMPs in the medical field as antibiotic alternatives and would add a high level of complexity to forming AMP hydrogel materials. While the hydrogel material is promising as a tool to utilize AMPs, a polymeric hydrogel design that eliminates the need for conjugation could increase the consistency and efficacy of AMPs while reducing the cost associated with losing a large and unclear portion of AMPs during the conjugation process.

Polymeric Hydrogels Comprising Artificial Protein Polymers

The major components of polymeric hydrogels are a three-dimensional lattice of physically or chemically crosslinked polymers and water[30]. The polymers can be natural (e.g., cellulose and collagen) or synthetic (e.g., polyethylene glycol and Pluronic F127). Natural protein polymers have high biocompatibility and tend to be simple to produce, but purifying natural proteins can be challenging, and precise control over the exact sequences, and thus the quantity of crosslinking functional groups, can be difficult. Synthetic polymers have been used extensively in the construction of hydrogels due to their excellent mechanical properties and swelling, as well as purification strategies that often do not require removing impurities. However, some synthetic polymers have biocompatibility issues and obtaining precise monodispersed sizes of synthetic polymers can be difficult, which can affect the mechanics of

polymer networks. To prepare AMP-incorporated materials, both synthetic and natural polymeric hydrogels have the same conjugation yield challenges mentioned previously. Artificial proteins have gained increasing attention for constructing polymeric hydrogels because they have the synthesis and biocompatibility advantages of natural proteins, as well as the design control afforded by synthetic polymers and beyond, with amino acid level precision to produce monodispersed polymer chain lengths and sequences[32].

These sizable advantages of artificial proteins have generated increasing research into generating artificial tissues from artificial proteins that have predictable mechanical properties[33], a feat that is particularly difficult to achieve with natural proteins or synthetic polymers. Finally, artificial proteins are uniquely positioned to generate AMP-incorporated hydrogels with tethers without the need for conjugation, because the DNA sequence of an AMP, artificial protein tether, and artificial protein material could all be included in one genetic code using genetic engineering, producing one protein strand containing all required components without extra post-processing steps. Typically, artificial proteins are purified using chromatography. For example, one strategy involves incorporating a string of histidine residues at the beginning or end of the artificial protein. Then, an electrostatic, pH-controlled affinity between the string of histidine residues and a nickel-based resin in the column can be used to selectively bind the artificial protein to the column and then release it in the elution[34]. However, chromatography can be expensive and time-consuming for large-scale purification, so finding artificial proteins with less expensive and simpler purification strategies would be preferred for translation to clinical utility.

Elastin-Like Polypeptides

Elastin-like polypeptides (ELPs) are a particular class of artificial proteins with intrinsically disordered structures. Intrinsically disordered proteins (IDPs), including ELPs, lack

stable secondary structures, but can self-assemble into micelles, cylinders, or more complex structures under specific conditions. IDP self-assembled structures are discussed further in a review paper that we prepared, including the IDP design parameters and environmental conditions that can be controlled to produce and stabilize various IDP self-assembled structures[35]. ELPs are inspired by a repetitive amino acid sequence found in elastin, a natural protein that is a common component of extracellular matrices and a major contributor to the elasticity of natural tissues. ELPs typically fit the amino acid sequence $(VPGXG)_n$, where X (i.e., guest residue) can be any amino acid except for proline (P), and V and G represent abbreviations for valine and glycine residues, respectively[36, 37]. These artificial proteins are well known for their stimulus-responsiveness and lower critical solution temperatures (LCSTs) and low immunogenicity[38, 39]. ELPs will phase-separate into a coacervate at solution temperatures above their LCST and will reversibly dissolve in solution temperatures below their LCST (Figure 5). The LCST can be modulated by several parameters, such as ELP chain length, salt concentration, ELP concentration, hydrophilicity of guest residues, and pH[37].

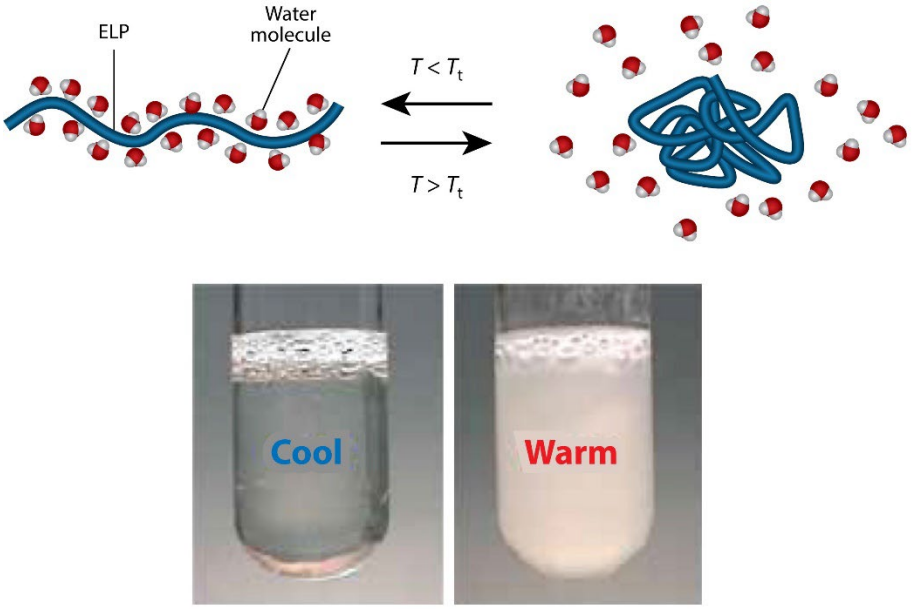

Figure 5. Diagram and photos showing the reversible temperature-responsive behavior of ELPs. ELPs are soluble below their LCST and aggregate into a coacervate state above their LCST. Reprinted with permission from Varanko, A. K.; Su, J. C.; Chilkoti, A. Elastin-Like Polypeptides for Biomedical Applications. *Annual Review of Biomedical Engineering* **2020**, *22* (1), 343-369. DOI: 10.1146/annurev-bioeng-092419-061127. Copyright 2020, Annual Reviews, Inc.

The temperature-responsive properties of ELPs enable a purification strategy that does not require chromatography. Inverse transition cycling (ITC) exploits the reversible phase change behavior of ELPs, which is uncommon among contaminants from protein biosynthesis (Figure 6)[39, 40]. When a solution containing ELPs and contaminants is heated above the LCST of the ELPs, the ELPs can be centrifuged such that the ELPs are contained in the pellet. Soluble contaminants can be discarded, and fresh cold buffer can be added to the pellet to dissolve the ELP below its LCST. Centrifuging at the cold temperature will keep the ELPs suspended, and

the insoluble contaminants can be removed. Repeating the cycle several times yields extremely pure ELPs relative to many conventional purification methods, and this process can also purify peptides that contain ELPs with other components, as well as ELP-fusion proteins.

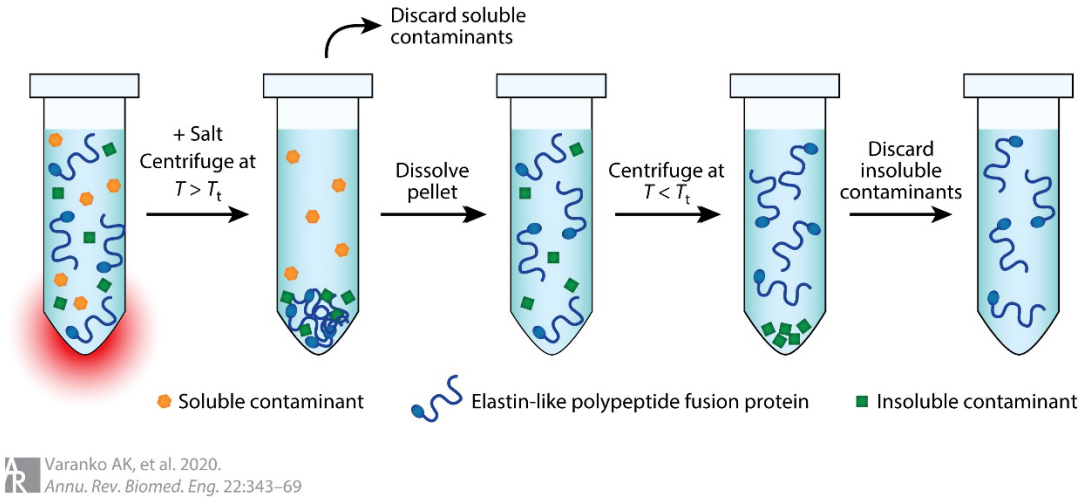

Figure 6. Diagram showing the inverse transition cycling of purifying ELPs using centrifugation. Reprinted with permission from Varanko, A. K.; Su, J. C.; Chilkoti, A. Elastin-Like Polypeptides for Biomedical Applications. *Annual Review of Biomedical Engineering* **2020**, *22* (1), 343-369. DOI: 10.1146/annurev-bioeng-092419-061127. Copyright 2020, Annual Reviews, Inc.

Artificial proteins that contain ELP can be biosynthesized, often in relatively high yield[41], and purified using ITC inexpensively without chromatography, which makes ELP a great candidate to form the hydrogel polymeric networks. In addition, under specific conditions, the same temperature-responsive properties can also cause ELPs to self-assemble into structures, such as micelles, cylinders, and fibers. This functionality is desired in applications such as drug delivery[42], vaccine carriers[39], and tissue engineering[41], where stable structures can enable a

longer half-life, improved targeting, and higher efficacy compared to similar unstructured components.

Elastin-Like Polypeptide Self-Assembled Structures

ELP homopolymers are the simplest type of ELP, where every monomer repeat contains the same guest residue, or a sequence of guest residues consistently repeats. In most cases, the ELP homopolymers will form large aggregates above their LCST, but specific designs can can self-assemble into defined nanoparticles[43] or fiber bundles[44] under particular environmental conditions. However, beyond ELP homopolymers, ELP block copolymers can form more complex self-assembled structures. ELP block copolymers have distinct blocks of various monomer sequences, and the blocks can respond differently to external stimuli, such as temperature. For example, a well-designed ELP block copolymer could self-assemble into micelles that contain targeting molecules or drugs (such as AMPs) on the external corona of the micelle, while other fusion components such as imaging agents can be on the inside core of the micelle (Figure 8). Typically, the temperature of the external environment would be higher than the LCST of one block but lower than the LCST of the other block. This causes one block to phase separate and end up in the core of the micelle, along with the fusion component to which it is attached. The soluble block stays on the outside of the micelle with the fusion components attached to that block[35, 45].

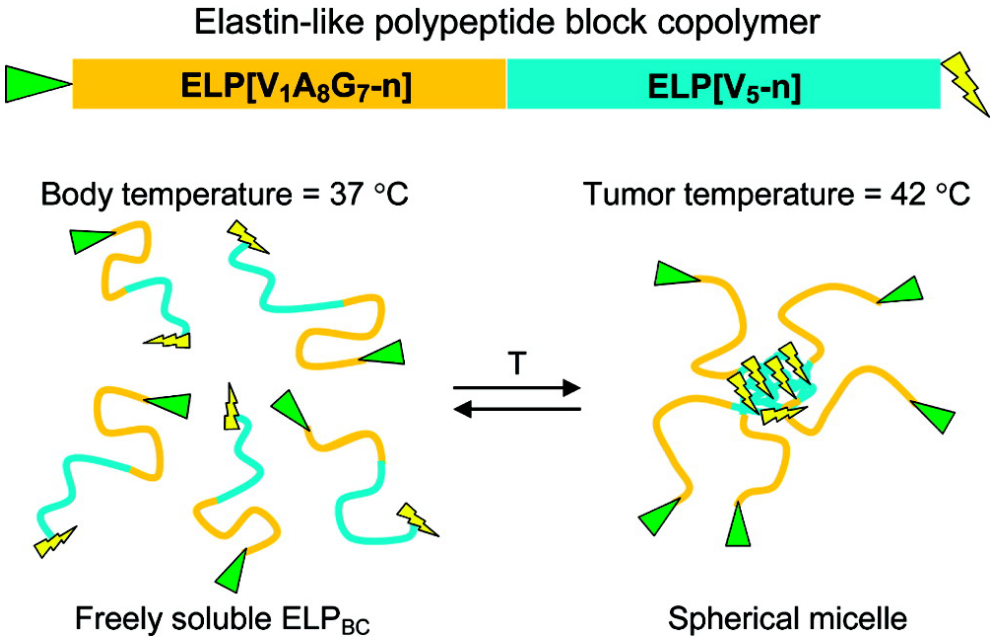

Figure 7. Self-assembled ELP micelles triggered by temperature change. Body temperature is above the LCST of the hydrophobic block (blue), while tumor temperature is below the LCST of the hydrophobic block, causing its phase-separation. The small molecules that are attached to the higher LCST block remain on the outside of the micelle (green triangle), while the small molecules attached to the block that phase separates are targeted to the inside (yellow lightning bolts). Reprinted with permission from Dreher, M. R.; Simnick, A. J.; Fischer, K.; Smith, R. J.; Patel, A.; Schmidt, M.; Chilkoti, A. Temperature Triggered Self-Assembly of Polypeptides into Multivalent Spherical Micelles. *Journal of the American Chemical Society* **2008**, *130* (2), 687-694. DOI: 10.1021/ja0764862. Copyright 2008, American Chemical Society.

Dityrosine Photocrosslinking to Form Polymeric Hydrogels

Chemical crosslinking is a good choice to form a strong polymer network that could potentially target natural tissues with high stiffness because physically crosslinked hydrogels tend to be weaker. Furthermore, rapid chemical crosslinking is preferred because many applications require setting a particular shape in seconds to minutes rather than hours[46], such as

3D printing. However, many rapid chemical crosslinking strategies have the disadvantage of forming crosslinks before the solution is completely mixed, leaving clumps of densely and sparsely crosslinked regions throughout the polymer network, leading to inconsistencies in the material mechanical properties[47]. Photocrosslinking is an attractive tool because the solution containing all activating reagents can be completely mixed before the solution is irradiated with light to activate the crosslinking. This strategy can produce a hydrogel with consistent mechanical properties throughout the hydrogel. Furthermore, to crosslink an artificial protein, dityrosine photocrosslinking can be utilized to form dityrosine covalent bonds between tyrosine amino acids[48]. If tyrosine is strategically placed in the artificial protein, it's possible to control where the crosslinking can occur. In addition, dityrosine photocrosslinking requires blue light, which is safer than UV light irradiation in situations when crosslinking would need to occur with a patient present.

An ELP block copolymer design with a material block, tether block, and AMP block can exploit these functionalities for AMP-incorporated materials. With tyrosine as guest residues evenly spaced throughout the material forming block, the ELP block copolymer can be dityrosine photocrosslinked to form hydrogels with a range of stiffness properties to match a variety of tissues by controlling the crosslinking density. The crosslinking density can be controlled by changing the concentrations of the photoinitiators used for photocrosslinking. The more hydrophilic, flexible ELP tether and AMP can be separated from the hydrogel for enhanced efficacy if the tether does not contain tyrosine residues. If the tether block is more hydrophilic, and the material forming block is more hydrophobic, the ELP block copolymer can also form micelles with the material forming block in the core and the tether and AMP forming the outer corona. Such a design can form an all-in-one artificial protein platform capable of forming

hydrogels and micelles to utilize AMPs in a variety of clinical scenarios, from engineered tissues to drug delivery vehicles depending on material processing, where crosslinking the polymers forms hydrogels and heating the polymers form micelles.

OVERVIEW OF DISSERTATION

The number of deaths associated with antibiotic resistant infections are predicted to increase exponentially in the coming decades, yet there are scarce antibiotics in the pipeline to replace the drugs that lose efficacy. There exists a great need for novel approaches to disrupt the current trends to treat antibiotic resistant infections, ranging from gram-positive methicillin resistant *Staphylococcus aureus* (MRSA)[49] and *Enterococcus faecalis*[50] to gram-negative *Pseudomonas aeruginosa*[51]. This includes efforts to reduce the use of antibiotics in hospitals and taking steps to limit the use of antibiotics in agriculture to keep the drugs in use efficacious, and to develop alternative treatments that fight infections while avoiding the development of microbial resistance.

Antimicrobial peptides (AMPs) represent an exciting alternative class of treatments to combat antibiotic resistant infections because they have broad-range efficacy against diverse pathogens and over 3,700 AMPs have been identified. Current research into utilizing AMPs include conjugation onto material surfaces to stabilize AMPs against degradation and organ filtration. Furthermore, separating AMPs from the material surface using a flexible, hydrophilic tether and controlling the orientation for which the AMPs are bound have shown to enhance the efficacy of AMPs. However, complicated and expensive processing and synthesis steps to produce such a therapeutic has slowed the clinical translation of AMP-material technology.

To solve the hurdles slowing the translation of AMP-incorporated materials, we designed and patented an all-in-one artificial protein platform that includes a material forming block, tether block, and AMP block in a single ELP block copolymer protein strand (Appendix A). We chose elastin-like polypeptides (ELPs) to comprise the material forming block and the tether block due to the cost-effective inverse transition cycling (ITC) method that avoids conventional

chromatography. ELPs also provide design flexibility because their $(VPGXG)_n$ sequence allow for X, the guest residue, to be any amino acid except for proline (P). Incorporating tyrosine into guest residue positions allows for dityrosine photocrosslinking to form hydrogel materials. Hydrophilic, flexible tethers, such as polyethylene glycol, have been used separate AMPs from materials to enhance the AMP efficacy. Therefore, it is necessary to choose relatively hydrophilic amino acids compared to tyrosine as the guest residues in the tether block.

To design the material block of the ELP block copolymer with the functionality of forming hydrogels, we incorporated tyrosine as guest residues. Tyrosine allows for dityrosine photocrosslinking to be utilized to form the polymer network, and the photocrosslinking method allows for the solution to be mixed completely prior to activation to form hydrogels with homogeneous crosslinking and elasticity. However, the LCST of a block with all tyrosine as guest residues would have a very low LCST below 0 °C within other design restrictions, such as molar mass and quantity of crosslinking sites. Amino acids, such as alanine, serine, and threonine, are less hydrophobic than average compared to tyrosine. The ELP LCST will increase if the average hydrophilicity of the guest residue increases. Therefore, to more easily utilize inverse transition cycling (ITC) purification, we incorporated alanine as guest residues in a 2:1 ratio to tyrosine, thus increasing the LCST of the material forming block near 18 °C. Because the protein must be centrifuged above and below the LCST at various steps of ITC, having the LCST near room temperature makes the purification process simpler.

The temperature-responsive properties of ELP block-copolymers can also permit the formation of micelles, where the more hydrophobic material forming block (i.e., ELP with tyrosine guest residues) will form the core of the micelle and the hydrophilic tether block will be on the outside of the micelle with the AMP attached on the outside of the tether. These micelles

can form when the external temperature is above the LCST of the hydrophobic material forming block and below the LCST of the tether block. Therefore, we designed the hydrophilic tether block to have a LCST around 37 °C, such that the ELP diblock copolymer will form micelles at body temperature but low enough to allow the ELP to be easily phase separated during ITC.

In my first manuscript published in *Frontiers in Chemistry* (Appendix B), we investigated a homopolymer that closely represents the material forming block of the all-in-one artificial protein platform but without the tether. The work represented a proof-of-concept that an ELP containing tyrosine residues could be crosslinked to target the elastic moduli of natural tissues using dityrosine photocrosslinking, which was not yet known. The homopolymer has the same numbers of alanine and tyrosine residues as the block copolymer, but the tyrosine and alanine residues were evenly spread out across the entire polymer in a 4:1 ratio of alanine to tyrosine. The molar mass and chain length of the homopolymer are also equal to the block copolymer.

We characterized the temperature responsiveness of the ELP homopolymer and found its LCST was 29 °C. As expected, the homopolymer does not form micelles. Rather, it is completely soluble below 29 °C and phase-separated above 29 °C. We then showed that the homopolymer was able to target any value up to 40 kPa by modulating the concentrations of the dityrosine photocrosslinking photoinitiators because research showed that it is critical for engineered tissues to match the elastic modulus of natural tissues to enable proper cell proliferation and differentiation. Furthermore, we evaluated the cytocompatibility of the material forming block and the photoinitiators and found that ammonium persulfate can be toxic to fibroblasts when it is used in excess, but that the materials were safe otherwise. Thus, we showed that the material forming block can form biocompatible hydrogels that can have its elastic

modulus targeted to match a range of soft tissues. However, since the homopolymer does not form micelles, the next step was to characterize a material forming block with an attached tether block and identify the ability of the polymer to form micelles when heated, and form hydrogels when crosslinked that can be targeted to match the mechanics of natural tissues.

The next proof-of-concept hurdle to translate the all-in-one artificial protein platform to clinical use was forming hydrogels with the tether block attached to the material block (Appendix C). The material block had a lower LCST in this design compared to the homopolymer that was tested in the first manuscript (Appendix B), which was 18 °C compared to the 29°C LCST of the homopolymer. We characterized the block copolymer (material block and attached tether) and found that it formed micelles between the LCST of the material forming block 18°C and the 37°C LCST of the tether block. However, those values were calculated at 1 mg/mL, while crosslinking was performed at 100 mg/mL. The LCST of ELPs is inversely proportional to concentration; thus, we expected the self-assembled structures could have been forming at 4°C in the crosslinking solution. The structures would be expected to have tyrosine on the inside of the structure with the material forming block, potentially reducing the efficiency of crosslinking and by extension the elastic moduli of the block copolymer hydrogels. We proceeded to evaluate the elastic moduli of hydrogels made from the diblock copolymer and found the elastic moduli of the hydrogels were much lower than the homopolymer under similar conditions.

To overcome this obstacle, we developed a method to increase the elastic moduli of the diblock copolymer hydrogels by blending the diblock copolymer with the homopolymer. We found that if 25% of the block copolymer was replaced with the homopolymer in the crosslinking solution, some of the block copolymer hydrogels had a much higher elastic

modulus, while others were low under the same conditions. We hypothesize that there is a trigger near 25% where the structure of the polymer network changes, but more research is required to find the precise mechanism, whether it is a very precise concentration or material processing differences. Altogether, this method keeps the protein concentration in the hydrogels constant but provides another method to control the hydrogel stiffness besides the photoinitiator concentrations. These data indicate the elastic modulus of the block copolymer hydrogels can increase dramatically by adding homopolymer mass percent, and shows it is possible to form block copolymer hydrogels with a reasonably high elastic modulus with only 25% homopolymer added.

CONCLUSIONS AND FUTURE WORKS

Altogether the all-in-one artificial protein platform design and research projects demonstrate the functionalities of forming biocompatible materials, including micelles at body temperature and crosslinking to form hydrogel materials that can target the elastic moduli of a range of natural tissues. We expect with this foundational work that the platform can be applied toward producing antimicrobial materials for testing against pathogenic microorganisms.

In this regard, preliminary data are promising with micelles that include the AMPs LL37 and pexiganan. Data show the ability of ELP diblock copolymers containing LL37 and pexiganan can significantly reduce the growth of *Pseudomonas aeruginosa* and *Staphylococcus aureus* antibiotic resistant bacteria compared to several controls. The ELP diblock copolymer without AMPs was unable to significantly reduce bacterial growth, and the ELP homopolymer with attached AMPs but without the tether was significantly less efficacious, suggesting the tether is required in this format to increase efficacy (*manuscript in preparation*).

While these data are exciting and promising, there are many avenues of research that are required to optimize the AMP efficacy. Using genetic engineering, all three blocks (material, tether, AMP) can be improved or replaced with amino acid-level precision. The material forming block forms self-assembled structures at low temperatures in the crosslinking solution causing a lower elastic modulus in hydrogels. Therefore, the alanine residues in the current ELP material forming block can be replaced with more hydrophilic residues, such that the LCST of the material block would increase and potentially prevent the self-assembled structures from forming. The LCST of the material forming block must be lower than body temperature to form micelles, but there is plenty room for the LCST to increase. For example, substituting the alanine

residues for serine or threonine would increase the LCST of the block because the average hydrophobicity of alanine is higher than serine or threonine.

As for the tether, the LCST of the block is near body temperature, which could cause larger structures to form at body temperature rather than stable micelles if the tether phase-separates in addition to the material forming block. Residues such as glycine, serine and threonine can replace alanine to make the tether more hydrophilic. The LCST would be expected to still be low enough to perform ITC to purify the protein (<~50 °C), especially if salt is used during purification to reduce the LCST during the phase separation step.

There are over 3,700 AMPs that have been identified, and one of the major benefits to this platform is all AMPs can be tested without the requirement to change conjugation chemistries or purification strategies. With genetic engineering, the DNA encoding for the AMP can be changed out for any AMP for which the sequence is known and tested against pathogens. Furthermore, combinations of multiple AMPs in the same hydrogel or micelle materials may have synergistic effects compared to single AMPs, and this platform allows for precise control of AMP concentrations in those materials for carefully controlled studies.

Finally, this platform is not limited to antimicrobial peptides. Small peptides that specialize in other applications such as cell or tumor targeting, imaging, and wound healing can be genetically fused to the hydrophilic tether. The protease degradation and organ filtration that limits the efficacy of antimicrobial peptides can also affect other small peptides. Therefore, stabilizing other small peptides using the all-in-one artificial protein platform can make advances in additional fields where the expense of producing small peptides and complexity of conjugating those peptides to materials are prohibitive to their clinical utilization.

I anticipate with the promising preliminary data and these promising hydrogel characteristics that the all-in-one artificial protein platform will be applied in the clinic as a versatile tool, allowing capabilities to mix and match AMPs or other small peptides, and test all parameters for each block in controlled optimization studies, as a next generation solution to antimicrobial resistant infections.[52]

REFERENCES

(1) O'Neill, J. *Tackling drug-resistant infections globally: final report and recommendations*; Government of the United Kingdom, 2016.

(2) National Action Plan for Combating Antibiotic-Resistant Bacteria 2020-2025. House, T. W., Ed.; 2020; pp 1-47.

(3) Hormozi, S. F.; Vasei, N.; Aminianfar, M.; Darvishi, M.; Saeedi, A. A. Antibiotic resistance in patients suffering from nosocomial infections in Besat Hospital. *Eur J Transl Myol* **2018**, *28* (3), 7594. DOI: 10.4081/ejtm.2018.7594 From NLM.

(4) Manyi-Loh, C.; Mamphweli, S.; Meyer, E.; Okoh, A. Antibiotic Use in Agriculture and Its Consequential Resistance in Environmental Sources: Potential Public Health Implications. *Molecules* **2018**, *23* (4), 795. DOI: 10.3390/molecules23040795.

(5) Shallcross, L. J.; Davies, D. S. Antibiotic overuse: a key driver of antimicrobial resistance. *Br J Gen Pract* **2014**, *64* (629), 604-605. DOI: 10.3399/bjgp14X682561 From NLM.

(6) Merlin, C. Reducing the Consumption of Antibiotics: Would That Be Enough to Slow Down the Dissemination of Resistances in the Downstream Environment? *Front Microbiol* **2020**, *11*, 33. DOI: 10.3389/fmicb.2020.00033 From NLM.

(7) Butler, M.; Gigante, V.; Sati, H.; Paulin, S.; Al-Sulaiman, L.; Rex, J.; Fernandes, P.; Arias, C.; Paul, M.; Thwaites, G.; et al. Analysis of the Clinical Pipeline of Treatments for Drug-Resistant Bacterial Infections: Despite Progress, More Action Is Needed. *Antimicrobial Agents and Chemotherapy* **2022**, *66*. DOI: 10.1128/AAC.01991-21.

(8) Nizet, V. Antimicrobial Peptide Resistance Mechanisms of Human Bacterial Pathogens. *Current Issues in Molecular Biology* **2006**. DOI: 10.21775/cimb.008.011.

(9) Chen, C. H.; Lu, T. K. Development and Challenges of Antimicrobial Peptides for Therapeutic Applications. *Antibiotics* **2020**, *9* (1), 24. DOI: 10.3390/antibiotics9010024.

(10) Cherkasov, A.; Hilpert, K.; Jenssen, H.; Fjell, C. D.; Waldbrook, M.; Mullaly, S. C.; Volkmer, R.; Hancock, R. E. Use of artificial intelligence in the design of small peptide antibiotics effective against a broad spectrum of highly antibiotic-resistant superbugs. *ACS Chem Biol* **2009**, *4* (1), 65-74. DOI: 10.1021/cb800240j From NLM.

(11) Mishra, B.; Reiling, S.; Zarena, D.; Wang, G. Host defense antimicrobial peptides as antibiotics: design and application strategies. *Current Opinion in Chemical Biology* **2017**, *38*, 87-96. DOI: 10.1016/j.cbpa.2017.03.014.

(12) Brogden, K. A. Antimicrobial peptides: pore formers or metabolic inhibitors in bacteria? *Nature Reviews Microbiology* **2005**, *3* (3), 238-250. DOI: 10.1038/nrmicro1098.

(13) Wimley, W. C. Describing the Mechanism of Antimicrobial Peptide Action with the Interfacial Activity Model. *ACS Chemical Biology* **2010**, *5* (10), 905-917. DOI: 10.1021/cb1001558.

(14) Hancock, R. E. W.; Sahl, H.-G. Antimicrobial and host-defense peptides as new anti-infective therapeutic strategies. *Nature Biotechnology* **2006**, *24* (12), 1551-1557. DOI: 10.1038/nbt1267.

(15) Zhang, Q.-Y.; Yan, Z.-B.; Meng, Y.-M.; Hong, X.-Y.; Shao, G.; Ma, J.-J.; Cheng, X.-R.; Liu, J.; Kang, J.; Fu, C.-Y. Antimicrobial peptides: mechanism of action, activity and clinical potential. *Military Medical Research* **2021**, *8* (1). DOI: 10.1186/s40779-021-00343-2.

(16) Zhang, L.-J.; Gallo, R. L. Antimicrobial peptides. *Current Biology* **2016**, *26* (1), R14-R19. DOI: 10.1016/j.cub.2015.11.017.

(17) Lei, J.; Sun, L.; Huang, S.; Zhu, C.; Li, P.; He, J.; Mackey, V.; Coy, D. H.; He, Q. The antimicrobial peptides and their potential clinical applications. *Am J Transl Res* **2019**, *11* (7), 3919-3931. From NLM.

(18) Dennison, S. R.; Reddy, S. M.; Morton, L. H. G.; Harris, F.; Badiani, K.; Phoenix, D. A. PEGylation enhances the antibacterial and therapeutic potential of amphibian host defence peptides. *Biochimica et Biophysica Acta (BBA) - Biomembranes* **2022**, *1864* (1), 183806. DOI: 10.1016/j.bbamem.2021.183806.

(19) Muszanska, A. K.; Rochford, E. T. J.; Gruszka, A.; Bastian, A. A.; Busscher, H. J.; Norde, W.; van der Mei, H. C.; Herrmann, A. Antiadhesive Polymer Brush Coating Functionalized with Antimicrobial and RGD Peptides to Reduce Biofilm Formation and Enhance Tissue Integration. *Biomacromolecules* **2014**, *15* (6), 2019-2026. DOI: 10.1021/bm500168s.

(20) Costa, F.; Carvalho, I. F.; Montelaro, R. C.; Gomes, P.; Martins, M. C. L. Covalent immobilization of antimicrobial peptides (AMPs) onto biomaterial surfaces. *Acta Biomaterialia* **2011**, *7* (4), 1431-1440. DOI: 10.1016/j.actbio.2010.11.005.

(21) Rai, A.; Ferrão, R.; Palma, P.; Patricio, T.; Parreira, P.; Anes, E.; Tonda-Turo, C.; Martins, M. C. L.; Alves, N.; Ferreira, L. Antimicrobial peptide-based materials: opportunities and challenges. *Journal of Materials Chemistry B* **2022**, *10* (14), 2384-2429. DOI: 10.1039/d1tb02617h.

(22) Sánchez-Trasviña, C.; Rito-Palomares, M.; González-Valdez, J. Development and Characterization of PEGylated Chromatographic Monoliths as a Novel Platform for the Separation of PEGylated RNase a Isomers. *Advances in Polymer Technology* **2019**, *2019*, 5067028. DOI: 10.1155/2019/5067028.

(23) Onaizi, S. A.; Leong, S. S. Tethering antimicrobial peptides: current status and potential challenges. *Biotechnol Adv* **2011**, *29* (1), 67-74. DOI: 10.1016/j.biotechadv.2010.08.012 From NLM.

(24) Bagheri, M.; Beyermann, M.; Dathe, M. Immobilization reduces the activity of surface-bound cationic antimicrobial peptides with no influence upon the activity spectrum. *Antimicrob Agents Chemother* **2009**, *53* (3), 1132-1141. DOI: 10.1128/aac.01254-08 From NLM.

(25) Bagheri, M. Cationic Antimicrobial Peptides (AMPs): Thermodynamic Characterization of Peptide-Lipid Interactions and Biological Efficacy of Surface-Tethered Peptides. *ChemistryOpen* **2015**, *4* (3), 389-393. DOI: 10.1002/open.201402149.

(26) Cao, H.; Duan, L.; Zhang, Y.; Cao, J.; Zhang, K. Current hydrogel advances in physicochemical and biological response-driven biomedical application diversity. *Signal Transduction and Targeted Therapy* **2021**, *6* (1), 426. DOI: 10.1038/s41392-021-00830-x.

(27) Huerta-López, C.; Alegre-Cebollada, J. Protein Hydrogels: The Swiss Army Knife for Enhanced Mechanical and Bioactive Properties of Biomaterials. *Nanomaterials (Basel)* **2021**, *11* (7). DOI: 10.3390/nano11071656 From NLM.

(28) Chaudhuri, O.; Gu, L.; Klumpers, D.; Darnell, M.; Bencherif, S. A.; Weaver, J. C.; Huebsch, N.; Lee, H.-P.; Lippens, E.; Duda, G. N.; et al. Hydrogels with tunable stress relaxation regulate stem cell fate and activity. *Nature Materials* **2016**, *15* (3), 326-334. DOI: 10.1038/nmat4489.

(29) Engler, A. J.; Sen, S.; Sweeney, H. L.; Discher, D. E. Matrix Elasticity Directs Stem Cell Lineage Specification. *Cell* **2006**, *126* (4), 677-689. DOI: 10.1016/j.cell.2006.06.044.

(30) Kaczmarek, B.; Nadolna, K.; Owczarek, A. Chapter 6 - The physical and chemical properties of hydrogels based on natural polymers. In *Hydrogels Based on Natural Polymers*, Chen, Y. Ed.; Elsevier, 2020; pp 151-172.

(31) Lozeau, L. D.; Alexander, T. E.; Camesano, T. A. Proposed Mechanisms of Tethered Antimicrobial Peptide Chrysophsin-1 as a Function of Tether Length Using QCM-D. *The Journal of Physical Chemistry B* **2015**, *119* (41), 13142-13151. DOI: 10.1021/acs.jpcb.5b06883.

(32) Kim, M.; Chen, W. G.; Kang, J. W.; Glassman, M. J.; Ribbeck, K.; Olsen, B. D. Artificially Engineered Protein Hydrogels Adapted from the Nucleoporin Nsp1 for Selective Biomolecular Transport. *Advanced Materials* **2015**, *27* (28), 4207-4212. DOI: 10.1002/adma.201500752.

(33) Wu, J.; Li, P.; Dong, C.; Jiang, H.; Bin, X.; Gao, X.; Qin, M.; Wang, W.; Bin, C.; Cao, Y. Rationally designed synthetic protein hydrogels with predictable mechanical properties. *Nature Communications* **2018**, *9* (1). DOI: 10.1038/s41467-018-02917-6.

(34) Spriestersbach, A.; Kubicek, J.; Schäfer, F.; Block, H.; Maertens, B. Purification of His-Tagged Proteins. *Methods Enzymol* **2015**, *559*, 1-15. DOI: 10.1016/bs.mie.2014.11.003 From NLM.

(35) Doole, F. T.; Camp, C. P.; Kim, M. Tailoring the formation and stability of self-assembled structures from precisely engineered intrinsically disordered protein polymers: A comprehensive review. *Giant* **2023**, *14*, 100158. DOI: https://doi.org/10.1016/j.giant.2023.100158.

(36) Meyer, D. E.; Chilkoti, A. Genetically Encoded Synthesis of Protein-Based Polymers with Precisely Specified Molecular Weight and Sequence by Recursive Directional Ligation: Examples from the Elastin-like Polypeptide System. *Biomacromolecules* **2002**, *3* (2), 357-367. DOI: 10.1021/bm015630n.

(37) Meyer, D. E.; Chilkoti, A. Purification of recombinant proteins by fusion with thermally-responsive polypeptides. *Nat Biotechnol* **1999**, *17* (11), 1112-1115. DOI: 10.1038/15100 From NLM.

(38) Li, Y.; Wang, Y.; Cheng, J.; Zhou, X.; Lu, H.; Zhang, X.; Xia, X.; Sun, H. Generation and immunogenicity assessment of ELPylated virus-like particles of porcine circovirus type 2. *Virology Journal* **2020**, *17* (1). DOI: 10.1186/s12985-020-01346-6.

(39) Ingrole, R. S.; Tao, W.; Tripathy, J. N.; Gill, H. S. Synthesis and Immunogenicity Assessment of Elastin-Like Polypeptide-M2e Construct as an Influenza Antigen. *Nano LIFE* **2014**, *04* (02), 1450004. DOI: 10.1142/s1793984414500044.

(40) MacEwan, S.; Hassouneh, W.; Chilkoti, A. Non-chromatographic Purification of Recombinant Elastin-like Polypeptides and their Fusions with Peptides and Proteins from Escherichia coli. *Journal of visualized experiments : JoVE* **2014**. DOI: 10.3791/51583.

(41) Camp, C. P.; Peterson, I. L.; Knoff, D. S.; Melcher, L. G.; Maxwell, C. J.; Cohen, A. T.; Wertheimer, A. M.; Kim, M. Non-cytotoxic Dityrosine Photocrosslinked Polymeric Materials With Targeted Elastic Moduli. *Frontiers in Chemistry* **2020**, *8*, Original Research. DOI: 10.3389/fchem.2020.00173.

(42) MacEwan, S. R.; Chilkoti, A. Applications of elastin-like polypeptides in drug delivery. *J Control Release* **2014**, *190*, 314-330. DOI: 10.1016/j.jconrel.2014.06.028 From NLM.

(43) Bahniuk, M. S.; Alshememry, A. K.; Elgersma, S. V.; Unsworth, L. D. Self-assembly/disassembly hysteresis of nanoparticles composed of marginally soluble, short elastin-like polypeptides. *Journal of Nanobiotechnology* **2018**, *16* (1). DOI: 10.1186/s12951-018-0342-5.

(44) Salvi, A. M.; Moscarelli, P.; Satriano, G.; Bochicchio, B.; Castle, J. E. Influence of amino acid specificities on the molecular and supramolecular organization of glycine-rich elastin-like polypeptides in water. *Biopolymers* **2011**, *95* (10), 702-721. DOI: 10.1002/bip.21636 From NLM.

(45) Dreher, M. R.; Simnick, A. J.; Fischer, K.; Smith, R. J.; Patel, A.; Schmidt, M.; Chilkoti, A. Temperature Triggered Self-Assembly of Polypeptides into Multivalent Spherical Micelles. *Journal of the American Chemical Society* **2008**, *130* (2), 687-694. DOI: 10.1021/ja0764862.

(46) Melchels, F. P. W.; Feijen, J.; Grijpma, D. W. A review on stereolithography and its applications in biomedical engineering. *Biomaterials* **2010**, *31* (24), 6121-6130. DOI: https://doi.org/10.1016/j.biomaterials.2010.04.050.

(47) Kroll, D. M.; Croll, S. G. Influence of crosslinking functionality, temperature and conversion on heterogeneities in polymer networks. *Polymer* **2015**, *79*, 82-90. DOI: https://doi.org/10.1016/j.polymer.2015.10.020.

(48) Aeschbach, R.; Amadoò, R.; Neukom, H. Formation of dityrosine cross-links in proteins by oxidation of tyrosine residues. *Biochimica et Biophysica Acta (BBA) - Protein Structure* **1976**, *439* (2), 292-301. DOI: https://doi.org/10.1016/0005-2795(76)90064-7.

(49) Bal, A. M.; David, M. Z.; Garau, J.; Gottlieb, T.; Mazzei, T.; Scaglione, F.; Tattevin, P.; Gould, I. M. Future trends in the treatment of methicillin-resistant Staphylococcus aureus (MRSA) infection: An in-depth review of newer antibiotics active against an enduring pathogen. *J Glob Antimicrob Resist* **2017**, *10*, 295-303. DOI: 10.1016/j.jgar.2017.05.019 From NLM.

(50) Akter, T.; Haque, M. N.; Ehsan, R.; Paul, S. I.; Foysal, M. J.; Tay, A. C. Y.; Islam, M. T.; Rahman, M. M. Virulence and antibiotic-resistance genes in Enterococcus faecalis associated with streptococcosis disease in fish. *Scientific Reports* **2023**, *13* (1), 1551. DOI: 10.1038/s41598-022-25968-8.

(51) Pang, Z.; Raudonis, R.; Glick, B. R.; Lin, T. J.; Cheng, Z. Antibiotic resistance in Pseudomonas aeruginosa: mechanisms and alternative therapeutic strategies. *Biotechnol Adv* **2019**, *37* (1), 177-192. DOI: 10.1016/j.biotechadv.2018.11.013 From NLM.

(52) Yahia, L. H.; Chirani, N.; Gritsch, L.; Motta, F. L.; SoumiaChirani; Fare', S. History and Applications of Hydrogels. 2015.

APPENDIX A

Antimicrobial Biopolymer Compositions, Methods of Synthesis, and Applications of Use

Cross-References to Related Applications

[0001] This application is a continuation-in-part and claims benefit of U.S. Patent Application No. 16/253,825 filed January 22, 2019, which is a non-provisional and claims benefit of U.S. Patent Application No. 62/619,430 filed January 19, 2018, the specifications of which are incorporated herein in its entirety by reference.

Reference to a Sequence Listing

[0002] Applicant asserts that the paper copy of the Sequence Listing is identical to the Sequence Listing in computer readable form found on the accompanying computer file, entitled UNIA 17.44 CIP Sequence Listing_ST25. The content of the sequence listing is incorporated herein by reference in its entirety.

Field of the Invention

[0003] The present invention relates to biopolymers, more particularly to biopolymers comprising tethered antimicrobial peptides (AMPs) for treating microbial infections.

Background of the Invention

[0004] Tethering antimicrobial peptides (AMPs) to a biomaterial surface is a promising therapeutic to treat a broad range of microbial infections (e.g., by enhancing AMP stability, prolonging AMP activity *in vivo*, reducing AMP dosage, reducing AMP toxicity, etc.), including antimicrobial-resistant microorganisms. However, complex chemical synthesis of conventional

AMP-incorporated materials limits the use of antimicrobial materials in clinical settings. Furthermore, the complex chemical synthesis and processing of conventional AMP-incorporated materials is impractical for many AMPs due to high cost burdens. For example, conventional AMP-incorporated materials are comprised of: an AMP; a long, flexible, hydrophilic polymer tether; and a biomaterial that is specific to the clinical application. Each component is synthesized individually and subsequently connected in additional steps.

[0005] AMP biopolymers can be synthesized as an artificially engineered protein (an "all-in-one" artificial protein) by genetically fusing (1) an AMP; (2) a protein that behaves similarly to polymer tethers; and (3) a protein as a modifiable material platform that can transform to self-standing nanoparticles and films, or adhesives to easily attach tethered AMPs onto any biomaterial surface for various clinical applications. Genetic engineering allows for modification of single amino acids of the artificial protein, e.g., for modifying the AMP sequence for better potency, changing to a different AMP, improving the material properties, etc. Biosynthesis using biological hosts precisely produces the artificial proteins as designed, reducing inconsistent antimicrobial activity by eliminating complex chemical processing. In addition, because these proteins can be purified without traditional chromatography, and because biosynthesis is scalable, there is significant potential for the clinical translation of the AMP-incorporated materials using cost-effective biomanufacturing.

[0006] The development of this "all-in-one" artificial protein as a universal material platform for AMPs serves to mitigate current barriers to the efficient and cost-effective development and application of AMP-incorporated materials for their use in the clinical setting.

Summary of the Invention

[0007] The present invention features biopolymers comprising antimicrobial peptides (AMPs), as

well as applications of use, methods of synthesis, and compositions for synthesis. The methods and compositions herein help to simplify and unify the synthesis of various AMP-incorporated materials.

[0008] The biopolymers of the present invention may be used for treating microbial infections, including bacterial infections, fungal infections, parasitic infections, viral infections, infections associated with antibiotic-resistant bacteria or antifungal-resistant fungi or antiviral-resistant viruses, biological warfare agents (BWAs) such as *Bacillus anthracis* and *Yersenia pestis*, etc. The biopolymers of the present invention may be used to kill or reduce the growth of the particular microbe (e.g., bacteria, fungus, parasite, virus, etc.).

[0009] The ELP(Tyr) design provided herein produces AMP antimicrobial agents in the form of nanoparticles, films/membranes, and strong adhesives to biomaterial surfaces. Elastin-like polypeptide (ELP)-fusion proteins self-assemble into multiple material structures in physiological conditions as a function of: (i) the designed phase transition temperature (T_t); (ii) molar mass ratio between the ELP and fused proteins; and (iii) concentration of ELP-fusion protein in solution. This helps guide the development of AMP nanoparticles.

[0010] The present invention provides antimicrobial material (AMP)-biopolymer compositions comprising an elastin-like polypeptide (ELP); an antimicrobial material (AMP); and a protein (polypeptide, e.g., with antifouling characteristics) tether connecting the ELP and the AMP. In certain embodiments, the ELP comprises at least one tyrosine residue (e.g., ELP(Tyr)). In certain embodiments, the ELP, e.g., ELP(Tyr), is according to the formula $(VPGXaaG)_m$ (SEQ ID NO: 1). In certain embodiments, the ELP, e.g., ELP(Tyr), is according to the formula $[(VPGXaaG)_j(VPGYG)_k(VPGXaaG)_l]_n$ (note VPGYG is SEQ ID NO: 2), thus the formula may

be written $[(\text{SEQ ID NO: 1})_j(\text{SEQ ID NO: 2})_k(\text{SEQ ID NO: 1})_l]_n$. In certain embodiments, Xaa is a polar amino acid, a non-polar amino acid, a charged amino acid, or a combination thereof, not including proline. For example, in certain embodiments, Xaa is alanine. In some embodiments, Xaa is serine. In some embodiments, Xaa is glycine. In some embodiments, Xaa is arginine. In some embodiments, Xaa is asparagine. In some embodiments, Xaa is aspartic acid. In some embodiments, Xaa is cysteine. In some embodiments, Xaa is glutamine. In some embodiments, Xaa is glutamic acid. In some embodiments, Xaa is histidine. In some embodiments, Xaa is isoleucine. In some embodiments, Xaa is leucine. In some embodiments, Xaa is lysine. In some embodiments, Xaa is methionine. In some embodiments, Xaa is phenylalanine. In some embodiments, Xaa is threonine. In some embodiments, Xaa is tryptophan. In some embodiments, Xaa is tyrosine. In some embodiments, Xaa is valine. In some embodiments, Xaa may be one or a combination of the aforementioned examples of amino acids. A composition may comprise a plurality of ELPs with one or different formulas.

[0011] Certain embodiments herein, e.g., compositions herein, may comprise an elastin-like peptide (ELP), an antimicrobial peptide (AMP) and a hydrophilic protein tether connecting the ELP and the AMP. In some embodiments, the ELP comprises one or more pentapeptide repeats consecutively linked. In other embodiments, at least one of the pentapeptide repeats comprises a tyrosine residue. In some embodiments, protein tether connects to the AMP at the AMP's N-terminus, C-terminus, or both. In further embodiments, the ELP is more hydrophobic than the protein tether.

[0012] The present invention also features antimicrobial material (AMP)-biopolymer compositions comprising: an elastin-like polypeptide (ELP); an antimicrobial material (AMP); and a protein tether connecting the ELP and the AMP, wherein the peptide tether connects to the AMP

at the AMP's N-terminus or C-terminus. In some embodiments, the ELP comprises at least one tyrosine residue.

[0013] The ELP may be according to the formula $[(\text{VPGXaaG, SEQ ID NO: 1})_j(\text{VPGYG, SEQ ID NO: 2})_k(\text{VPGXaaG, SEQ ID NO: 1})_l]_n$. In some embodiments, Xaa is alanine, serine, arginine, asparagine, aspartic acid, cysteine, glutamine, glutamic acid, glycine, histidine, isoleucine, leucine, lysine, methionine, phenylalanine, threonine, tryptophan, tyrosine, or valine.

[0014] In some embodiments, the protein tether comprises $[\text{VPGSG}]_i$ (SEQ ID NO: 4) or $[\text{AGAGAGPEG}]_n$ (SEQ ID NO: 5). In some embodiments, the composition self-assembles into nanoparticles. In some embodiments, tyrosine residues are cross-linked to form a self-standing film, a membrane material, or a hydrogel.

[0015] In some embodiments, the tyrosine residue allows the composition to adhere to a surface after hydroxylation by tyrosinase. In other embodiments, the tyrosine residue allows the composition to adhere to a surface after hydroxylation. In some embodiments, the surface is a cloth, a plastic, a glass, a metal, or a combination thereof. In some embodiments, the surface is a medical device, a dressing, a clothing, or a combination thereof. In some embodiments, the protein tether has anti-fouling characteristics. In some embodiments, the composition is for killing an infectious agent or for reducing growth of an infectious agent. In some embodiments, the infectious agent is a bacteria, a virus, a fungus, or a parasite.

[0016] In certain embodiments, the AMP is selected from the group consisting of LL37, RL37, Dermcidin, Protegrin (e.g., PG-1, PG-2, PG-3, PG-4, or PG-5), Pexiganan, etc., or a combination thereof. However, the present invention is not limited to the aforementioned AMPs.

[0017] In certain embodiments, the AMP biopolymer composition self-assembles into nanoparticles. In certain embodiments, the tyrosine residues are cross-linked (e.g., by photo-crosslinking using a photoinitiator, e.g., riboflavin (vitamin B2), Tris(2,2-bipyridine)ruthenium(II), etc., to form a self-standing film, a membrane material, or a hydrogel.

[0018] The tyrosine residue(s) of the composition allow the composition to adhere to a surface (e.g., cloth, plastic, metal, glass, a combination thereof; e.g., a medical device such as an endoscope or an implant, a dressing, clothing, or a combination thereof), e.g., after hydroxylation by tyrosinase.

[0019] In certain embodiments, AMP is connected to the tether by its N-terminus. In certain embodiments, the AMP is connected to the tether by its C-terminus. In certain embodiments, the composition comprises an AMP molecule connected to the tether at its N-terminus and an AMP molecule connected to the tether at its C-terminus. For example, in certain embodiments, the composition is ELP(Tyr)-tether-AMP. In certain embodiments, the composition is AMP-tether-ELP(Tyr). In certain embodiments, the composition is ELP-tether-AMP. In certain embodiments, the composition is AMP-tether-ELP. In certain embodiments, the composition comprises a mix of different compositions, e.g., a mix of AMP-tether-ELP and ELP-tether-AMP.

[0020] In certain embodiments, the composition is for treating an infection, e.g., a bacterial infection, a viral infection, a fungal infection, or a parasitic infection. In certain embodiments, the infection is caused by a biological warfare agent. In certain embodiments, the infection is caused by an antimicrobial-resistant microorganism. In certain embodiments, the composition is for killing an infectious agent or for reducing growth of an infectious agent.

[0021] The present invention also provides films comprising an antimicrobial material (AMP)-

biopolymer according to the present invention as described herein. For example, the AMP-biopolymer may comprise an elastin-like polypeptide (ELP) (e.g., ELP(Tyr)); an antimicrobial peptide (AMP); and a protein tether connecting the ELP and the AMP. In some embodiments, the AMP-biopolymer comprises: an elastin-like polypeptide ELP(Tyr) according to the formula $[(\text{VPGXaaG, SEQ ID NO: 1})_j(\text{VPGYG, SEQ ID NO: 3})_k(\text{VPGXaaG, SEQ ID NO: 1})_l]_n$; an antimicrobial peptide (AMP); and a protein tether connecting the ELP and the AMP. The protein tether connects to the AMP at the AMP's N-terminus or C-terminus. The ELP may be cross-linked to form the film material. For example, the tyrosines in the ELP(Tyr) may be cross-linked to form a film.

[0022] In some embodiments, Xaa is alanine, serine, arginine, asparagine, aspartic acid, cysteine, glutamine, glutamic acid, glycine, histidine, isoleucine, leucine, lysine, methionine, phenylalanine, threonine, tryptophan, tyrosine, or valine. In some embodiments, the AMP is selected from the group consisting of LL37, RL37, Dermcidin, Protegrin, Pexiganan or a combination thereof. However, the present invention is not limited to the aforementioned AMPs. In some embodiments, the protein tether comprises $[\text{VPGSG}]_i$ (SEQ ID NO: 42) or $[\text{AGAGAGPEG}]_i$ (SEQ ID NO: 43).

[0023] The present invention also provides therapeutic cocktail compositions comprising two or more different antimicrobial (AMP)-biopolymer compositions according to the present invention. For example, in some embodiments, each AMP biopolymer composition comprises an elastin-like polypeptide ELP(Tyr) according to the formula $[(\text{VPGXaaG, SEQ ID NO: 1})_j(\text{VPGYG, SEQ ID NO: 3})_k(\text{VPGXaaG, SEQ ID NO: 1})_l]_n$; an antimicrobial peptide (AMP); and a protein tether connecting the ELP and the AMP. The protein tether may connect to the AMP at the AMP's N-terminus or C-terminus. In some embodiments, the AMP is selected from the group consisting of LL37, RL37, Dermcidin, Protegrin, Pexiganan or a combination thereof. However, the AMP is not

limited to the aforementioned examples of AMPs.

[0024] The present invention also provides designed nucleic acid sequences encoding AMP-biopolymer compositions according to the present invention. The present invention also features isolated nucleic acid sequences encoding AMP-biopolymer compositions according to the present invention. The present invention also provides amino acid sequences of AMP-biopolymer compositions according to the present invention.

[0025] The present invention also provides methods of synthesizing AMP-biopolymer compositions according to the present invention. In certain embodiments, the method comprises introducing (to a host for gene expression such as but not limited to a bacterial host) a vector encoding the AMP-biopolymer composition; expressing the AMP-biopolymer composition; and purifying the AMP-biopolymer composition. In certain embodiments, the gene expression host is a bacterial host, e.g., *Escherichia coli*. The gene expression host is not limited to *E. coli*. In certain embodiments, purifying the AMP biopolymer composition comprises an inverse transition cycling (ITC) method.

[0026] The present invention also provides methods for purifying AMP biopolymer compositions according to the present invention, wherein the method comprises an inverse transition cycling (ITC) method.

[0027] Any feature or combination of features described herein are included within the scope of the present invention provided that the features included in any such combination are not mutually inconsistent as will be apparent from the context, this specification, and the knowledge of one of ordinary skill in the art. Additional advantages and aspects of the present invention are apparent in the following detailed description and claims.

Brief Description of the Drawings

[0028] This patent application contains at least one drawing executed in color. Copies of this patent or patent application publication with color drawing(s) will be provided by the Office upon request and payment of the necessary fee.

[0029] The features and advantages of the present invention will become apparent from a consideration of the following detailed descriptions presented in connection with the accompanying drawings in which:

[0030] FIG. 1 shows a schematic view of the synthesis of AMP biopolymers (e.g., ELPs) of the present invention as well as applications thereof.

[0031] FIG. 2A shows SDS-PAGE analysis of ELP$(A_1Y_1A_1)_{24}$-LL37 purified by inverse transition cycling methods.

[0032] FIG. 2B shows SDS-PAGE analysis of ELP$(S_2Y_1S_2)_8$-LL37 purified by salting out methods.

[0033] FIG. 2C shows UV/Vis spectrophotometer analysis of the phase-transitioning temperatures of ELP$(A_2Y_1A_2)_{24}$ and ELP$(A_2Y_1A_2)_{36}$, respectively.

[0034] FIG. 3 shows ELP$(S_2Y_2S_2)_{16}$-LL37 with PBS containing 25 wt % ammonium sulfate. At 40°C, the protein was not in solution (a), but the protein was in precipitate (b) and dissolved (c) at 4°C.

[0035] FIG. 4 shows a hydrogel made of cross-linked ELP$(A_2Y_1A_2)_{24}$ showing hydrogel thermoresponsive behavior where the hydrogel is clear below the transition temperature (e.g., below 25°C, left panel) and cloudy above the transition temperature (e.g., above 25°C, right panel).

Detailed Description of the Invention

[0036] For purposes of summarizing the disclosure, certain aspects, advantages, and novel features of the disclosure are described herein. It is to be understood that not necessarily all such advantages may be achieved in accordance with any particular embodiments of the disclosure. Thus, the disclosure may be embodied or carried out in a manner that achieves or optimizes one advantage or group of advantages as taught herein without necessarily achieving other advantages as may be taught or suggested herein.

[0037] Additionally, although embodiments of the disclosure have been described in detail, certain variations and modifications will be apparent to those skilled in the art, including embodiments that do not provide all the features and benefits described herein. It will be understood by those skilled in the art that the present disclosure extends beyond the specifically disclosed embodiments to other alternative or additional embodiments and/or uses and obvious modifications and equivalents thereof. Moreover, while a number of variations have been shown and described in varying detail, other modifications, which are within the scope of the present disclosure, will be readily apparent to those of skill in the art based upon this disclosure. It is also contemplated that various combinations or sub-combinations of the specific features and aspects of the embodiments may be made and still fall within the scope of the present disclosure. Accordingly, it should be understood that various features and aspects of the disclosed embodiments can be combined with or substituted for one another in order to form varying modes of the present disclosure. Thus, it is intended that the scope of the present disclosure herein disclosed should not be limited by the particular disclosed embodiments described herein.

[0038] As used herein, the singular forms “a,” “an,” and “the” are intended to include the plural forms as well, unless the context clearly indicates otherwise. Furthermore, to the extent that the

terms “including,” “includes,” “having,” “has,” “with,” or variants thereof are used in either the detailed description and/or the claims, such terms are intended to be inclusive in a manner similar to the term “comprising.”

[0039] As used herein, the “amino acids” refers to the twenty amino acids that are found in nature, i.e. occur naturally. The natural amino acids are as follows: alanine, arginine, glycine, asparagine, aspartic acid, cysteine, glutamine, glutamic acid, serine, threonine, histidine, lysine, methionine, proline, valine, isoleucine, leucine, tyrosine, tryptophan, and phenylalanine. This application adheres to the IUPAC rules of standard abbreviations for amino acids.

[0040] A conservative substitution, as known to one of ordinary skill in the art, refers to a complete replacement of an amino acid residue with a different residue having similar biochemical characteristics, such as size, charge, polarity, etc. For instance, the aromatic Tyrosine may be conservatively substituted with aromatic phenylalanine, or basic Arginine may be conservatively substituted with basic Lysine. TABLE 1A and 1B show non-limiting examples of conservative amino acid substitutions.

[0041] **TABLE 1A**

Original Residue	**Conservative Substitutions**
Ala (A)	Cys, Gly, Ser, Thr, Val
Arg (R)	Asn, Gln, Glu, His, Lys
Asn (N)	Arg, Asp, Gln, Glu, His, Lys, Ser,

	Thr
Asp (D)	Asn, Gln, Glu, Ser
Cys (C)	Ala, Ser
Gln (Q)	Arg, Asn, Asp, Glu, His, Lys, Met, Ser
Glu (E)	Arg, Asn, Asp, Gln, His, Lys, Ser
Gly (G)	Ala, Ser, Glu, Asp
Ile (I)	Leu, Met, Phe, Val
Leu (L)	Ile, Met, Phe, Val
Lys (K)	Arg, Asn, Gln, Glu, Ser
Met (M)	Gln, Ile, Leu, Phe, Val
Phe (F)	Ile, Leu, Met, Trp, Tyr
Pro (P)	None
Ser (S)	Ala, Asn, Asp, Gln, Glu, Gly, Lys,

	Thr
Thr (T)	Ala, Asn, Ser, Val
Trp (W)	Phe, Tyr
Tyr (Y)	His, Phe, Trp,
Val (V)	Ala, Ile, Leu, Met, Thr

[0042] **TABLE 1B**

Amino Acid Property	**Amino Acid Substitutions**
Hydrophobic	Cys, Ile, Leu, Met, Phe, Pro, Trp, Val
Aliphatic	Ala, Ile, Leu, Pro, Val
Aromatic	His, Phe, Trp, Tyr
Amide	Asn, Gln
Nucleophilic	Cys, Ser, Thr

Polar	Arg, Asp, Asn, Gln, Glu, Lys
Negative	Asp, Glu
Positive	Arg, Lys, His
Small	Ala, Gly, Pro, Ser
C-beta	Ile, Thr, Val

[0043] As used herein, "micelle" and "nanoparticle" may be used interchangeably and refer to self-assembled molecules. In some embodiments, a nanoparticle describes a micelle of a particular size (i.e., nanoscale micelle).

[0044] The present invention features biopolymers comprising antimicrobial peptides (AMPs), as well as applications of use, methods of synthesis, and compositions for synthesis. The present invention provides compositions (e.g., a material platform) that stabilize AMPs and helps improve the ability to use AMPs as therapeutic agents for treating infections, e.g., bacterial infections, fungal infections, parasitic infections, viral infections, infections associated with antibiotic-resistant bacteria or antifungal-resistant fungi or antiviral-resistant viruses, biological warfare agents (BWAs) such as *Bacillus anthracis* and *Yersenia pestis*, etc. The biopolymers of the present invention may be used to kill or reduce the growth of the particular microbe or infectious agent (e.g., bacteria, fungus, parasite, virus, etc.).

[0045] Certain embodiments herein, e.g., compositions herein, may comprise an elastin-like

peptide (ELP), an antimicrobial peptide (AMP) and a hydrophilic protein tether connecting the ELP and the AMP. In some embodiments, the ELP comprises one or more pentapeptide repeats consecutively linked. In other embodiments, at least one of the pentapeptide repeats comprises a tyrosine residue. In some embodiments, protein tether connects to the AMP at the AMP's N-terminus, C-terminus, or both. In further embodiments, the ELP is more hydrophobic than the protein tether. In further embodiments, the composition described herein self-assembles into nanoparticles

[0046] In some embodiments, the one or more pentapeptide repeat is according to the formula $(WaaPXaaYaaG \text{ (SEQ ID NO: 2)})_m$, where Waa is valine, isoleucine or leucine, where Xaa is any amino acid, where Yaa is any amino acid except for proline, and where m is 10 to 400. In other embodiments, the one or more pentapeptide repeat is according to the formula $(VPGXaaG \text{ (SEQ ID NO: 1)})_m$, where Xaa is any amino acid except for proline and where m is from 10 to 400.

[0047] In further embodiments, the one or more pentapeptide repeats is selected from a group consisting of: SEQ ID NO: 3, SEQ ID NO: 4, SEQ ID NO: 5, SEQ ID NO: 6, SEQ ID NO: 7, SEQ ID NO: 8, SEQ ID NO: 9, SEQ ID NO: 10, SEQ ID NO: 11, SEQ ID NO: 12, SEQ ID NO: 13, SEQ ID NO: 14, SEQ ID NO: 15, SEQ ID NO: 16, SEQ ID NO: 17, SEQ ID NO: 18, SEQ ID NO: 19, SEQ ID NO: 20, SEQ ID NO: 21, SEQ ID NO: 22, SEQ ID NO: 23, SEQ ID NO: 24, SEQ ID NO: 25, SEQ ID NO: 26, SEQ ID NO: 27, SEQ ID NO: 28, SEQ ID NO: 29, SEQ ID NO: 30, SEQ ID NO: 31, SEQ ID NO: 32, SEQ ID NO: 33, SEQ ID NO: 34, SEQ ID NO: 35, SEQ ID NO: 36, SEQ ID NO: 37, SEQ ID NO: 38, SEQ ID NO: 39, SEQ ID NO: 40, and SEQ ID NO: 41. In certain embodiments, the one or more pentapeptide repeats comprising the tyrosine is selected from a group consisting of SEQ ID NO: 3, SEQ ID NO: 24, SEQ ID NO: 25, SEQ ID NO: 26, SEQ ID NO: 27, SEQ ID NO: 28, SEQ ID NO: 30, EQ ID NO: 32, SEQ ID NO: 33, SEQ

ID NO: 34, SEQ ID NO: 36, SEQ ID NO: 38, SEQ ID NO: 39, and SEQ ID NO: 40.

[0048] In some embodiments, the tyrosine residues are cross-linked to form a self-standing film, a membrane material, or a hydrogel. In some embodiments, the tyrosine residue allows the composition to adhere to a surface after hydroxylation. In other embodiments, the tyrosine residue allows the composition to adhere to a surface after hydroxylation by tyrosinase. In some embodiments, the surface is a cloth, a plastic, a glass, a metal, or a combination thereof. In other embodiments, the surface is a medical device, a dressing, a clothing, or a combination thereof.

[0049] The present invention discloses AMP-biopolymer compositions and methods for synthesizing the AMP-biopolymer compositions by integrating the synthesis of the AMP, the tether, and a biomaterial. To enable this approach, the biomaterial (platform, scaffold) may need to be able to transform into self-assembled nanoparticles, into adhesives to form a coating, and/or cross-link to form a film, gel, filter, antimicrobial clothing material, etc. The biopolymer may also need to contain a region that behaves structurally and physically similar to polymer tethers for enhanced AMP activity and stability.

[0050] The AMP biopolymer compositions (e.g., platforms, scaffolds) feature (1) a biocompatible scaffold (e.g., elastin-like polypeptide (ELP), resilin-like polypeptide (RLP), etc.); (2) a protein tether, and (3) an AMP. Without wishing to limit the present invention to any theory or mechanism, it is believed that the ELP platform is advantageous because of its tractability to transform into many types of biomaterials: (i) biocompatible ELP self-assembles into nanoparticles when heated above its phase-transitioning temperature (T_t), (ii) covalently bonded Tyr residues can form a self-standing film or membrane, and (iii) Tyr hydroxylation allows Tyr-containing materials to strongly adhere to surfaces. FIG. 1 illustrates the overall strategy of the compositions (e.g., ELPs) herein,

wherein AMP biopolymers can be designed and synthesized as a single unit. A gene is designed to yield a particular ELP (e.g., ELP(Tyr)) linked to a tether linked to an AMP, wherein the whole unit is called the biopolymer. Because the biopolymer is designed at the genetic level, modification of the components can be made by altering the nucleic acid sequence that encodes the biopolymer through genetic engineering. The biopolymer can self-assemble, e.g., to create a nanoparticle drug. In some embodiments, the tyrosine residues are utilized for photo-crosslinking or for attaching to surfaces such as but not limited to medical device surfaces or clothing, or for creating a biofilm for applications such as wound dressings.

Elastin-Like Polypeptide (ELP) Scaffold

[0051] As used herein, "elastin-like polypeptides (ELPs)" refer to a class of artificial, disordered polypeptide polymers comprising repeats of short peptide motifs. For example, an ELP may comprise pentapeptide repeat units (e.g., VPGXaaG (SEQ ID NO: 1)—where Xaa can be any amino acid except proline. In some embodiments, ELPs are based on the sequence of an elastin protein, an extracellular matrix protein that provides elasticity to tissues such as arteries, lungs, and skin. In other embodiments, the ELPs are derived from the hydrophobic domain of tropoelastin.

[0052] In some embodiments, the scaffold component of the AMP biopolymer compositions described herein may comprise an elastin-like polypeptide (ELP). In some embodiments, the ELP comprises pentapeptide repeats such as $(VPGXaaG (SEQ ID NO: 1))_m$, where Xaa is any amino acid except for proline and where m is from 10 to 400. In some embodiments, when two or more pentapeptide repeats such as $(VPGXaaG (SEQ ID NO: 1))_m$ are consecutively linked together Xaa may be one or a plurality of amino acids (not including proline) (e.g., polar amino acids, non-polar

amino acids, charged amino acids, or a combination thereof). For example, an ELP may comprise the sequence ((VPGXaaG (SEQ ID NO: 1))$_m$(VPGXaaG (SEQ ID NO: 1))$_m$), where both Xaa are the same amino acid (e.g., Y; i.e., ((VPG**Y**G (SEQ ID NO: 3))$_m$(VPG**Y**G (SEQ ID NO: 3))$_m$), or where the Xaa are two different amino (e.g., Y and A; i.e., ((VPG**Y**G (SEQ ID NO: 3))$_m$(VPG**A**G (SEQ ID NO: 4))$_m$). In other embodiments, the ELP comprises a pentapeptide repeats such as (WaaPXaaYaaG (SEQ ID NO: 2))$_m$, where Waa in position 1 is valine, isoleucine or leucine, where Xaa in position 3 is any amino acid, where Yaa in position 4 is any amino acid except for proline, and where m is 10 to 400.

[0053] In certain embodiments, m is 10. In other embodiments, m is a number from 10 to 15, or from 10 to 20, or from 10 to 25, or from 10 to 50, or from 10 to 100, or from 10 to 150, or from 10 to 200, or from 10 to 250, or from 10 to 300, or from 10 to 350, or from 10 to 400, or from 10 to 450. In certain embodiments, m is 15. In other embodiments, m is a number from 15 to 20, or from 15 to 25, or from 15 to 50, or from 15 to 100, or from 15 to 150, or from 15 to 200, or from 15 to 250, or from 15 to 300, or from 15 to 350, or from 15 to 400, or from 15 to 450. In certain embodiments, m is 20. In other embodiments, m is a number from 20 to 25, or from 20 to 50, or from 20 to 100, or from 20 to 150, or from 20 to 200, or from 20 to 250, or from 20 to 300, or from 20 to 350, or from 20 to 400, or from 20 to 450.

[0054] In certain embodiments, m is 25. In some embodiments, m is a number from 25 to 50. In some embodiments, m is a number from 25 to 100. In some embodiments, m is a number from 25 to 150. In some embodiments, m is a number from 25 to 200. In some embodiments, m is a number from 25 to 250. In some embodiments, m is a number from 25 to 300. In some embodiments, m is a number from 25 to 350. In some embodiments, m is a number from 25 to 400. In some embodiments, m is a number from 25 to 450.

[0055] In certain embodiments, m is 50. In some embodiments, m is a number from 50 to 100. In some embodiments, m is a number from 50 to 150. In some embodiments, m is a number from 50 to 200. In some embodiments, m is a number from 50 to 250. In some embodiments, m is a number from 50 to 300. In some embodiments, m is a number from 50 to 350. In some embodiments, m is a number from 10 to 400. In some embodiments, m is a number from 50 to 450.

[0056] In certain embodiments, m is 100. In other embodiments, m is a number from 100 to 150, or from 100 to 200, or from 100 to 250, or from 100 to 300, or from 100 to 350, or from 100 to 400, or from 100 to 450. In certain embodiments, m is 150. In other embodiments, m is a number from 150 to 200, or from 150 to 250, or from 150 to 300, or from 150 to 350, or from 150 to 400, or from 150 to 450. In certain embodiments, m is 200. In other embodiments, m is a number from 200 to 250, or from 200 to 300, or from 200 to 350, or from 200 to 400, or from 200 to 450. In certain embodiments, m is 250. In other embodiments, m is a number from 250 to 300, or from 250 to 350, or from 250 to 400, or from 250 to 450. In certain embodiments, m is 300. In other embodiments, m is a number from 300 to 350, or from 300 to 400, or from 300 to 450. In certain embodiments, m is 350. In other embodiments, m is a number from 350 to 400, or from 350 to 450. In certain embodiments, m is 400. In other embodiments, m is a number from 400 to 450.

[0057] In some embodiments, m is a number from 100 to 200. In some embodiments, m is a number from 200 to 300. In some embodiments, m is a number from 10 to 400 or more. In some embodiments, m = 3x, wherein x is a number from 1 to100, e.g., x = 1 and m = 3; x = 2 and m = 6; x = 20 and m = 60; x = 50 and m = 150; x = 60 and m = 180; etc. The present invention is not limited to the aforementioned values for m.

[0058] In some embodiments, the number of pentapeptide repeats (i.e., the aforementioned m

variable and the below mentioned n variable) are chosen such that the resulting ELP has a preferred size of about 100 kg/mol. In other embodiments, the preferred size of the ELP is ≤ 100 kg/mol. In certain embodiments, the maximum size of the ELP is 150-200 kg/mol. In further embodiments, the minimum size of the ELP is 10 kg/mol. In other embodiments, the number of pentapeptide repeats (i.e., the aforementioned m variable) is chosen such that the resulting ELP has a size of about 10 kg/mol to 50 kg/mol, or about 10 kg/mol to 100 kg/mol, or about 10 kg/mol to 125 kg/mol, or about 10 kg/mol to 150 kg/mol, or about 10 kg/mol to 175 kg/mol, or about 10 kg/mol to 200 kg/mol, or about 10 kg/mol to 225 kg/mol, or about 10 kg/mol to 250 kg/mol, or about 100 kg/mol to 125 kg/mol, or about 100 kg/mol to 150 kg/mol, or about 100 kg/mol to 175 kg/mol, or about 100 kg/mol to 200 kg/mol, or about 100 kg/mol to 225 kg/mol, or about 100 kg/mol to 250 kg/mol, or about 125 kg/mol to 150 kg/mol, or about 125 kg/mol to 175 kg/mol, or about 125 kg/mol to 200 kg/mol, or about 125 kg/mol to 225 kg/mol, or about 125 kg/mol to 250 kg/mol, or about 150 kg/mol to 175 kg/mol, or about 150 kg/mol to 200 kg/mol, or about 150 kg/mol to 225 kg/mol, or about 150 kg/mol to 250 kg/mol, or about 175 kg/mol to 200 kg/mol, or about 175 kg/mol to 225 kg/mol, or about 175 kg/mol to 250 kg/mol, or about 200 kg/mol to 225 kg/mol, or about 200 kg/mol to 250 kg/mol, or about 225 kg/mol to 250 kg/mol.

[0059] **Table 2:** Shows non-limiting examples of pentapeptide repeats that could be as an ELP in the AMP biopolymer compositions as described herein:

Pentapeptide Repeat	**SEQ ID NO:**		**Pentapeptide Repeat**	**SEQ ID NO:**
$(VPGYG)_m$	3		$(VGGVG)_m$	22

$(VPGAG)_m$	4		$(KGGVG)_m$	23
$(VPGSG)_m$	5		$(VPYGG)_m$	24
$(VPGGG)_m$	6		$(VPYVG)_m$	25
$(VPGRG)_m$	7		$(VPYNG)_m$	26
$(VPGNG)_m$	8		$(VPYCG)_m$	27
$(VPGDG)_m$	9		$(VPYLG)_m$	28
$(VPGCG)_m$	10		$(VPNGG)_m$	29
$(VPGQG)_m$	11		$(IPGYG)_m$	30
$(VPGEG)_m$	12		$(IPGVG)_m$	31
$(VPGHG)_m$	13		$(IPYGG)_m$	32
$(VPGIG)_m$	14		$(IPYVG)_m$	33
$(VPGLG)_m$	15		$(IPYLG)_m$	34
$(VPGKG)_m$	16		$(IPNGG)_m$	35

$(VPGMG)_m$	17		$(LPGYG)_m$	36
$(VPGFG)_m$	18		$(LPGVG)_m$	37
$(VPGTG)_m$	19		$(LPYGG)_m$	38
$(VPGWG)_m$	20		$(LPYVG)_m$	39
$(VPGVG)_m$	21		$(LPYLG)_m$	40
			$(LPNGG)_m$	41
where m is from 10 to 400.				

[0060] In some embodiments, the ELP of the AMP biopolymer compositions as described herein may comprise one or more pentapeptide repeats (see Table 2) consecutively linked. In other embodiments, the one or more pentapeptide repeats may comprise varying m values. For example, an ELP may comprise the sequence $((VPGYG\ (SEQ\ ID\ NO:\ 3))_{10}(VPGAG\ (SEQ\ ID\ NO:\ 4))_{20})_n$, where n is 1 to 14. In some embodiments, the pentapeptide repeats may be arranged in various configurations to create an ELP. For example, $((SEQ\ ID\ NO:\ 1)_m(SEQ\ ID\ NO:\ 3)_m(SEQ\ ID\ NO:\ 1)_m)_n$, or $((SEQ\ ID\ NO:\ 1)_m(SEQ\ ID\ NO:\ 24)_m(SEQ\ ID\ NO:\ 1)_m)_n$, or $((SEQ\ ID\ NO:\ 1)_m(SEQ\ ID\ NO:\ 30)_m(SEQ\ ID\ NO:\ 1)_m)_n$, or $((SEQ\ ID\ NO:\ 1)_m(SEQ\ ID\ NO:\ 33)_m(SEQ\ ID\ NO:\ 1)_m)_n$, or $((SEQ\ ID\ NO:\ 1)_m(SEQ\ ID\ NO:\ 36)_m(SEQ\ ID\ NO:\ 1)_m)_n$, or $((SEQ\ ID\ NO:\ 1)_m(SEQ\ ID\ NO:$

39)$_m$(SEQ ID NO: 1)$_m$)$_n$, or ((SEQ ID NO: 2)$_m$(SEQ ID NO: 3)$_m$(SEQ ID NO: 2)$_m$)$_n$, or ((SEQ ID NO: 2)$_m$(SEQ ID NO: 24)$_m$(SEQ ID NO: 2)$_m$)$_n$, or ((SEQ ID NO: 2)$_m$(SEQ ID NO: 30)$_m$(SEQ ID NO: 2)$_m$)$_n$, or ((SEQ ID NO: 2)$_m$(SEQ ID NO: 33)$_m$(SEQ ID NO: 2)$_m$)$_n$, or ((SEQ ID NO: 2)$_m$(SEQ ID NO: 36)$_m$(SEQ ID NO: 2)$_m$)$_n$, or ((SEQ ID NO: 2)$_m$(SEQ ID NO: 39)$_m$(SEQ ID NO: 2)$_m$)$_n$, or ((SEQ ID NO: 2)$_m$(SEQ ID NO: 40)$_m$(SEQ ID NO: 2)$_m$)$_n$, where m is 10-400 and n is 10-400.

[0061] In the subsequent examples of ELP formulas shown below, it is noted that the pentapeptide repeats comprising the ELP are shown with varying m values. Therefore for ease of understanding m has been expanded to include j, k, and l. For example, (VPGAG (SEQ ID NO: 4))$_{\mathbf{m}}$(VPGYG (SEQ ID NO: 3))$_{\mathbf{m}}$(VPGAG (SEQ ID NO: 4))$_{\mathbf{m}}$ is the same as (VPGAG (SEQ ID NO: 4))$_{\mathbf{j}}$(VPGYG (SEQ ID NO: 3))$_{\mathbf{k}}$(VPGAG (SEQ ID NO: 4))$_{\mathbf{l}}$ or ELP($A_jY_kA_l$) (as shown below).

[0062] In some embodiments, the ELP comprises the formula ELP($X_jY_kX_l$)$_n$, wherein X is SEQ ID NO: 1 (VPGXaaG), and Y is SEQ ID NO: 3 (VPGYG). Thus, the ELP may comprise the formula [(VPGXaaG)$_j$(VPGYG)$_k$(VPGXaaG)$_l$]$_n$, e.g., [(SEQ ID NO: 1)$_j$(SEQ ID NO: 3)$_k$(SEQ ID NO: 1)$_l$]$_n$. For example, in some embodiments, Xaa is alanine and the formula is ELP($A_jY_kA_l$)$_n$, which = [(VPGAG)$_j$(VPGYG)$_k$(VPGAG)$_l$]$_n$ (wherein VPGAG is SEQ ID NO: 4).

[0063] In some embodiments, Xaa is serine and the formula is ELP($S_jY_kS_l$)$_n$, which = [(VPGSG)$_j$(VPGYG)$_k$(VPGSG)$_l$]$_n$ (wherein VPGSG is SEQ ID NO: 5). Xaa is not limited to serine or alanine. In some embodiments, Xaa is glycine (and the formula is ELP($G_jY_kG_l$)$_n$). In some embodiments, Xaa is arginine (and the formula is ELP($R_jY_kR_l$)$_n$). In some embodiments, Xaa is asparagine (and the formula is ELP($N_jY_kN_l$)$_n$). In some embodiments, Xaa is aspartic acid (and the formula is ELP($D_jY_kD_l$)$_n$). In some embodiments, Xaa is cysteine (and the formula is ELP($C_jY_kC_l$)$_n$). In some embodiments, Xaa is glutamine (and the formula is ELP($Q_jY_kQ_l$)$_n$). In

some embodiments, Xaa is glutamic acid (and the formula is $ELP(E_jY_kE_l)_n$). In some embodiments, Xaa is histidine (and the formula is $ELP(H_jY_kH_l)_n$). In some embodiments, Xaa is isoleucine (and the formula is $ELP(I_jY_kI_l)_n$). In some embodiments, Xaa is leucine (and the formula is $ELP(L_jY_kL_l)_n$). In some embodiments, Xaa is lysine (and the formula is $ELP(K_iY_kK_l)_n$). In some embodiments, Xaa is methionine (and the formula is $ELP(M_jY_kM_l)_n$). In some embodiments, Xaa is phenylalanine (and the formula is $ELP(F_jY_kF_l)_n$). In some embodiments, Xaa is threonine (and the formula is $ELP(T_jY_kT_l)_n$). In some embodiments, Xaa is tryptophan (and the formula is $ELP(W_iY_kW_l)_n$). In some embodiments, Xaa is tyrosine (and the formula is $ELP(Y_jY_kY_l)_n$). In some embodiments, Xaa is valine (and the formula is $ELP(V_jY_kV_l)_n$).

[0064] In some embodiments, ranges for j, k, and l for the pentapeptide repeats depend on the hydrophobicity of the amino acids in the selected pentapeptide repeats. In some embodiments, the variables j, k, and l are equivalent to the m variable and thus may be any number that m is equal to.

[0065] For example, in certain embodiments, the variables j, k, or l are 10. In other embodiments, the variables j, k, and l are a number from 10 to 15, or from 10 to 20, or from 10 to 25, or from 10 to 50, or from 10 to 100, or from 10 to 150, or from 10 to 200, or from 10 to 250, or from 10 to 300, or from 10 to 350, or from 10 to 400, or from 10 to 450. In certain embodiments, the variables j, k, or l are 15. In other embodiments, the variables j, k, or l are a number from 15 to 20, or from 15 to 25, or from 15 to 50, or from 15 to 100, or from 15 to 150, or from 15 to 200, or from 15 to 250, or from 15 to 300, or from 15 to 350, or from 15 to 400, or from 15 to 450. In certain embodiments, the variables j, k, or l are 20. In other embodiments, the variables j, k, or l are a number from 20 to 25, or from 20 to 50, or from 20 to 100, or from 20 to 150, or from 20 to 200, or from 20 to 250, or from 20 to 300, or from 20 to 350, or from 20 to 400, or from 20 to 450.In

certain embodiments, the variables j, k, or l are 25. In some embodiments, the variables j, k, or l are a number from 25 to 50, or from 25 to 100, or from 25 to 150, or from 25 to 200 or from 25 to 250, or from 25 to 300, or from 25 to 350, or from 25 to 400 or from 25 to 450.In certain embodiments, the variables j, k, or l are 50. In some embodiments, the variables j, k, or l are a number from 50 to 100 or from 50 to 150 or from 50 to 200, or from 50 to 250, or from 50 to 300, or from 50 to 350, or from 10 to 400, or from 50 to 450.

[0066] In certain embodiments, the variables j, k, or l are 100. In other embodiments,the variables j, k, or l are a number from 100 to 150, or from 100 to 200, or from 100 to 250, or from 100 to 300, or from 100 to 350, or from 100 to 400, or from 100 to 450. In certain embodiments, the variables j, k, or l are 150. In other embodiments, the variables j, k, or l are a number from 150 to 200, or from 150 to 250, or from 150 to 300, or from 150 to 350, or from 150 to 400, or from 150 to 450. In certain embodiments, the variables j, k, or l are 200. In other embodiments, the variables j, k, or l are a number from 200 to 250, or from 200 to 300, or from 200 to 350, or from 200 to 400, or from 200 to 450. In certain embodiments, the variables j, k, or l are 250. In other embodiments, the variables j, k, or l are a number from 250 to 300, or from 250 to 350, or from 250 to 400, or from 250 to 450. In certain embodiments, the variables j, k, or l are 300. In other embodiments, the variables j, k, or l are a number from 300 to 350, or from 300 to 400, or from 300 to 450. In certain embodiments, the variables j, k, or l are 350. In other embodiments, the variables j, k, or l are a number from 350 to 400, or from 350 to 450. In certain embodiments, the variables j, k, or l are 400. In other embodiments, the variables j, k, or l are a number from 400 to 450.

[0067] In further embodiments, j = 1, 2, 3, 4, 5, 6, etc. In some embodiments, k = 1, 2, 3, 4, 5, 6, etc. In some embodiments, l = 1, 2, 3, 4, 5, 6, etc.

[0068] In some embodiments, n is greater than 10. In other embodiments, n is less than 400. In certain embodiments, n is 10. In other embodiments, n is a number from 10 to 450, or from 10 to 400, or from 10 to 350, or from 10 to 300, or from 10 to 250, or from 10 to 200, or from 10 to 150, or from 10 to 100, or from 10 to 50. In certain embodiments, n is 50. In other embodiments, n is a number from 50 to 450, or from 50 to 400, or from 50 to 350, or from 50 to 300, or from 50 to 250, or from 50 to 200, or from 50 to 150, or from 50 to 100. In certain embodiments, n is 100. In other embodiments, n is a number from 100 to 450, or from 100 to 400, or from 100 to 350, or from 100 to 300, or from 100 to 250, or from 100 to 200, or from 100 to 150. In certain embodiments, n is 150. In other embodiments, n is a number from 150 to 450, or from 150 to 400, or from 150 to 350, or from 150 to 300, or from 150 to 250, or from 150 to 200. In certain embodiments, n is 200. In other embodiments, n is a number from 200 to 450, or from 200 to 400, or from 200 to 350, or from 200 to 300, or from 200 to 250. In certain embodiments, n is 250. In other embodiments, n is a number from 250 to 450, or from 250 to 400, or from 250 to 350, or from 250 to 300. In certain embodiments, n is 300. In other embodiments, n is a number from 300 to 450, or from 300 to 400, or from 300 to 350. In certain embodiments, n is 350. In other embodiments, n is a number from 350 to 450, or from 350 to 400. In certain embodiments, n is 400. In other embodiments, n is a number from 400 to 450.

[0069] In further embodiments, n = 1, 2, 3, 4, 5, 6, 7, 8, 9, 10, 11, 12, 13, 14, 15, 16, 17, 18, 19, 20, 21, 22, 23, 24, 25, 26, 27, 28, 29, 30, 31, 32, 33, 34, 35, 36, 37, 38, 39, 40, 41, 42, 43, 44, 45, 46, 47, 48, 49, 50, more than 50 etc.

[0070] In some embodiments, the variable for the ELP (e.g., ((pentapeptide repeats)$_j$(pentapeptide repeats)$_k$(pentapeptide repeats)$_l$)$_n$, where the variables are j, k, l and n) are selected such that $10 \leq ((j+k+l) \times n) \leq 400$. In some embodiments, the variable for the ELP (e.g., ((pentapeptide

repeats)$_j$(pentapeptide repeats)$_k$(pentapeptide repeats)$_l$)$_n$, where the variables are j, k, l and n) are selected according to the formula $10 \leq ((j+k+l) \times n) \leq 400$.

[0071] Without wishing to limit the present invention to any theory or mechanism, n may be determined based on what works well for purification processes, e.g., n may need to be large enough for purification. However, n is not limited to any particular number. In some embodiments, n is 3 or more, 4 or more, 5 or more, etc., e.g., in some embodiments, n = 4, 5, 6, 7, 8, 9, 10, 11, 12, 13, 14, 15, 16, 17, 18, 19, 20, 21, 22, 23, 24, 25, 26, 27, 28, 29, 30, 31, 32, 33, 34, 35, 36, 37, 38, 39, 40, 41, 42, 43, 44, 45, 46, 47, 48, 49, 50, more than 50, etc.

[0072] In some embodiments, the n variable (and the aforementioned m variable) is chosen such that the resulting ELP has a preferred size of about 100 kDa to 150 kDa. In some embodiments, the n variable and the aforementioned m variable) is chosen such that the resulting ELP has a size of about 10 kDa to 250 kDa, or about 10 kDa to 200 kDa, or about 10 kDa to 150 kDa, or about 10 kDa to 100 kDa, or about 10 kDa to 50 kDa, or about 10 kDa to 25 kDa, 25 kDa to 250 kDa, or about 25 kDa to 200 kDa, or about 25 kDa to 150 kDa, or about 25 kDa to 100 kDa, or about 25 kDa to 50 kDa, or about 50 kDa to 250 kDa, or about 50 kDa to about 200 kDa, or about 50 kDa to about 150 kDa, or about 50 kDa to about 100 kDa, or about 100 kDa to 250 kDa, or about 100 kDa to about 200 kDa, or about 100 kDa to about 150 kDa, or about 150 kDa to 250 kDa, or about 150 kDa to about 200 kDa, or about 200 kDa to 250 kDa.

[0073] In some embodiments, n is from 10 to 400. In other embodiments, n is greater than 10 and less than 400. In further embodiments, the ELP formula comprises $10 \leq (j + k + l) \times n \leq 400$. In some embodiments, the ELP formula comprises $10 \leq (j + k + l) \times n \leq 450$.

[0074] In some embodiments, the ELP comprises tyrosine residues (ELP(Tyr)) $(VPGYG)_m$SEQ

ID NO: 3)). In some embodiments, an ELP comprising a pentapeptide repeat comprising a tyrosine residue (Y) allows for it to be photo-crosslinked to ultimately create a hydrogel or biopolymer material.

[0075] The T_t of an ELP is adjustable by combining polar and non-polar amino acids in the non-conserved X_{aa} position, and controlling the ELP molar masses. An ELP with Tyr and Ala or Tyr and Ser residues in the X_{aa} position of SEQ ID NO: 1 is shown in Table 3 below. Note that ELP $(A_2Y_1A_2)_{36}$ = $[(VPGAG)_2(VPGYG)_1(VPGAG)_2]_{36}$ (Xaa is alanine). ELP $(S_2Y_1S_2)_{36}$ = $[(VPGSG)_2(VPGYG)_1(VPGSG)_2]_{36}$ (Xaa is serine). ELP $(S_2Y_1S_1)_{45}$ = $[(VPGSG)_2(VPGYG)_1(VPGSG)_1]_{45}$ (Xaa is serine). ELP $(A_2Y_1A_1)_{45}$ = $[(VPGAG)_2(VPGYG)_1(VPGAG)_1]_{45}$ (Xaa is alanine).

[0076] In some embodiments, an ELP has high conformational flexibility at low temperatures such that it appears clear and has a disordered molten globule aggregate at higher temperatures such that it appears cloudy (see FIG. 4)

Table 3. Proposed ELP(Tyr) sequences and their expected and experimental transition temperature (T_t)

ELP (Tyr)	**$T_{t,\ expected}$**	**Number of ELP pentapeptide (m)**	**$T_{t,\ experimental}$ of ELP (Tyr)**
ELP $(A_2Y_1A_2)_{36}$	25°C	180	25°C
ELP	29°C	180	29°C (expected)

$(S_2Y_1S_2)_{36}$			
ELP $(S_2Y_1S_1)_{45}$	24°C	180	TBD
ELP $(A_2Y_1A_1)_{45}$	20°C	180	TBD

[0077] Expected T_t ($T_{t,expected}$) and Experimental T_t ($T_{t,experimental}$) are according to previous research by Ingrole, R., Tao et al. "*Synthesis and Immunogenicity Assessment of Elastin-Like Polypeptide-M2e Construct as an Influenza Antigen*" Nano Life, 2014. These results were obtained using alanine in the Xaa position instead of serine, e.g. ELP$(A_2Y_1A_2)_n$ vs. ELP$(S_2Y_1S_2)_n$. The expected T_t ($T_{t,expected}$) of ELP$(A_2Y_1A_2)_n$ matched the experimental T_t ($T_{t,experimental}$) when the number of ELP pentapeptide repeats were 180 (n = 36). The T_t of the ELP can be changed when fused to AMPs but the larger ELP$(A_2Y_1A_2)_{36}$ had less change in T_t when fused to a hydrophilic peptide relative to the smaller ELP$(A_2Y_1A_2)_{24}$.

[0078] The ELPs herein were designed based on ELP(Tyr) sequences with the same number of ELP pentapeptide repeats (to similarly match the $T_{t,experimental}$ of ELP(Tyr) with the $T_{t,expected}$ (see Table 3). The sequence variants facilitate: (i) T_t of ELP(Tyr) between room temperature (RT) and body temperature (BT) when fused with amphiphilic AMPs; and (ii) investigation of the relationship between AMP activity and the quantity of Tyr residues, which influences the strength of the film/coating materials. LL37 is a cationic, amphiphilic, antimicrobial peptide, composed of 37 amino acids. The present invention provides a fusion of the LL37 peptide to the C-terminus of ELP(Tyr): ELP(Tyr)-LL37. LL37 can damage microbial membranes, including *E.coli* and *S.*

aureus, via carpet or toroidal models. Solid-state NMR spectroscopy revealed that LL37 forms dimer or tetramer oligomer structures like the Barrel-Stave pore model when they bind to the membrane. Since LL37 covers the most-widely accepted microbe lysis mechanisms, it was chosen as a representative model of AMP lysis activity as part of the artificial protein.

[0079] The short ELP$(S_2Y_1S_2)_8$–LL37 gene was designed with multiple restriction enzyme sites for gene editing. The gene was cloned into a protein expression vector (see FIG. 1 for a schematic view) and was produced in *E. coli*. The T_t of ELP$(S_2Y_1S_2)_8$–LL37 was too high to apply non-chromatographic T_t purification (> 70ºC). Its size was confirmed by metal ion affinity chromatography by attaching the affinity tag to the protein (see FIG. 3). FIG. 2A shows SDS-PAGE analysis of $(S_2Y_1S_2)_8$–LL37 purified by Ni-NTA chromatography methods. FIG. 2B shows SDS-PAGE analysis of ELP$(A_1Y_1A_1)_{24}$-LL37 purified by inverse transition cycling methods. FIG. 2C shows UV/Vis spectrophotometer analysis of the phase-transitioning temperatures of ELP$(A_2Y_1A_2)_{24}$ and ELP$(A_2Y_1A_2)_{36}$, respectively.

[0080] The size of the ELP was doubled using the golden gate cloning method, and the phase transition of ELP was captured by decreasing the T_t in a solution with high salt concentration (see FIG. 3). This approach did not work with the shorter ELP, indicating larger ELPs exhibit lower $T_{t,experimental}$ and more closely matched $T_{t,expected}$. Without wishing to limit the present invention to any theory or mechanism, ELP(Tyr)-LL37 proteins may reach the target T_t and facilitate non-chromatographic ELP-fusion protein purification by using the inverse transition cycling (ITC) method that utilizes ELP phase changes above and below its T_t (see FIG. 3).

[0081] Inexpensive purification of elastin-like polypeptides (ELP), including ELP(Tyr) and biopolymers containing ELP is carried out through the Inverse Transition Cycling (ITC) method

by utilizing the ELP phase change behavior, where ELP phase changes occur at its transition temperature (T_t). T_t is determined by the polarity of amino acids in the Xaa position and quantity of pentapeptide repeats in ELP. Below its T_t, ELP is soluble and above its T_t, ELP is insoluble. The ITC method to purify an ELP mixture is carried out by first centrifuging the ELP mixture at a temperature below T_t when ELP is soluble and discarding the pellet. This removes insoluble impurities when ELP is soluble. Next, the temperature of the ELP mixture is raised above T_t causing ELPs to display increased hydrophobic behavior, aggregate and collapse from solution. The ELP mixture is then centrifuged, and the soluble portion is removed. This removes soluble impurities when ELP is insoluble. Repeating this process several times yields highly pure ELP as many impurities cannot reversibly precipitate and dissolve in solutions.
To capture target proteins, chromatography often requires expensive columns as in ion-exchange or size exclusion, or peptide tags (e.g. His-Tag, Strep-Tag, etc.) on the protein as well as expensive beads (e.g. Ni-NTA beads) used for binding. ITC purification is a less expensive option because it simply requires heating, cooling and centrifugation.

[0082] FIG. 4 shows a hydrogel made of cross-linked ELP$(A_2Y_1A_2)_{24}$ showing hydrogel thermoresponsive behavior where the hydrogel is clear below the transition temperature (e.g., below 25°C, left panel) and cloudy above the transition temperature (e.g., above 25°C, right panel).

[0083] By genetically fusing AMP to an ELP, *E. coli* host expression, and ITC purification, ELP-AMP can be produced at low cost. T_t behavior of the ELP may depend on environmental factors such as temperature, pH and salt concentrations.

[0084] The present invention is not limited to the aforementioned ELPs, e.g., ELP(Tyr). For example, in some embodiments, the ELP comprises ELP(DOPA) after Tyr hydroxylation by

tyrosinase.

[0085] In some embodiments, the ELP sequence needs to be more hydrophobic than the protein tether. For example, the ratio of hydrophobic to hydrophilic amino acids in ELP needs to be greater than the ratio of hydrophobic to hydrophilic amino acids in the protein tether. In some embodiments, hydrophobic amino acids comprise Valine (Val or V), Isoleucine (Ile or I), Leucine (Leu or L), Methionine (Met or M), Phenylalanine (Phe or F), Tryptophan (Trp or W), Cysteine (Cys or C). In other embodiments, the remaining amino acids (i.e., those not mentioned above) can be considered as hydrophilic or less hydrophobic.

Protein Tethers

[0086] As used herein, a "protein tether" or a "peptide tether" may be used interchangeably, and refers to a hydrophilic and unstructured synthetic peptide. In some embodiments, the peptide tether of the antimicrobial composition described herein is more hydrophilic than the ELP sequence. In other embodiments, the ELP sequence of the antimicrobial composition described herein is more hydrophobic than the peptide tether. In further embodiments, the ELP sequence of the antimicrobial composition described herein is more hydrophobic than the peptide tether when counting the number of hydrophobic amino acids in each part (e.g., the ELP sequence has more hydrophobic amino acids than the peptide tether).

[0087] One of the unique and inventive technical features of the present invention is utilizing a peptide tether that is more hydrophilic or less hydrophobic than the ELP of the antimicrobial biopolymer composition described herein. Without wishing to limit the invention to any theory or mechanism, it is believed that the technical feature of the present invention advantageously allows for the ELP to form a micelle core and the hydrophilic tether act as a corona in the micelle. This

allows the separation of the AMP from the ELP micelle core which improves the AMP activity. If there are no tethers, then some of the ELPs can still form micelle structure but there will be no gap between ELP and AMP. In this design, many AMPs will be buried in the ELP micelle core and thus, the amounts of active AMPs, outside of the micelle cores, will be less than the ELP-tether-AMP design and thus, the relative activity will be dropped.

[0088] In some embodiments, the peptide tether comprises the sequence (VSGSG (SEQ ID NO: 42))$_i$, where i is 10 to 400. In other embodiments, the peptide tether comprises the sequence (AGAGAGPEG (SEQ ID NO: 43))$_i$, where i is 1 to 200. In some embodiments, the peptide tether comprises the sequence (VPGAG (SEQ ID NO: 44))$_i$, where i is 10 to 400. In some embodiments, the peptide tether comprises the sequence (VPGGG (SEQ ID NO: 45))$_i$, where i is 10 to 400. In some embodiments, the peptide tether comprises the sequence (VPGEG (SEQ ID NO: 46))$_i$, where i is 10 to 400. In some embodiments, the peptide tether comprises the sequence (VPGEGVPGKG (SEQ ID NO: 47))$_i$, where i is 1 to 200. In some embodiments, the peptide tether comprises the sequence (AGAGAGPEG (SEQ ID NO: 43))$_i$, where i is less than 200. In some embodiments, the peptide tether comprises a sequence (ASPAAPAPASPAAPAPSAPAA (SEQ ID NO: 48))$_i$, where i is 1 to 100. In some embodiments, the peptide tether comprises the sequence (GEQGKPGNQGEPGNPGSPGQPGNPGQPGS
PGNPGQPGNEGPQGSQGNPGQPGEPGSNGQPGQPGQNGKNGQPGSPGSQGSPGNQGSP
GNQGQPGNKGEQGKPGNQGPA (SEQ ID NO: 49))$_i$, where i is is 1 to 20.

[0089] In some embodiments, the length or size of the peptide tether (i.e., the i value) is selected to keep the antimicrobial biopolymer composition less than or equal to 100 kDa. In other embodiments, the length or size of the peptide tether (i.e., the i value) is selected to keep the antimicrobial biopolymer composition about 50 kDa. In some embodiments, the length or size of

the peptide tether (i.e., the i value) is selected to keep the antimicrobial biopolymer composition about 150 kDa. In other embodiments, the length or size of the peptide tether (i.e., the i value) is selected to keep the antimicrobial biopolymer composition about 100 kDa. In further embodiments, the length or size of the peptide tether (i.e., the i value) is selected to keep the antimicrobial biopolymer composition within about 200 kDa.

[0090] In certain embodiments, i is 5. In other embodiments, i is a number from 5 to 10, or from 5 to 20, or from 5 to 25, or from 5 to 50, or from 5 to 100, or from 5 to 150, or from 5 to 200, or from 5 to 250, or from 5 to 300, or from 5 to 350, or from 5 to 400, or from 5 to 450. In certain embodiments, i is 10. In other embodiments, i is a number from 10 to 20, or from 10 to 25, or from 10 to 50, or from 10 to 100, or from 10 to 150, or from 10 to 200, or from 10 to 250, or from 10 to 300, or from 10 to 350, or from 10 to 400, or from 10 to 450. In certain embodiments, i is 20. In other embodiments, i is a number from 20 to 25, or from 20 to 50, or from 20 to 100, or from 20 to 150, or from 20 to 200, or from 20 to 250, or from 20 to 300, or from 20 to 350, or from 20 to 400, or from 20 to 450. In certain embodiments, i is 50. In other embodiments, i is a number from 50 to 100, or from 50 to 150, or from 50 to 200, or from 50 to 250, or from 50 to 300, or from 50 to 350, or from 50 to 400, or from 50 to 450.

[0091] In certain embodiments, i is 100. In other embodiments, i is a number from 100 to 150, or from 100 to 200, or from 100 to 250, or from 100 to 300, or from 100 to 350, or from 100 to 400, or from 100 to 450. In certain embodiments, i is 150. In other embodiments, i is a number from 150 to 200, or from 150 to 250, or from 150 to 300, or from 150 to 350, or from 150 to 400, or from 150 to 450. In certain embodiments, i is 200. In other embodiments, i is a number from 200 to 250, or from 200 to 300, or from 200 to 350, or from 200 to 400, or from 200 to 450. In certain embodiments, i is 250. In other embodiments, i is a number from 250 to 300, or from 250 to 350,

or from 250 to 400, or from 250 to 450. In certain embodiments, i is 300. In other embodiments, i is a number from 300 to 350, or from 300 to 400, or from 300 to 450. In certain embodiments, i is 350. In other embodiments, i is a number from 350 to 400, or from 350 to 450. In certain embodiments, i is 400. In other embodiments, i is a number from 400 to 450.

[0092] The protein tether separates the ELP and the AMP to increase AMP activity. The protein tether is designed based on currently used synthetic polymer tethers, e.g., polyethylene glycol (PEG), with similar properties: size controlled, hydrophilic, and unstructured. The benefit of designing a protein tether is that the tether can be genetically encoded with ELP and AMP, e.g., ELP-tether-AMP is synthesized together in one polymer unit via bio-manufacturing, and purified (e.g., by ITC), which the conventional approach needs to prepare biomaterials and synthesize and purify polymer tethers and AMPs separately, and then attached end-to-end, resulting in high cost and time.

[0093] Without wishing to limit the present invention to any theory or mechanism it is believed that the hydrophilic properties of a synthetic polymer tethers improve AMP stability because the hydration characteristic repels the adherence of nonspecific biomolecules (e.g., proteases), thus preventing peptide (i.e., AMP) degradation. In some embodiments, AMP activity (i.e., antimicrobial activity) may be extended (e.g., extended from hours to days) *in vivo* when attached to hydrophilic unstructured proteins and indicates that unstructured protein tethers with hydrophilic properties prevent AMP degradation and enhance the stability and activity.

[0094] Without wishing to limit the present invention to any theory or mechanism it is believed that the use of a hydrophilic peptide tether helps to improve the stability of the entire antimicrobial composition described herein and enhances antimicrobial activity. Surprisingly, the present

invention was able to make use of a hydrophilic peptide tether rather than a synthetic polymer tether to create the biopolymer. The use of a peptide tether is novel in the formation of AMP-biopolymers, because prior art teaches the use of synthetic tether polymers. Additionally, the use of a hydrophilic peptide tether allows the preparation of a cost-effective antimicrobial biopolymer material (i.e., antimicrobial biopolymer composition).

[0095] In some embodiments, the hydrophilic tether described herein allows for the AMP and ELP to remain associated together. In other embodiments, the hydrophilic tether described herein allows for the AMP and ELP to remain associated together through the synthesis and purification of the antimicrobial biopolymer composition. Without wishing to limit the present invention to any theory or mechanism it is believed that the ability to to allow the entire antimicrobial biopolymer composition described herein (i.e., the ELP, the AMP, and the peptide tether) to remain associated together through the synthesis and purification of the antimicrobial biopolymer composition allows for a cost effective method of producing the composition described herein because there is no need to methods to attach the three pieces.

[0096] Intrinsically disordered proteins have similar flexibility to PEG due to a similar chain stiffness with a persistent length of ~0.4 nm. Hydrophilic unstructured proteins are available with precisely controllable lengths, allowing the development of the protein tether.

[0097] The tether is to be hydrophilic, unstructured, and of a certain length. For example, in certain embodiments, the tether length is at least 3000 g/mol, which is equal to a degree of polymerization (DP) of 70. In certain embodiments, for better separation between the self-assembled ELP nanoparticle and AMP, the ratio of tether size to whole biopolymer size (f_{tether}) = (molar mass of tether)/ (molar mass of ELP-tether-AMP) is about 0.2 as described by Widder et al. in their article

"*Characterization of hydration and nanophase separation during the temperature response in hydrophobic/hydrophilic elastin-like polypeptide (ELP) diblock copolymers*", published in the Soft Matter in 2017 (see Table 4).

[0098] In some embodiments, the f_{tether} is greater than or equal to 0.2. In other embodiments, the f_{tether} is less than or equal to 0.5. In further embodiments, the f_{tether} is about 0.10, or about 0.15, or about 0.20, or about 0.25, or about 0.30, or about 0.35, or about 0.40, or about 0.45, or about 0.50, or about 0.55, or about 0.60. In some embodiments, the f_{tether} ranges from 0.10 to 0.60, or from 0.10 to 0.50, or from 0.10 to 0.40, or from 0.10 to 0.30, or from 0.10 to 0.20, or from 0.20 to 0.60, or from 0.20 to 0.50, or from 0.20 to 0.40, or from 0.20 to 0.30, or from 0.30 to 0.60, or from 0.30 to 0.50, or from 0.30 to 0.40, or from about 0.40 to 0.60, or from about 0.40 to about 0.50, or about 0.50 to about 0.60.

[0099] Without wishing the limit the present invention to any theory or mechanism it is believed that an antimicrobial biopolymer composition (e.g., ELP-tether-AMP) wherein the ratio of tether molar mass (or molecular weight) to total ELP-tether AMP (i.e, f_{tether}) is from 0.2 and 0.5, the hydrophobic ELP will form micelle core while hydrophilic or less hydrophobic tether will segregate AMP from the ELP core, meaning that the tether will be the corona of the micelle. In other words, from center to the outside of the micelle will be ELP, tether and AMP, sequentially.

[00100] Referring to Table 4 two protein tethers (DP > 70 and f_{tether}: ~0.2) were introduced into the ELPs: (i) hydrophilic polymer-like unstructured protein C_{30}; and (ii) $ELP(S)_m$. $ELP(S)_i$ = VPGSG (SEQ ID NO: 5)$_m$; C_i = $[AGAGAGPEG]_i$ (SEQ ID NO: 43). Note m is not limited to 36 and 45, and i is not limited to 30 per Table 4.

Table 4: Shows non-limiting examples of ELP(Tyr)-protein tether design with LL37

ELP (Tyr)-tether ($(ELP(S)_m$ or C_i)	**$T_{t,\ expected}$[37]**	**m**	**F_{tether} (Molar mass of tether/molar mass of ELP(Tyr)-tether)**	**$T_{t,\ experimental}$**	**$T_{t,\ experimental}$ with LL37**
$ELP(S_2Y_1S_2)_{36}$ –$ELP(S)_{36}$	29°C	180	0.19	29°C (expected)	TBD
$ELP(A_2Y_1A_2)_{36}$ –$ELP(S)_{36}$	26°C	180	0.20	26°C (expected)	TBD
$ELP(S_2Y_1S_1)_{45}$ –$ELP(S)_{45}$	24°C	180	0.19	TBD	TBD
$ELP(A_2Y_1A_1)_{45}$ –$ELP(S)_{45}$	21°C	180	0.19	TBD	TBD
$ELP(S_2Y_1S_2)_{36}$ –C_{30}	>29°C	180 (tether not included)	0.21	TBD	TBD
$ELP(A_2Y_1A_2)_{36}$ –C_{30}	>25°C	180 (tether not included)	0.22	TBD	TBD
$ELP(S_2Y_1S_1)_{45}$	>25°C	180 (tether	0.21	TBD	TBD

$-C_{30}$		not included)			
$ELP(A_2Y_1A_1)_{45}-C_{30}$	>20°C	180 (tether not included)	0.22	TBD	TBD

[00101] To test hydration characteristics of hydrophilic protein tethers, the hydrodynamic radius (r_h) of nanoparticles can be measured to observe changes of particle sizes compared to $ELP(S_2Y_1S_2)_{36}$ (Table 3) vs. $ELP(S_2Y_1S_1)_{36}$ - $ELP(S)_{36}$ (Table 4), which have the same amino acid compositions but different distributions; in the absence and presence of protein tethers, the contact angle of water droplets on the AMP biopolymer films and coatings on silica can be analyzed (Table 3 and Table 4); and (iii) anti-adhesion or anti-fouling functionality will be identified via fluorescent microscopy using fluorescent-tagged bovine serum albumin on the AMP biopolymer coatings, and the result can be compared to PEG coatings. Since hydrophilic synthetic polymer PEG is a well-known conventional tether with excellent antifouling property, the last test will help to select a protein tether in Table 4 that shows promising results.

[00102] To examine plasma or serum stability of LL37 in the compositions of the present invention, samples of LL37 and ELP(Tyr)-tether-LL37 nanoparticles will be collected in 80% human plasma or serum at 37ºC in time intervals. Biomolecules in the serum will be heat-inactivated right after the sample collection to prevent additional LL37 degradation, and the percentage of degradation will be analyzed by HPLC.

Antimicrobial Peptides (AMPs)

[00103] As used herein, "antimicrobial peptides (AMPs)" refers to a class of small, positively charged peptides that widely exist in nature and they are an important part of the innate immune system of different organisms. AMPs are evolutionarily conserved and have a broad range of antimicrobial activity inhibitory effects against bacteria, fungi, parasites, and viruses. Additionally, AMPs are relatively short, commonly comprising 10–60 amino acids, contain a substantial proportion (typically 50%) of hydrophobic residues, and are often cationic or zwitterionic. In some embodiments, AMPs may be classified into four categories based on their secondary structure, i.e., (i) α-helical, (ii) β-sheet, (iii) αβ, or (iv) non-αβ elements.

[00104] Without wishing to limit the present invention to any theories or mechanisms it is believed that because AMPs are generally small peptides (e.g., 10-60aa) with a simple structure, AMPs are able to maintain their activities over time because they are less likely to lose their structure and therefore their function.

[00105] In some embodiment, the antimicrobial peptide (AMP) selected for the antimicrobial compositions described herein may be selected based on the resulting material (e.g., micelle or nanoparticles, hydrogel, films or adhesives) in which the antimicrobial composition will be utilized in. For example, in some embodiments, to create a hydrogel, a film or an adhesive material using the antimicrobial composition described herein, tyrosine residues of the ELP need to be photocrosslinked or hydrolyzed and thus, AMPs without tyrosine residues should be used. Otherwise, AMPs will be also crosslinked or hydrolyzed and thus cannot be used as AMPs. In other embodiments, to create a micelle or nanoparticle material using the antimicrobial composition described herein AMPs with tyrosine residues may still be used. In some

embodiments, to create a micelle or nanoparticle material the total amount of hydrophobic amino acid residues in the AMP needs to be less than the ELP. Without wishing to limit the present invention to any theory or mechanisms it is believed that an antimicrobial composition (such as the one described herein) with an ELP that is more hydrophobic than the AMP, can form a micelle core at a certain threshold temperature and peptide tether will segregate AMPs away from the ELP micelle core.

[00106] In some embodiments, the antimicrobial compositions described herein comprise an antimicrobial peptide (AMP). In other embodiments, the antimicrobial compositions described herein comprise an antimicrobial peptide (AMP) with no tyrosine amino acids. In some embodiments, the AMP comprises no tyrosine amino acid residues within its sequence. In other embodiments, the AMP sequence comprises no tyrosine amino acid residues. In some embodiments, the antimicrobial peptide (AMP) can be any AMP with no tyrosine amino acid residue.

[00107] The antimicrobial peptide (AMP) may be selected from one of many known AMPs or those in future development. The present invention is not limited to the AMPs disclosed herein. A non-limiting example of an AMP is LL37, which is a cationic, amphiphilic, antimicrobial peptide, composed of 37 amino acids (LLGDFFRKSKEKIGKEFKRIVQRIKDFLRNLVPRTES, SEQ ID NO: 50).

[00108] In some embodiments, the antimicrobial peptides (AMPs) of the compositions as described herein may comprise antibacterial, antifungal, anti-parasitic, antiviral activity (i.e., properties) or a combination thereof. In some embodiments, any antimicrobial peptide (AMP) may be utilized in the composition of the present invention as described herein. In other embodiments, any synthetic

or native AMP may be utilized in the composition of the present invention as described herein. Non-limiting examples of AMPs are described in Wang et al., in the article "*APD3: the antimicrobial peptide database as a tool for research and education*," published in Nucleic Acid Research in 2016.

[00109] Non-limiting examples of AMPs with antibacterial activity include be are not limited to LL37, RL37, dermcidin, protegrin 1, protegrin 2, protegrin 3, protegrin 4, protegrin 5, abaecin, andropin, bactenecin, bovine neutrophil beta-defensin 12 (bBD-1), Pexiganan, Lytixar, hLF1-11, LL-37, Omiganan, Corticostatin I, Corticostatin VI, NP-3a, Pediocin PA-1/AcH, Lacticin 3147, As-CATH5, Dalbavancin, Baciim, Vancocin, Daptomycin, Colistin, Telavancin, Gramicidin, D2A21, PXL01, Omiganan, Nisin, Polylysine, NKL-24, Caerin1.1, Caerin 1.9, Dicentracin, Thanatin, Ponericin W1, Mastoparan, or a combination thereof.

[00110] Non-limiting examples of AMPs with antifungal activity include but are not limited to Lactoferricin B (LfcinB), bombinin-like peptide 1, bombinin-like peptide 3, bombinin-like peptide 7, Antifungal protein (AFP), hLF1-11, Novexatin, CZEN-002, PAC-113, NP-3a, As-CATH5, PAC-113, P-113, D2A21, Omiganan, Polylysine, PAF26, 03TR/C12O3TR, Thanatin, Ponericin W1, or a combination thereof.

[00111] Non-limiting examples of AMPs with antiparasitic activity include but are not limited to gaegurin-1, gaegurin-2, gaegurin-3, DefMT7 (defensin MT7), or a combination thereof.

[00112] Non-limiting examples of AMPs with antiviral activity include but are not limited to antiviral protein Y3, human neutrophil peptide-4 (HNP-4), human defensin 5 (HD-5), human defensin 6 (HD-6), NP-3a, Polylysine, or a combination thereof.

[00113] Non-limiting examples of AMPs with anti-cancer activity include but are not limited to Iseganan or Mastoparan. Non-limiting examples of AMPs with anti spermicidal activity include but are not limited to Pediocin PA-1/AcH, or Lacticin 3147. Non-limiting examples of AMPs with anti-sepsis activity include but are not limited to As-CATH5. Non-limiting examples of AMPs with anti-HIV-1 activity include but are not limited to Fuzeon.

[00114] Non-limiting examples of AMPs include but are not limited to LL37, RL37, dermcidin, protegrin 1, protegrin 2, protegrin 3, protegrin 4, protegrin 5, abaecin, andropin, bactenecin, bovine neutrophil beta-defensin 12 (bBD-1), Pexiganan, Lytixar, hLF1-11, LL-37, Omiganan, Corticostatin I, Corticostatin VI, NP-3a, Pediocin PA-1/AcH, Lacticin 3147, As-CATH5, Dalbavancin, Baciim, Vancocin, Daptomycin, Colistin, Telavancin, Gramicidin, D2A21, PXL01, Omiganan, Nisin, Polylysine, NKL-24, Caerin1.1, Caerin 1.9, Dicentracin, Thanatin, Ponericin W1, Mastoparan, Lactoferricin B (LfcinB), bombinin-like peptide 1, bombinin-like peptide 3, bombinin-like peptide 7, Antifungal protein (AFP), hLF1-11, Novexatin, CZEN-002, PAC-113, NP-3a, As-CATH5, PAC-113, P-113, D2A21, Omiganan, Polylysine, PAF26, 03TR/C12O3TR, Thanatin, Ponericin W1, gaegurin-1, gaegurin-2, gaegurin-3, DefMT7 (defensin MT7), antiviral protein Y3, human neutrophil peptide-4 (HNP-4), human defensin 5 (HD-5), human defensin 6 (HD-6), NP-3a, Polylysine, Iseganan, Mastoparan, Pediocin PA-1/AcH, Lacticin 3147, As-CATH5, Fuzeon, or a combination thereof. However, the present invention is not limited to the aforementioned AMPs.

[00115] Regarding orientation of the AMP, AMPs tethered by their N- or C- termini may be more potent than an AMP randomly attached to tethers between its ends. In some embodiments, the AMP is attached to the protein tether at the N-terminal of the AMP. In other embodiments, the AMP is attached to the protein tether at the C-terminal of the AMP.

[00116] Without wishing to limit the present invention to any theory or mechanism it is believed that there are three mechanisms that are most-widely accepted for microbe lysis by AMPs (e.g., carpet model, barrel-stave model and toroidal model). First, in the carpet model, AMPs (e.g., cationic AMPs) bind to the membrane surface of the microbe via electrostatic interactions and cover the membrane in a carpet-like manner. Once a critical concentration of AMPs is reached, the AMPs insert into the membrane and distort it; leading to micellization. In the barrel-stave model, AMPs interact laterally with one another and interact with the membrane (e.g., the hydrophobic part of the AMPs interact with the membrane) resulting in the formation of a transmembrane pore with the hydrophilic part of the AMPs facing the inner channel. In the third model, the toroidal pore model, specific AMP-AMP interactions are not present. Instead, AMPs affect the local curvature of the bilayer in a cooperative manner such that a toroid of high curvature forms. The membrane is caused to curve inward, resulting in the formation of a pore made up of AMPs and lipid head groups.

[00117] Without wishing to limit the present invention to any theory or mechanism it is believed that AMPs can form barrel-stave pores on microbe membranes, however, for antimicrobial activity, several AMPs in an antiparallel formation are required to form the pore. For example, several LL37 peptides form a barrel structure in an antiparallel orientation and follow the carpet or toroidal model to lyse the bacterial membrane. This covers the three most widely accepted microbe lysis mechanisms. In some embodiments, AMPs described herein for use in the antimicrobial composition described herein may utilize any of the three lysis mechanisms for killing microbes (e.g., bacteria, viruses, fugi, parasites).

[00118] The present invention features simple gene editing to encode the AMPs to be connected to a protein tether by either the N- or C- terminus for the same AMP orientation (ELP-tether-AMP

or AMP-tether-ELP) within the material. For AMP orientation with opposite direction in the same material, either two AMP molecules can be attached, one by the N- and one by the C-terminus (e.g., AMP-tether-ELP-tether-AMP), or by mixing two proteins (ELP-tether-LL37 and LL37-tether-ELP) in the same biomaterial, the orientation of LL37 can be alternated in the ELP-based nanoparticle, films, and adhesives.

Development of ELP(Tyr)-Tether-AMP Nanoparticle, Film, and Coating Materials

[00119] The designed T_t of ELP(Tyr)-AMP facilitates ELP self-assembled nanoparticles at body temperature (BT), while Tyr residues in ELP(Tyr) can be photo-cross-linked to construct ELP(Tyr)-AMP films and hydroxylated to form ELP(DOPA)-AMP adhesives for coating biomaterial surfaces. In some embodiments, L-3,4-dihydroxyphenylalanine (DOPA) is a precursor to dopamine.

[00120] For example, because Tyr residues are rare in AMPs, Tyr-crosslinking using ELP(Tyr) helps to mitigate random cross-linking of AMPs and maximize AMP activity.

[00121] ELP(DOPA) may be produced by hydroxylating Tyr residues in ELP(Tyr) with commercially available mushroom tyrosinase. The ELP(DOPA)-AMP solution may be dip coated to deposit the ELP(DOPA)-AMP on biomaterial surfaces, such as alumina, Ti alloy, and polymers (e.g., ePTFE). The dwelling time of ELP(DOPA)-AMP adhesives will be monitored on surfaces in physiological buffers at BT, and the concentration of detached ELP(DOPA)-AMP proteins in solution can be determined over time using UV absorbance (280 nm) and the Beer-Lambert law.

[00122] An automated antibacterial susceptibility testing instrument can measure the minimal inhibitory concentration of free LL37 and ELP-LL37 nanoparticles against *E. coli* and *S. aureus*. The agar disk-diffusion method can be adapted to test the activity of ELP(Tyr)-LL37

nanoparticles, films and coatings on biomaterial surfaces. For example, MacConkey agar can be prepared for *E.coli* and tryptic soy agar can be prepared for *S. aureus* to determine the LL37 activity level by measuring the zone inhibition around the film or coating material, where > 1mm is indicative of a good antibacterial agent based on Swiss Norm 195920 - ASTM E 2149-01.

[00123] As previously discussed, the ELP(Tyr)-AMP films herein, using Tyr which is not found in most AMPs for cross-linking, may enhance AMP activity relative to the previously developed ELP-AMP film because AMPs were unintentionally cross-linked, resulting in a decrease in AMP activity.

[00124] One of the unique and inventive technical features of the present invention is utilizing specific amino acid residues (i.e, tyrosine (Y)) to crosslink the ELPs and selecting AMPs with no tyrosine (Y) amino acid residues to create an antimicrobial biopolymer composition described herein. Without wishing to limit the invention to any theory or mechanism, it is believed that the technical feature of the present invention advantageously provides for a method to specifically cross-link only the ELP part of the antimicrobial biopolymer composition while other parts of the composition (i.e., the peptide tether and AMPs) will not be cross-linked and thus, the activity (i.e., the antimicrobial activity) of the AMPs will not be hindered.

[00125] By cross-linking specific amino acid residues (i.e, tyrosine (Y)) in the platform (i.e., in the ELP) for AMPs, biopolymer networks can be prepared in aqueous conditions (e.g., a hydrogel). The platform design of the present invention reduces unintentional cross-linking of the peptide tether and AMPs. For example, the ELPs are photo-crosslinked using "Y" residues. Selected AMPs for the antimicrobial biopolymer composition described herein do not include "Y" residues and thus, the present invention can specifically cross-link only ELP parts while other parts (i.e.,

the peptide tether and AMPs) will not be cross-linked, and thus, cross-linking will not hinder AMP activity. All AMP constituents in the ELP-tether-AMP design are expected to be active in the cross-linked or hydrogel materials

[00126] Furthermore, the prior references teach away from the present invention. For example, in previous designs, platforms were crosslinking by using certain amino acid side chains. However, with this method of crosslinking it is difficult to avoid crosslinking of AMPs. This causes unintentional crosslinking of AMPs and will inhibit the activity of AMPs.

[00127] In some embodiments, the antimicrobial biopolymer compositions described herein (e.g., ELP-tether-AMP) will be genetically encoded together on the same plasmid using DNA cloning technology. Then, this ELP-tether-AMP sequence will be expressed using a biosystem (e.g., *E. coli.*) Therefore, "all-in-one" ELP-tether-AMP (i.e., “all-in-one antimicrobial biopolymer composition) will be synthesized together without additional methods to attach them. In some embodiments, the antimicrobial biopolymer composition of the present invention is an “all-in-one” composition and utilizes various DNA and protein engineering technologies.

[00128] Without wishing to limit the present invention to any theories or mechanisms, it is believed that the antimicrobial biopolymer composition of the present invention is cost effective than previous designs because the three components (i.e., the ELP, the AMP, and the peptide tether) are continuously linked throughout the synthesis and purification steps.

Applications

[00129] As previously discussed, the biopolymer-AMP compositions (e.g., AMP-ELP platform) have a variety of applications that include but are not limited to: antimicrobial nanoparticles as AMR therapeutics or as a pharmaceutical to treat infected individuals, antimicrobial coatings on

clothing, on surfaces of implants, or on medical devices, such as endoscopes, to prevent secondary microorganism infection from the device to patient, antimicrobial filters to prevent transmission and directly kill a broad range of biological pathogens, antimicrobial films for wound dressings, etc.

[00130] Without wishing to limit the present invention to any theory or mechanism, it is believed that large-scale production and storage of AMP-ELPs may be a versatile defensive strategy against of a biological warfare agents (BWAs; e.g., *Bacillus anthracis* and *Yersenia pestis*) attack or epidemic since the material can be used directly in applications ranging from a surface coating to protect personnel and infrastructure to a nanoparticle to treat BWA exposure. AMPs have shown efficacy against an extensive range of weaponizable biological pathogens such that having it on hand is invaluable preparation for an unknown or new BWA.

[00131] The present invention also provides methods for treating infections. The methods may feature the introduction of a biopolymer-AMP composition of the present invention, wherein the biopolymer-AMP composition kills the infectious agent or reduces the growth of the infectious agent.

[00132] The present invention also provides cocktails, e.g., for therapeutic purposes, wherein the cocktails comprise two or more AMP-ELPs such as ELPs with different AMPs, different ELPs with different AMPs, etc.

[00133] Various modifications of the invention, in addition to those described herein, will be apparent to those skilled in the art from the foregoing description. Such modifications are also intended to fall within the scope of the appended claims. Each reference cited in the present application is incorporated herein by reference in its entirety.

[00134] Although there has been shown and described the preferred embodiment of the present invention, it will be readily apparent to those skilled in the art that modifications may be made thereto which do not exceed the scope of the appended claims. Therefore, the scope of the invention is only to be limited by the following claims. In some embodiments, the figures presented in this patent application are drawn to scale, including the angles, ratios of dimensions, etc. In some embodiments, the figures are representative only and the claims are not limited by the dimensions of the figures. In some embodiments, descriptions of the inventions described herein using the phrase "comprising" includes embodiments that could be described as "consisting of", and as such the written description requirement for claiming one or more embodiments of the present invention using the phrase "consisting of" is met.

What is Claimed is:

1. An antimicrobial biopolymer composition comprising,
    a) an elastin-like polypeptide (ELP), wherein the ELP comprises one or more pentapeptide repeats consecutively linked, wherein at least one of the pentapeptide repeats comprises a tyrosine residue;
    b) an antimicrobial peptide (AMP); and
    c) a hydrophilic peptide tether connecting the ELP and the AMP;

    wherein the peptide tether connects to the AMP at the AMP's N-terminus, C-terminus, or both;

    wherein the ELP is more hydrophobic than the peptide tether.

2. The composition of claim 1, wherein the one or more pentapeptide repeats is selected from a group consisting of: SEQ ID NO: 3, SEQ ID NO: 4, SEQ ID NO: 5, SEQ ID NO: 6, SEQ ID NO: 7, SEQ ID NO: 8, SEQ ID NO: 9, SEQ ID NO: 10, SEQ ID NO: 11, SEQ ID NO: 12, SEQ ID NO: 13, SEQ ID NO: 14, SEQ ID NO: 15, SEQ ID NO: 16, SEQ ID NO: 17, SEQ ID NO: 18, SEQ ID NO: 19, SEQ ID NO: 20, SEQ ID NO: 21, SEQ ID NO: 22, SEQ ID NO: 23, SEQ ID NO: 24, SEQ ID NO: 25, SEQ ID NO: 26, SEQ ID NO: 27, SEQ ID NO: 28, SEQ ID NO: 29, SEQ ID NO: 30, SEQ ID NO: 31, SEQ ID NO: 32, SEQ ID NO: 33, SEQ ID NO: 34, SEQ ID NO: 35, SEQ ID NO: 36, SEQ ID NO: 37, SEQ ID NO: 38, SEQ ID NO: 39, SEQ ID NO: 40, and SEQ ID NO: 41.
3. The composition of claim 1, wherein the one or more pentapeptide repeats comprising the tyrosine is selected from a group consisting of SEQ ID NO: 3, SEQ

ID NO: 24, SEQ ID NO: 25, SEQ ID NO: 26, SEQ ID NO: 27, SEQ ID NO: 28, SEQ ID NO: 30, EQ ID NO: 32, SEQ ID NO: 33, SEQ ID NO: 34, SEQ ID NO: 36, SEQ ID NO: 38, SEQ ID NO: 39, and SEQ ID NO: 40.

4. The composition of claim 1, wherein the tyrosine residues are cross-linked to form a self-standing film or membrane material.
5. The composition of claim 1, wherein the tyrosine residue allows the composition to adhere to a surface after hydroxylation by tyrosinase.
6. The composition of claim 5, wherein the surface is a cloth, a plastic, a glass, a metal, or a combination thereof.
7. The composition of claim 5, wherein the surface is a medical device, a dressing, a clothing, or a combination thereof.
8. The composition of claim 1, wherein the pentapeptide repeat is according to the formula (WaaPXaaYaa4G (SEQ ID NO: 2))$_m$, where Waa is valine, isoleucine or leucine, where Xaa is any amino acid, where Yaa is any amino acid except for proline, and where m is 10 to 400.
9. The composition of claim 1, wherein the ELP is according to the formula [(VPGXaaG (SEQ ID NO: 1))$_j$(VPGYG (SEQ ID NO: 3))$_k$(VPGXaaG (SEQ ID NO: 1))$_l$]$_n$, where j ranges from 10-400, k ranges from 10-400, l ranges from 10-400, and n ranges from 10-400, such that $10 \leq (j+k+l)xn \leq 400$.
10. The composition of claim 9, wherein one Xaa of the formula is identical to or different from another Xaa of the formula.
11. The composition of claim 9, wherein Xaa is alanine, serine, arginine, asparagine, aspartic acid, cysteine, glutamine, glutamic acid, glycine, histidine, isoleucine,

leucine, lysine, methionine, phenylalanine, threonine, tryptophan, tyrosine, or valine.

12. The composition of claim 9, wherein tyrosine residues are cross-linked to form a self-standing film, a membrane material, or a hydrogel.
13. The composition of claim 9, wherein the tyrosine residues allow the composition to adhere to a surface after hydroxylation.
14. The composition of claim 13, wherein the surface is a cloth, a plastic, a glass, a metal, or a combination thereof.
15. The composition of claim 13, wherein the surface is a medical device, a dressing, a clothing, or a combination thereof.
16. The composition of claim 1, wherein the AMP comprises antibacterial activity, antiviral activity, antifungal activity, antiparasitic activity or a combination thereof.
17. The composition of claim 16, wherein the antibacterial AMP comprises LL37, RL37, dermcidin, protegrin 1, protegrin 2, protegrin 3, protegrin 4, protegrin 5, abaecin, andropin, bactenecin, bovine neutrophil beta-defensin 12 (bBD-1), Pexiganan, Lytixar, hLF1-11, LL-37, Omiganan, Corticostatin I, Corticostatin VI, NP-3a, Pediocin PA-1/AcH, Lacticin 3147, As-CATH5, Dalbavancin, Baciim, Vancocin, Daptomycin, Colistin, Telavancin, Gramicidin, D2A21, PXL01, Omiganan, Nisin, Polylysine, NKL-24, Caerin1.1, Caerin 1.9, Dicentracin, Thanatin, Ponericin W1, Mastoparan or a combination thereof.
18. The method of claim 1, wherein the hydrophilic peptide tether comprises $[VPGSG]_i$ (SEQ ID NO: 42) or $[AGAGAGPEG]_m$ (SEQ ID NO: 43), wherein i is equal to 36 or 45 and m is equal to 30.

19. The composition of claim 1, wherein the composition self-assembles into nanoparticles.
20. The composition of claim 1, wherein the hydrophilic peptide tether has anti-fouling characteristics.

Abstract

Biopolymer compositions comprising antimicrobial peptides (AMPs) for treating infections such as bacterial infections, viral infections, fungal infections, and parasitic infections. The compositions herein may also be used for treating infections associated with antibiotic-resistant bacteria, antifungal-resistant fungi, antiviral-resistant viruses, or for treating biological warfare agents (BWAs) such as *Bacillus anthracis* and *Yersenia pestis*. The present invention also provides methods of synthesis of said biopolymer compositions, wherein AMP biopolymers can be synthesized as an artificially engineered protein by genetically fusing an AMP; a protein that behaves similarly to polymer tethers; and a protein as a modifiable material platform that can transform to self-assembled nanoparticles, self-standing films, or adhesives to easily attach tethered AMPs onto any biomaterial surface for various clinical applications.

APPENDIX B

Non-cytotoxic Dityrosine Photocrosslinked Polymeric Materials With Targeted Elastic Moduli

Christopher P. Camp[1], Ingrid L. Peterson[2], David S. Knoff[1], Laruen G. Melcher[3], Connor J. Maxwell[1], Audrey T. Cohen[1], Anne M. Wertheimer[3,*], and Mikyu Kim[1,3,4,*]

[1]*Department of Biomedical Engineering, University of Arizona, Tucson, AZ, United States*

[2]*Applied Biosciences GIDP, University of Arizona, Tucson, AZ, United States*

[3]*BIO5 Institute, University of Arizona, Tucson, AZ, United States*

[4]*Department of Materials Science & Engineering, University of Arizona, Tucson, AZ, United States*

*Correspondence Anne M. Wertheimer, **awerth@email.arizona.edu**;

Minkyu Kim, **minkyukim@email.arizona.edu**

Reproduced from *Frontiers in Chemistry*, **2020**, 8:173.

with permission form the Frontiers Media S.A.

Abstract

Controlling mechanical properties of polymeric biomaterials, including the elastic modulus, is critical to direct cell behavior, such as proliferation and differentiation. Dityrosine photocrosslinking is an attractive and simple method to prepare materials that exhibit a wide range of elastic moduli by rapidly crosslinking tyrosyl-containing polymers. However, high concentrations of commonly used oxidative crosslinking reagents, such as ruthenium-based photoinitiators and persulfates, present cytotoxicity concerns. We found the elastic moduli of materials prepared by crosslinking an artificial protein with tightly controlled tyrosine molarity can be modulated up to 40 kPa by adjusting photoinitiator and persulfate concentrations. Formulations with various concentrations of the crosslinking reagents were able to target a similar material elastic modulus, but excess unreacted persulfate resulted in cytotoxic materials. Therefore, we identified a systematic method to prepare non-cytotoxic photocrosslinked polymeric materials with targeted elastic moduli for potential biomaterials applications in diverse fields, including tissue engineering and 3D bioprinting.

Introduction

Polymeric biomaterials that are designed to mimic the mechanical properties of tissue matrices can direct cellular behaviors, such as proliferation and differentiation (Engler et al., 2006; Guvendiren and Burdick, 2012; Chaudhuri et al., 2016). Polymers can be chemically crosslinked to form polymer-network materials, such as hydrogels, that mimic the elastic moduli of natural tissues, ranging from 1 kPa in brain tissue to over 100 kPa in bone (Engler et al., 2006; Chaudhuri et al., 2016). Furthermore, crosslinking strategies that rapidly form hydrogels on the order of seconds to minutes are advantageous to precisely fix complex material shapes. However, rapid chemical crosslinking strategies often result in clusters of densely and sparsely crosslinked regions because polymers quickly crosslink before the reagents are well-mixed, resulting in diminished mechanical properties (Kroll and Croll, 2015; Gu et al., 2017, 2020). Therefore, a rapid crosslinking strategy with improved crosslinking homogeneity is necessary to fabricate tissue-mimicking polymeric biomaterials.

Photochemical crosslinking is a potential method to improve the consistency of crosslinking density in rapidly formed polymeric materials because solutions can be thoroughly mixed prior to activating photocrosslinking reagents. Dityrosine photocrosslinking is an attractive and simple approach that exploits light and photoinitiator-activated phenolic coupling of tyrosyl groups within synthetic or natural polymers (Aeschbach et al., 1976; Fancy and Kodadek, 1999; Partlow et al., 2016). The photoinitiator tris(2,2′-bipyridyl)ruthenium(II) ($[Ru(II)bpy_3]^{2+}$) and persulfate oxidizing agents are often used for rapid dityrosine photocrosslinking (Elvin et al., 2005, 2010; Fang and Li, 2012; Ding et al., 2013; Jeon et al., 2015; Yang et al., 2015; Kim et al., 2017; Zhang et al., 2017; Min et al., 2018; Sakai et al., 2018; Khanmohammadi et al., 2019; Lim

et al., 2019). $[Ru(II)bpy_3]^{2+}$ functions by absorbing visible light and reducing a persulfate anion to reach a higher energy state, $[Ru(II)bpy_3]^{3+}$. The persulfate anion is consumed in the reaction through decomposition from $S_2O2{-}8O82$- to $SO2{-}4SO42$- and $SO\bullet{-}4SO4\bullet$-. $[Ru(II)bpy_3]^{3+}$ oxidizes tyrosyl phenyl groups into free radicals that spontaneously dimerize (Nickel et al., 1994). The complete process of $[Ru(II)bpy_3]^{2+}$ (Ru)-mediated crosslinking occurs on the order of seconds to minutes, and the strategy has been used to form polymeric materials, such as hydrogels, with elastic moduli ranging from 6 kPa to over 100 kPa (Elvin et al., 2010; Ding et al., 2013; Zhang et al., 2017). The range of potential elastic moduli makes the technology sufficient to form biomaterials that mimic particular tissue matrices.

Despite the benefits of Ru-mediated dityrosine photocrosslinking, there is disagreement about the possible cytotoxicity of the Ru and persulfate crosslinking reagents (Annabi et al., 2017). In preparation of dityrosine photocrosslinked polymeric materials, persulfate concentrations have ranged from at least 1 to 200 mM, and Ru concentrations from 0.1 to 3 mM (Elvin et al., 2005, 2010; Fang and Li, 2012; Ding et al., 2013; Jeon et al., 2015; Kim et al., 2017; Zhang et al., 2017; Min et al., 2018; Sakai et al., 2018; Khanmohammadi et al., 2019; Lim et al., 2019). Persulfates are strong oxidizing agents that can stress cell membranes and lead to an increased rate of apoptosis (Song et al., 2017). Ru is an intercalator that can affect DNA and cell replication (Ang and Dyson, 2006; Gill et al., 2016). Due to the potential cytotoxicity of Ru and persulfates, dityrosine photoinitiators including riboflavin or flavin mononucleotide (Kato et al., 1994; Applegate et al., 2016; Donnelly et al., 2017; Liu et al., 2018), and Rose Bengal (Spikes et al., 1999) have been used as alternatives. However, these approaches come at the cost of slower crosslinking that limit potential time-sensitive biomaterials applications, such as stereolithographic 3D bioprinting, where rapid crosslinking is beneficial (Melchels et al.,

2010; Bajaj et al., 2014; Valot et al., 2019). Therefore, an evaluation of Ru photocrosslinking parameters is necessary to carefully utilize Ru crosslinking technology and guide the rapid production of non-cytotoxic dityrosine photocrosslinked polymeric materials.

We hypothesized that elastic moduli of Ru-mediated photocrosslinked materials can be targeted by controlling concentrations of Ru and persulfate where the limiting reagent dictates the elastic modulus. Moreover, we expected that hydrogels prepared from formulations where both reagents are at limiting concentrations could enhance the survivability and growth of cells compared to excessive reagent concentrations. To investigate the Ru-mediated fabrication of non-cytotoxic dityrosine polymeric materials with targeted elastic moduli, we used artificial proteins as model polymers. Advantages of artificial polypeptides include precise genetic engineering for well-controlled Tyr molarity in the system and monodispersed biosynthesis to reduce batch-to-batch variations of polymer lengths (Kim et al., 2015; Yang et al., 2017; Dzuricky et al., 2018). We utilized elastin-like polypeptides (ELP) incorporated with tyrosine residues, ELP(Tyr), as an unstructured polymer model (Roberts et al., 2015) to form dityrosine photocrosslinked hydrogels.

Artificial protein ELPs are typically composed of repeating ($GX_{aa}GVP$) pentapeptide sequences, where X_{aa} can be any amino acid except proline (Urry et al., 1985). Tyrosine and alanine residues comprise the X_{aa} positions, $[(GAGVP)_2\text{-}GYGVP\text{-}(GAGVP)_2]_{24}$, to construct ELP(Tyr). Tyrosine residues allow for photocrosslinking, and together with alanine residues, set the lower critical solution temperature (LCST) at 29°C to utilize the inverse transition cycling (ITC) method, a purification strategy that exploits the reversible, temperature-dependent, phase separation property of ELP (Meyer and Chilkoti, 1999; Christensen et al., 2013). The biocompatibility of ELP-based scaffolds, micelles, and hydrogels has led to its utilization in

biomedical applications (Urry et al., 1991; Simnick et al., 2007), making ELP(Tyr) a suitable polymer to examine potential cytotoxic effects of Ru and persulfate concentrations when used to form dityrosine photocrosslinked materials with targeted elastic moduli (Figure 1).

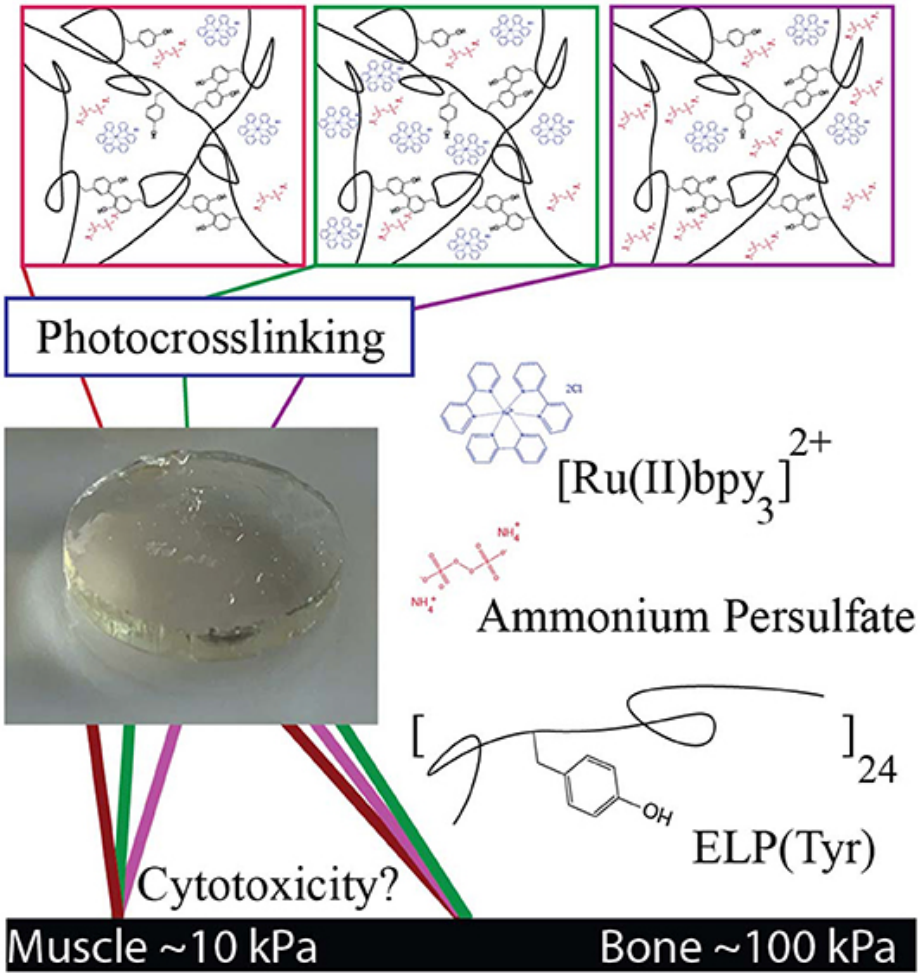

Figure 1. Schematic of tyrosine-photocrosslinked hydrogels with targeted elastic moduli. Multiple formulations with various concentrations of Ru and persulfate can potentially produce hydrogels with similar elastic moduli. Each formulation may have a different degree of cytotoxicity depending on crosslinking reagent concentrations. Reagents in images are an artistic representation of higher concentrations than what is optimal for target G′ and are not representative of actual molar concentrations.

In this study, we controlled the elastic modulus (G′) of photocrosslinked hydrogels by tuning Ru and ammonium persulfate (APS) concentrations with a constant ELP(Tyr) concentration to control the tyrosine molarity in each crosslinking formulation. Hydrogels with similar G′ that were formed by different crosslinking formulations were evaluated in cytotoxicity assays to understand changes in cytotoxicity due to differences in Ru and APS concentrations. The cytotoxicity assay tests the utility of Ru-mediated dityrosine crosslinked hydrogels in applications for which buffer exchange of the hydrogel is difficult, such as *in-situ* hydrogel applications (Bang et al., 2018) where crosslinking reagents necessarily come into direct contact with cells. This study demonstrates a systematic approach to prepare non-cytotoxic biomaterials with targeted elastic moduli given any appropriate tyrosyl-containing polymer by controlling the concentrations of Ru and APS used during photocrosslinking.

Materials and Methods

ELP(Tyr) Synthesis

The ELP(Tyr) plasmid (Figure S1) was kindly provided by the Dr. Harvinder Gill laboratory (Ingrole et al., 2014). The pET-24 a(+) ELP(Tyr) plasmid was transformed into BL21(DE3) competent *Escherichia coli* (*E. coli*) cells (New England Biolabs, Ipswich, MA). One colony was amplified in 10 mL LB media with 50 mg/L kanamycin overnight at 37°C and 220 rpm. The overnight culture was centrifuged at 3,000 × g for 15 min at 4°C. The pellet was resuspended in 2 mL LB media, and 500 µL of cell culture was added to 1 L terrific broth media with 50 mg/L kanamycin. Cultures were incubated at 37°C and 220 rpm for 24 h, centrifuged at 6,000 × g for 5 min to harvest cells, then frozen at −80°C for at least 1 h. Cell pellets were resuspended in pH 7.5 phosphate buffer and lysed using a Branson Sonifier 250 (Branson Ultrasonics, Danbury, CT). Cell debris were removed by centrifuging at 25°C, 10,800 × g for 15 min. ELP(Tyr) was purified using the inverse transition cycling method (Meyer and Chilkoti, 1999) using the described protocol (Ingrole et al., 2014). The cell lysate was heated to 40°C then centrifuged at 40°C, 8,000 × g for 15 min to pellet phase-separated ELP(Tyr). The pellet, including ELP(Tyr), was resuspended in 4°C deionized water to dissolve ELP(Tyr). The resuspended pellet solution was then centrifuged at 4°C, 20,000 × g for 15 min to remove impurities. The supernatant was transferred to a new bottle and the pellet was discarded. The process was repeated for two more cycles and purity was confirmed via SDS PAGE (Figure S2). The purified protein was dialyzed in 4.5 L deionized water and changed every 3+ h 7 times at 4°C. Then the soluble fraction was centrifuged and lyophilized, yielding about 350 mg ELP(Tyr) per 1 L cell culture. Lyophilized ELP(Tyr) was stored at −20°C.

Photocrosslinked ELP(Tyr) Hydrogels

The photocrosslinking solution was prepared containing 10% w/v ELP(Tyr) in pH 7.5 phosphate buffer and was mixed with various concentrations of ammonium persulfate and tris(2,2′-bipyridyl)ruthenium(II) chloride hexahydrate (Sigma-Aldrich, St. Louis, MO, USA). Molds were printed by a Formlabs FORM 2 printer with Dental SG resin (Formlabs, MA, USA). Cylindrical 14 mm diameter × 2 mm height molds were prepared for rheology. Cylindrical 20 mm diameter × 1 mm height and 8 mm diameter × 1 mm height molds were prepared for cytotoxicity assays. The crosslinking solution filled the molds and was then irradiated at a distance of 10 inches under a 24 W, 460 nm, 14 × 14 LED array for 10 min. The hydrogels were removed from the molds and stored in glass scintillation vials covered with aluminum foil.

Rheology

The viscoelastic mechanical properties of the hydrogels were analyzed by small amplitude oscillatory shear rheology on a Discovery Hybrid Rheometer 2 (TA Instruments, USA) with a sandblasted 8 mm parallel plate geometry and a sandblasted stage. Inertia, friction, and rotational mapping calibrations were performed prior to each experiment. A Peltier temperature-controlled stage maintained 4°C for all rheology testing. The cylindrical hydrogel was cut to 8 mm diameter, transferred to the stage, and aligned with the geometry before lowering the gap height until the axial force reached 0.05 N. Strain sweeps were performed from 0.01 to 1,000% shear strain at a constant 10 rad/s angular frequency. G′ was determined by averaging the data points within the linear viscoelastic region of the strain sweep (Figure S3). Frequency sweeps were performed from 0.01 to 100 rad/s at a constant 0.1% shear strain where it showed the chemical gel behavior, G′ > G″. The statistical data analysis was conducted using Prism 8 software (GraphPad Software Inc., CA, USA; Tables S1–S3).

Fibroblast Culturing

For the hydrogel cytotoxicity and the MTT (3-(4,5-dimethylthiazol-2-yl)-2,5-diphenyltetrazolium bromide) assay, low passage (per ATCC guidelines) human neonatal foreskin fibroblast cells (ATCC CRL-2097) were cultured in Iscove's Modified Dulbecco's Media (IMDM) with 10% fetal bovine serum (FBS) without antibiotics at passage 12. Culturing conditions were kept at 37°C, 5% CO_2, and over 95% humidity. Assay plates (either 96 well or 12 well tissue culture treated plates) were seeded from fresh cultures that were harvested at about 75% confluence, as follows: 12-well tissue culture plates were seeded at 125,000 cells/1 mL, and 96-well tissue culture plates at 10,000 cells/100 µL per well.

Hydrogel Cytotoxicity Assay

A live dead viability/cytotoxicity kit (Invitrogen Cat# L3224) was used to assess hydrogel cytotoxicity. Prepared hydrogels remained protected from light at 4°C for up to 16 h before cytotoxicity testing. Prior to introduction to the 70–80% confluent monolayer, each hydrogel was soaked in 70% ethanol for 10 min protected from light at room temperature, soaked in 3 mL culture media for 5–10 min twice, then gently placed into a 12 well dish. Bright field images were taken at 48 h of co-culture with human neonatal foreskin fibroblast cells (ATCC CRL-2097), then hydrogels were gently removed from the 12 well plates. Culture media was carefully discarded without disturbing the monolayer. Cells were washed three times using 1 mL of dye solution (4 µM Ethidium homodimer-1 and 0.4 µM Calcein AM dye from the kit in D-PBS). After the wash, the dye solution was removed and discarded. A final application of 500 µL dye solution was added and the plate was incubated at room temperature for 1 h, then wrapped in foil and protected from light until imaging on the Bio-Rad ZOE Fluorescent Imager.

MTT Assay

Tissue culture treated 96 well plates were seeded with 10,000 fibroblast cells/100 µL of media (IMDM + 10% FBS). After 48 h, the plate was treated with varying final concentrations of freshly prepared sterile filtered solutions as follows: ammonium persulfate (APS) (0.75 mM, 0.25 mM); $[Ru(II)bpy_3]^{2+}$ (Ru) (125, 9 µM); as well as combinations: (9 µM Ru + 0.25 mM APS, 9 µM Ru + 0.75 mM APS). Each treatment was conducted in duplicate and placed in the incubator for 24 h. After 24 h, all media was removed and replaced with 100 µL phenol red free IMDM + 10% FBS. Cells were exposed to 1.2 mM MTT solution (Invitrogen Cat# M6494) and incubated for 4 h at 37°C. Per the manufacturer's rapid protocol, after incubation, 75 µL of media was removed and 50 µL of standard cell culture dimethyl sulfoxide (DMSO) (Invitrogen Cat# D12345) was added to each well, gently mixed and incubated at 37°C for 10 min. After 10 min, the plate was placed in a standard plate reader, shaken for 20 s and read at 540 nm. The assay was repeated on 4 separate days.

Results and Discussion

To investigate targeted hydrogel elastic moduli (G′), photocrosslinked ELP(Tyr) hydrogels were prepared using assorted molar concentrations of Ru ([Ru]) and APS ([APS]), then evaluated using rheology. The cytotoxicity of hydrogels from different photocrosslinking formulations with similar G′ were examined to develop a method to prepare non-cytotoxic materials using Ru-catalyzed dityrosine photocrosslinking.

Targeted Hydrogel Elastic Moduli With Multiple Material Formulations

Typical concentrations of Ru and APS used in dityrosine photocrosslinked hydrogels range from 100 to 1,000 μM Ru and 10 to 100 mM APS (Elvin et al., 2010; Fang and Li, 2012; Ding et al., 2013; Zhang et al., 2017; Min et al., 2018). The conversion of $[Ru(II)bpy_3]^{2+}$ to $[Ru(II)bpy_3]^{3+}$ consumes APS, thus we expect G′ can be controlled by modulating [APS] in the crosslinking formulation. We investigated variable [APS] from 15 to 120 mM with [Ru] held constant at 125 μM (squares in Figure 2A). We observed that a particular G′ can be targeted below 24 kPa by modulating [APS] up to 60 mM. There was no significiant difference between G′ with 60 mM APS and 120 mM APS ($P = 0.769$, Table S2), indicating that either a limited molarity of tyrosine or Ru was keeping G′ from increasing between 60 and 120 mM APS. To determine whether G′ plateaued due to limited [Ru] or [tyrosine] in the crosslinking formulation, we prepared hydrogels with higher concentrations of Ru, the same concentration of ELP(Tyr), and the same range of APS concentrations.

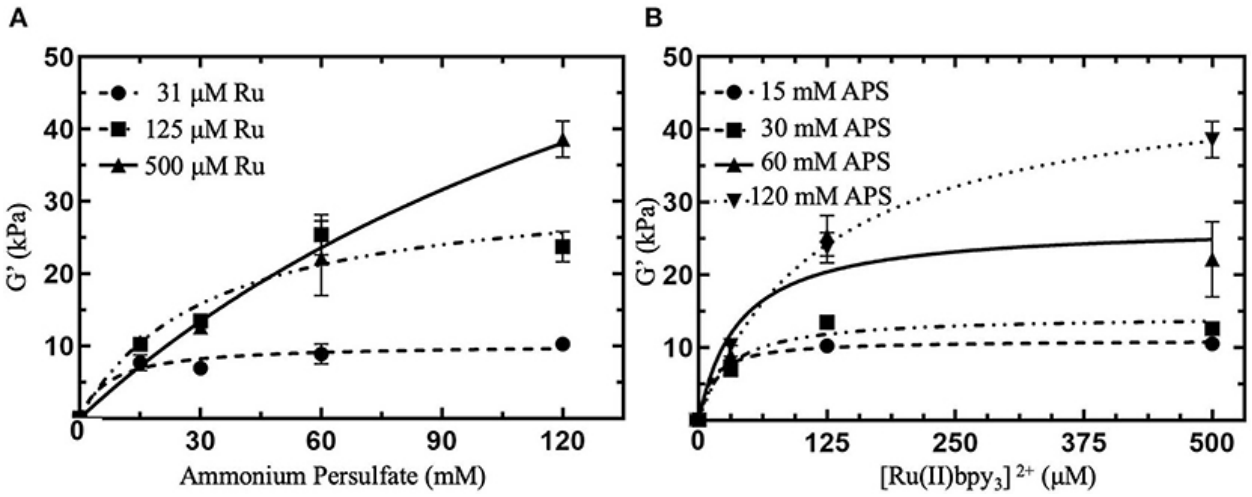

Figure 2. Shear elastic modulus (G′) of photocrosslinked polymeric hydrogels with various concentrations of crosslinking reagents. G′ were collected from linear viscoelastic region from small amplitude oscillatory shear measurements (Figure S3) and averaged (N = 3 for each data point). **(A)** G′ for hydrogels with APS molar concentrations, [APS], ranging from 15 to 120 mM with constant [Ru] between 31 and 500 μM. **(B)** G′ for hydrogels with [Ru] varied from 31 to 500 μM with constant [APS] ranging from 15 to 120 mM. All hydrogels contained 10 w/v % ELP(Tyr) dissolved in pH 7.5 phosphate buffer and were subject to 10 min of blue light photoactivation for crosslinking. Error bars represent standard deviation. Curves are least square fitting to the hyperbolic model that assumes the independent variable is a reagent that reaches saturating concentrations. **(B)** Is the reformatting of data in **(A)** with the x-axis relevent to [Ru] to investigate constant [APS]. For formulations with 0 mM [Ru] or [APS], we assumed G′ = 0 kPa since the hydrogel was not formed.

Photocrosslinked hydrogels were prepared with a 4-fold higher [Ru] to explore a possible increase in hydrogel G′. When [Ru] was increased from 125 to 500 μM at 120 mM APS, G′ of hydrogels were enhanced from ~24 to 38.6 ± 2.5 kPa (triangles in Figure 2A). Contrasting with 125 μM Ru, G′ (22.2 ± 5.2 kPa) for 500 μM Ru was enhanced by 74% when increasing APS from 60 to 120

mM. We attempted to examine the maximum G′ for 500 μM Ru by increasing [APS] beyond 120 mM, but these hydrogels fractured during crosslinking, making further hydrogel measurements not reproducible (Figure S4). Consequently, for ELP(Tyr) hydrogels with 500 μM Ru, [APS] can be modulated to target a particular G′ up to 40 kPa.

To investigate further control of hydrogel G′ using Ru, we tested a 4-fold decrease in [Ru] from 125 to 31 μM. G′ of prepared hydrogels with 31 μM Ru ranged from ~8–10 kPa (circles in Figure 2A), and showed no significant differences in G′ for [APS] between 15 and 120 mM ($P > 0.05$ for all comparisons, Table S2). In summary, 31 μM Ru caused G′ to plateau at all measured APS concentrations (circles in Figure 2A), 125 μM Ru caused G′ to increase between 15 and 60 mM APS but plateau between 60 and 120 mM APS (squares in Figure 2A), while for 500 μM Ru, G′ increased continuously without plateauing (triangles in Figure 2A). This confirms that [Ru] must be high enough (≥500 μM) for APS to be used to modulate G′ up to 40 kPa.

Furthermore, we investigated controlling G′ by holding [APS] constant and modulating [Ru] from 31 to 500 μM to ascertain whether both Ru and APS can act as limiting reagents (Figure 2B). In crosslinking formulations with 15 mM APS, all hydrogels had similar G′ ranging from ~8 to 11 kPa (circles in Figure 2B; $P > 0.05$ for all comparisons, Table S3). For constant 30 and 60 mM APS, there was an increase in G′ when [Ru] was increased from 31 to 125 μM ($P = 0.0022$; $P < 0.0001$, Table S3). However, G′ plateaued when [Ru] was increased from 125 to 500 μM ($P > 0.05$, Table S3). While 120 mM APS was held constant in crosslinking formulations, G′ continously increased from 10.3 ± 0.8 kPa at 31 μM Ru to 38.6 ± 2.5 kPa at 500 μM Ru (inverted triangles in Figure 2B; $P < 0.0001$, Table S3). Altogether, G′ was enhanced when [Ru] increased between 125 and 500 μM for constant 120 mM APS but plateaued when [APS] was 60 mM or

below. Thus, controlling the concentration of Ru can be used to target G′ of ELP(Tyr) hydrogels when the APS concentration is not limiting.

When either [Ru] or [APS] is held constant, the other reagent concentration can be modulated to change hydrogel G′. While it has been shown that G′ of Ru-mediated dityrosine crosslinked materials can be altered by modulating persulfate or polymer concentrations in crosslinking formulations with high [Ru] (≥1 mM) (Jeon et al., 2015; Yang et al., 2015), with these results, it can be concluded that [Ru], [APS], and the tyrosyl-incorporated polymer concentration can all control G′ of Ru-mediated dityrosine photocrosslinked hydrogels independent of an excess concentration of other parameters.

Multiple photocrosslinking formulations with different concentrations of Ru and APS can target similar G′ of polymeric materials because Ru and APS can each function as a limiting reagent with respect to G′. For example, 31 μM Ru limits G′ for APS between 15 and 120 mM, resulting in ~8–10 kPa hydrogels (circles in Figure 2A), while 15 mM APS limits G′ for Ru between 31 and 500 μM, also resulting in ~8–11 kPa hydrogels (circles in Figure 2B). Additionally, optimal formulations can be prepared that contain limiting concentrations of both reagents that target a specific G′, such as 8–11 kPa (Figure S5). Although multiple formulations can be used to prepare polymeric materials with similar G′, excess reagents can impact hydrogel cytotoxicity. Therefore, it is necessary to investigate how reagent concentrations that prepare hydrogels can adversely affect cytotoxicity to inform if they are suitable to prepare biomaterials.

Cytotoxicity Analysis of Hydrogels Prepared by Multiple Crosslinking Formulations

To examine potential cytotoxic effects of different formulations when preparing Ru-mediated crosslinked polymeric hydrogels with similar elastic moduli (G′), we prepared three formulations

of various [Ru] and [APS] that each target G′ to ~10 kPa (Figure 2): low [Ru] and low [APS] (31 μM Ru, 15 mM APS), high [Ru] and low [APS] (125 μM Ru, 15 mM APS), and low [Ru] and high [APS] (31 μM Ru, 120 mM APS).

The prepared hydrogels were applied to human primary fibroblasts at 70–80% confluence in clutures to understand if some formulations can negatively impact cell growth. We found that hydrogels prepared with low APS and either low or high Ru (Figures 3A,B) showed no cytotoxicity compared to controlled cell growth with no hydrogel added (Figure 3D). In contrast, the hydrogels prepared with low Ru and high APS were cytotoxic (Figure 3C). Therefore, the amount of APS leaching out from the hydrogel and coming into contact with the fibroblasts is likely correlated with the increase in cytotoxicity.

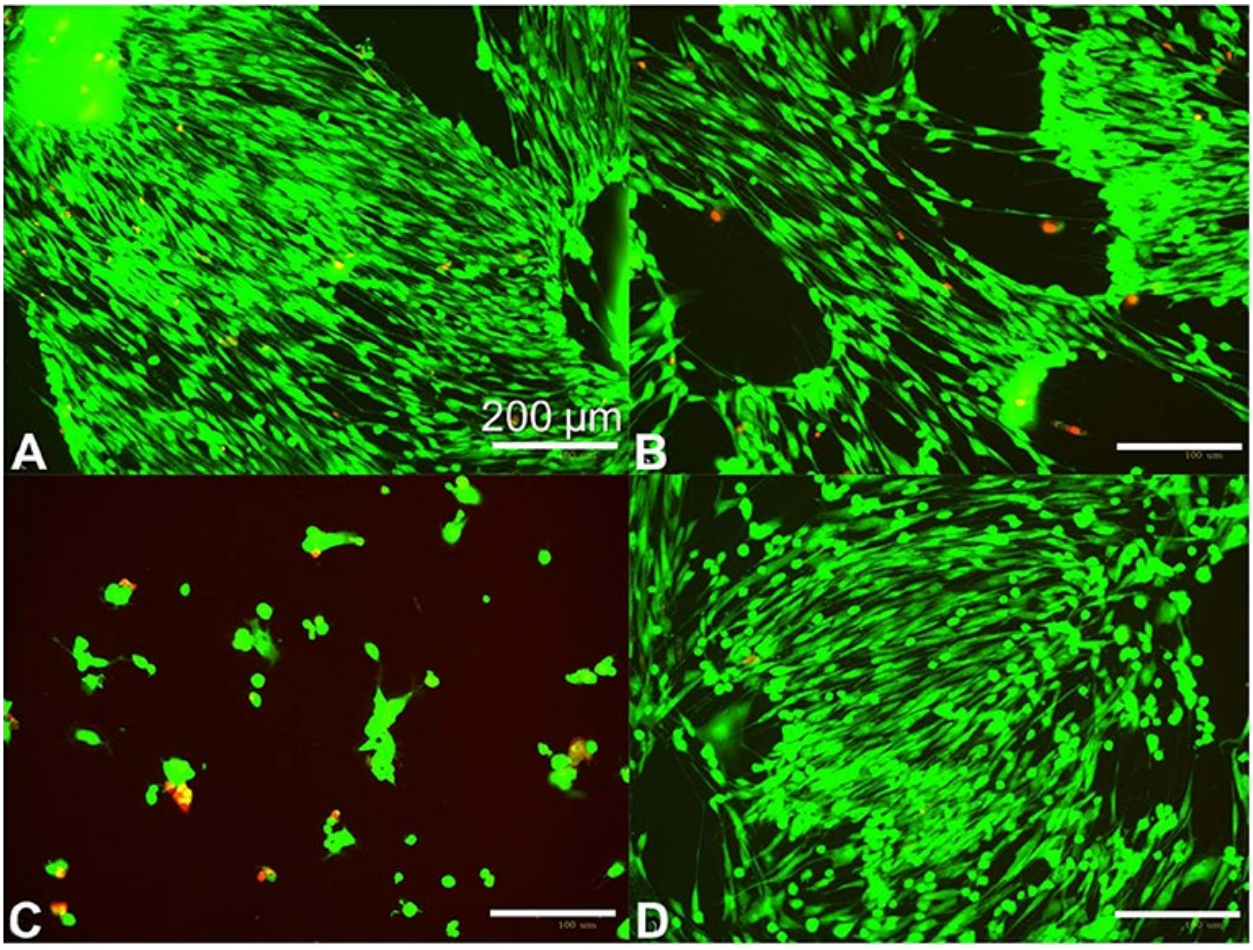

Figure 3. Human fibroblast cytotoxicity/viability assay for ~10 kPa hydrogels prepared using different photocrosslinking formulations. Fibroblasts were seeded at 125,000 cells per well and grown overnight in standard 12 well dishes, then treated at 70–80% confluence with 20 mm diameter × 1 mm height crosslinked hydrogels for 48 h. Hydrogels were prepared with 10 w/v% ELP(Tyr) and 125 μM Ru/15 mM APS **(A)**, 31 μM Ru/15 mM APS **(B)**, and 31 μM Ru/120 mM APS **(C)**. The hydrogel was omitted in the control well **(D)**. Green fluorescence indicates live cells while red indicates dead cells. Bright field images are available in Figure S7.

We anticipated that the total mass of APS in the hydrogel could be the major factor compared to the APS molar concentration in the hydrogel because the total mass of released APS will increase the APS concentration in a given cell culture volume for the fibroblast cytotoxicity assay. To understand the impact of hydrogel volume on fibroblast cytotoxicity, we compared the 20 mm diameter × 1 mm height hydrogels that caused cytotoxicity (Figure 3C) to 8 mm diameter × 1 mm height hydrogels with various formulations in fibroblast cytotoxicity assays. The hydrogel volume to well volume ratio was 1:3 for the larger hydrogels and 1:20 for the smaller hydrogels. The smaller hydrogels showed no fibroblast cytotoxicity irrespective of formulation after 48 h (Table S4), while the larger hydrogels with 31 μM Ru and 120 mM APS were cytotoxic after 48 h (Figure 3C), indicating that the hydrogel with the greater total mass of APS showed increased cytotoxicity.

To confirm that the mass of APS in hydrogels will impact cytotoxicity, we added the total mass of APS used in the cytotoxic 20 mm diameter hydrogels with 120 mM APS to 8 mm diameter hydrogels, bringing the concentration in the 8 mm hydrogels to 750 mM APS. We found that the hydrogels with 120 mM APS did not disrupt cell growth compared to the control with no hydrogels added (Figures S6A,C), but despite constant G′ and hydrogel volume, hydrogels with 750 mM APS disrupted cell growth (Figure S6B). Thus, the total amount of APS is the major parameter

that determines cytotoxicity. Cytotoxicity assays performed by other groups have shown that biomaterials prepared with Ru-mediated crosslinking showed no cytotoxicity (Elvin et al., 2009; Syedain et al., 2009; Lv et al., 2013; Keating et al., 2019). This may be a result of lower amounts of excess APS in crosslinking formulations, testing being conducted on confluent monolayers or cells with low rates of proliferation (Williams et al., 2005), or the testing of hydrogels with smaller volumes and a lower total mass of crosslinking reagents relative to cell media volume to dilute excess reagents.

The direct impact of [Ru] and [APS] on fibroblast cytotoxicity was quantified using MTT assays. We found [Ru] up to 125 μM did not affect fibroblast cytotoxicity, while [APS] even at 0.25 mM showed cytotoxicity (Figure S8). These data indicate that high APS concentrations should be carefully avoided in crosslinking formulations due to acute cytotoxicity. It has been suggested that the consumption of APS in the reaction reduces the toxicity of produced hydrogels compared to the formulation before photoactivation (Elvin et al., 2009). Yet, hydrogels with the higher [APS] depicted in Figure 3C were cytotoxic. In those hydrogels, 120 mM APS is in excess of the concentration necessary to reach ~10 kPa because similar G′ can be obtained with 15 mM APS at the same low Ru concentration (circles in Figure 2A). It is expected that the excess APS was not consumed in the reaction since G′ was limited by low [Ru]. Thus, the hydrogel leaked unreacted APS into the fibroblast media and caused cytotoxicity. The hydrogel cytotoxicity was reduced for smaller hydrogels because the amount of excess APS that leaked out into the media was less than the larger hydrogel prepared with the same [APS] in the constant well volume. However, smaller hydrogels or larger well volumes to reduce [APS] in cell media may not realistically represent possible clinical applications. Therefore, hydrogels that are prepared with just enough APS to

target the elastic modulus while avoiding excess [APS] can result in lower unreacted [APS] in the prepared hydrogel for reduced cytotoxicity.

A similar approach to preparing crosslinking formulations is necessary when considering [Ru]. Since Ru is implicated as a DNA intercalator, avoiding excess [Ru] in crosslinking formulations could improve biocompatibility of Ru-mediated photocrosslinked materials. We found that modulation of [Ru] was effective to control G′ such that low [Ru] could consistently target a lower G′ independent of [APS] and excess crosslinking time. Yet, the recyclability of Ru in this reaction has led to speculation that Ru cannot be effectively used to modulate G′ (Syedain et al., 2009). The cyclic conversion of $[Ru(II)bpy_3]^{2+}$ to $[Ru(II)bpy_3]^{3+}$ by APS oxidation and back to $[Ru(II)bpy_3]^{2+}$ by tyrosyl reduction would seem to allow for lower [Ru] to reach the same G′ given more time. However, the activity of Ru was temporally limited for the photocrosslinking of ELP(Tyr), shown by formulations with excess [APS] but lower G′ compared to formulations with the same [APS] but increased [Ru] (circles compared to triangles in Figure 2A). This finding indicates [Ru] and [APS] must be high enough to target a particular G′. Yet, excess [Ru] and [APS] can be avoided for enhanced biocompatibility by systematically evaluating possible formulations to reach a target G′ value for a given tyrosyl-containing polymer.

Funding

This research was supported by the Accelerate for Success award from Research, Discovery & Innovation at the University of Arizona and in part by the University of Arizona Biomedical Engineering Department (CC), the University of Arizona Applied Biosciences GIDP (IP), the National Heart, Lung, and Blood Institute of the National Institutes of Health (T32HL007955; DK), and the ARCS Foundation Templin Endowment (DK). The content was solely the responsibility

of the authors and does not necessarily represent the official views of the National Institutes of Health.

Conflict of Interest

The authors declare that the research was conducted in the absence of any commercial or financial relationships that could be construed as a potential conflict of interest.

Acknowledgments

The authors would like to thank Dr. Dongkyun Kang laboratory at the University of Arizona for providing 3D-printed molds to fabricate hydrogels.

References

Aeschbach, R., Amado, R., and Neukom, H. (1976). Formation of dityrosine cross-links in proteins by oxidation of tyrosine residues. *Biochim. Biophys. Acta* 439, 292–301. doi: 10.1016/0005-2795(76)90064-7

Ang, W. H., and Dyson, P. J. (2006). Classical and non-classical ruthenium-based anticancer drugs: towards targeted chemotherapy. *Eur. J. Inorg. Chem.* 20, 4003–4018. doi: 10.1002/ejic.200600723

Annabi, N., Zhang, Y. N., Assmann, A., Sani, E. S., Cheng, G., Antonio, D. L., et al. (2017). Engineering a highly elastic human protein-based sealant for surgical applications. *Sci. Transl. Med.* 9:eaai7466. doi: 10.1126/scitranslmed.aai7466

Applegate, M. B., Partlow, B. P., Coburn, J., Marelli, B., Pirie, C., Roberto, P., et al. (2016). Photocrosslinking of silk fibroin using riboflavin for ocular prostheses. *Adv. Mater. Technol.* 28, 2417–2420. doi: 10.1002/adma.201504527

Bajaj, P., Schweller, R. M., Khademhosseini, A., West, J. L., and Bashir, R. (2014). 3D biofabrication strategies for tissue engineering and regenerative medicine. *Annu. Rev. Biomed. Eng.* 16, 247–276. doi: 10.1146/annurev-bioeng-071813-105155

Bang, S., Jung, U., and Noh, I. (2018). Synthesis and biocompatibility characterizations of *in situ* chondroitin sulfate-gelatin hydrogel for tissue engineering. *Tissue Eng. Regen. Med.* 15, 25–35. doi: 10.1007/s13770-017-0089-3

Chaudhuri, O., Gu, L., Klumpers, D., Darnell, M., Bencherif, S. A., James, C., et al. (2016). Hydrogels with tunable stress relaxation regulate stem cell fate and activity. *Nat. Mater.* 15, 326–334. doi: 10.1038/nmat4489

Christensen, T., Hassouneh, W., Trabbic-Carlson, K., and Chilkoti, A. (2013). Predicting transition temperatures of elastin-like polypeptide fusion proteins. *Biomacromolecules* 14, 1514–1519. doi: 10.1021/bm400167h

Ding, Y., Li, Y., Qin, M., Cao, Y., and Wang, W. (2013). Photo-cross-linking approach to engineering small tyrosine-containing peptide hydrogels with enhanced mechanical stability. *Langmuir* 29, 13299–13306. doi: 10.1021/la4029639

Donnelly, P. E., Chen, T., Finch, A., Brial, C., Maher, S. A., and Torzilli, P. A. (2017). Photocrosslinked tyramine-substituted hyaluronate hydrogels with tunable mechanical properties improve immediate tissue-hydrogel interfacial strength in articular cartilage. *J. Biomater. Sci. Polym. Ed.* 28, 582–600. doi: 10.1080/09205063.2017.1289035

Dzuricky, M., Roberts, S., and Chilkoti, A. (2018). Convergence of artificial protein polymers and intrinsically disordered proteins. *Biochemistry* 57, 2405–2414. doi: 10.1021/acs.biochem.8b00056

Elvin, C. M., Brownlee, A. G., Huson, M. G., Tebb, T. A., Kim, M., Russell, E., et al. (2009). The development of photochemically crosslinked native fibrinogen as a rapidly formed and mechanically strong surgical tissue sealant. *Biomaterials* 30, 2059–2065. doi: 10.1016/j.biomaterials.2008.12.059

Elvin, C. M., Carr, A. G., Huson, M. G., Maxwell, J. M., Pearson, R. D., Tony, V., et al. (2005). Synthesis and properties of crosslinked recombinant pro-resilin. *Nature* 437, 999–1002. doi: 10.1038/nature04085

Elvin, C. M., Vuocolo, T., Brownlee, A. G., Sando, L., Huson, M. G., Nancy, E., et al. (2010). A highly elastic tissue sealant based on photopolymerised gelatin. *Biomaterials* 31, 8323–8331. doi: 10.1016/j.biomaterials.2010.07.032

Engler, A. J., Sen, S., Sweeney, H. L., and Discher, D. E. (2006). Matrix elasticity directs stem cell lineage specification. *Cell* 126, 677–689. doi: 10.1016/j.cell.2006.06.044

Fancy, D. A., and Kodadek, T. (1999). Chemistry for the analysis of protein-protein interactions: rapid and efficient cross-linking triggered by long wavelength light. *Proc. Natl. Acad. Sci. U.S.A.* 96, 6020–6024. doi: 10.1073/pnas.96.11.6020

Fang, J., and Li, H. (2012). A facile way to tune mechanical properties of artificial elastomeric proteins-based hydrogels. *Langmuir* 28, 8260–8265. doi: 10.1021/la301225w

Gill, M. R., Harun, S. N., Halder, S., Boghozian, R. A., Ramadan, K., Haslina, A., et al. (2016). A ruthenium polypyridyl intercalator stalls DNA replication forks, radiosensitizes human cancer cells and is enhanced by Chk1 inhibition. *Sci. Rep.* 6:31973. doi: 10.1038/srep39363

Gu, Y., Zhao, J., and Johnson, J. A. (2020). Polymer networks: from plastics and gels to porous frameworks. *Angew. Chem. Int. Ed. Engl.* 59, 2–30. doi: 10.1002/anie.201902900

Gu, Y. W., Kawamoto, K., Zhong, M. J., Chen, M., Hore, M. J. A., Alex, M. J., et al. (2017). Semibatch monomer addition as a general method to tune and enhance the mechanics of polymer networks via loop-defect control. *Proc. Natl. Acad. Sci. U.S.A.* 114, 4875–4880. doi: 10.1073/pnas.1620985114

Guvendiren, M., and Burdick, J. A. (2012). Stiffening hydrogels to probe short- and long-term cellular responses to dynamic mechanics. *Nat. Commun.* 3:792. doi: 10.1038/ncomms1792

Ingrole, R. S., Tao, W., Tripathy, J. N., and Gill, H. S. (2014). Synthesis and immunogenicity assessment of elastin-like polypeptide-M2e construct as an influenza antigen. *Nano Life* 4:1450004. doi: 10.1142/S1793984414500044

Jeon, E. Y., Hwang, B. H., Yang, Y. J., Kim, B. J., Choi, B. H., Gyu, Y. J., et al. (2015). Rapidly light-activated surgical protein glue inspired by mussel adhesion and insect structural crosslinking. *Biomaterials* 67, 11–19. doi: 10.1016/j.biomaterials.2015.07.014

Kato, Y., Uchida, K., and Kawakishi, S. (1994). Aggregation of collagen exposed to uva in the presence of riboflavin–a plausible role of tyrosine modification. *Photochem. Photobiol.* 59, 343–349. doi: 10.1111/j.1751-1097.1994.tb05045.x

Keating, M., Lim, M., Hu, Q., and Botvinick, E. (2019). Selective stiffening of fibrin hydrogels with micron resolution via photocrosslinking. *Acta Biomater.* 87, 88–96. doi: 10.1016/j.actbio.2019.01.034

Khanmohammadi, M., Nemati, S., Ai, J., and Khademi, F. (2019). Multipotency expression of human adipose stem cells in filament-like alginate and gelatin derivative hydrogel fabricated through visible light-initiated crosslinking. *Mater. Sci. Eng. C Mater. Biol. Appl.* 103:109808. doi: 10.1016/j.msec.2019.109808

Kim, C. S., Yang, Y. J., Bahn, S. Y., and Cha, H. J. (2017). A bioinspired dual-crosslinked tough silk protein hydrogel as a protective biocatalytic matrix for carbon sequestration. *NPG Asia Mater.* 9:e391. doi: 10.1038/am.2017.71

Kim, M., Chen, W. G., Kang, J. W., Glassman, M. J., Ribbeck, K., and Olsen, B. D. (2015). Artificially engineered protein hydrogels adapted from the nucleoporin NSP1 for selective biomolecular transport. *Adv. Mater.* 27, 4207–4212. doi: 10.1002/adma.201500752

Kroll, D. M., and Croll, S. G. (2015). Influence of crosslinking functionality, temperature and conversion on heterogeneities in polymer networks. *Polymer* 79, 82–90. doi: 10.1016/j.polymer.2015.10.020

Lim, K. S., Klotz, B. J., Lindberg, G. C. J., Melchels, F. P. W., Hooper, G. J., Jos, M., et al. (2019). Visible light cross-linking of gelatin hydrogels offers an enhanced cell microenvironment with improved light penetration depth. *Macromol. Biosci.* 19:e1900098. doi: 10.1002/mabi.201900098

Liu, H. Y., Nguyen, H. D., and Lin, C. C. (2018). Dynamic peg-peptide hydrogels via visible light and fmn-induced tyrosine dimerization. *Adv. Healthc. Mater.* 7:e1800954. doi: 10.1002/adhm.201800954

Lv, S., Bu, T., Sayser, J., Bausch, A., and Li, H. (2013). Towards constructing extracellular matrix-mimetic hydrogels: an elastic hydrogel constructed from tandem modular proteins containing tenascin FnIII domains. *Acta Biomater*. 9, 6481–6491. doi: 10.1016/j.actbio.2013.01.002

Melchels, F. P. W., Feijen, J., and Grijpma, D. W. (2010). A review on stereolithography and its applications in biomedical engineering. *Biomaterials* 31, 6121–6130. doi: 10.1016/j.biomaterials.2010.04.050

Meyer, D. E., and Chilkoti, A. (1999). Purification of recombinant proteins by fusion with thermally-responsive polypeptides. *Nat. Biotechnol.* 17, 1112–1115. doi: 10.1038/15100

Min, K. I., Kim, D. H., Lee, H. J., Lin, L. W., and Kim, D. P. (2018). Direct synthesis of a covalently self-assembled peptide nanogel from a tyrosine-rich peptide monomer and its biomineralized hybrids. *Angew. Chem. Int. Ed. Engl.* 57, 5630–5634. doi: 10.1002/anie.201713261

Nickel, U., Chen, Y. H., Schneider, S., Silva, M. I., Burrows, H. D., and Formosinho, S. J. (1994). Mechanism and kinetics of the photocatalyzed oxidation of p-phenylenediamines by peroxydisulfate in the presence of tri-2,2′-bipyridylylruthenium(Ii). *J. Phys. Chem.* 98, 2883–2888. doi: 10.1021/j100062a026

Partlow, B. P., Applegate, M. B., Omenetto, F. G., and Kaplan, D. L. (2016). Dityrosine cross-linking in designing biomaterials. *ACS Biomater. Sci. Eng.* 2, 2108–2121. doi: 10.1021/acsbiomaterials.6b00454

Roberts, S., Dzuricky, M., and Chilkoti, A. (2015). Elastin-like polypeptides as models of intrinsically disordered proteins. *FEBS Lett.* 589, 2477–2486. doi: 10.1016/j.febslet.2015.08.029

Sakai, S., Kamei, H., Mori, T., Hotta, T., Ohi, H., Masaki, N., et al. (2018). Visible light-induced hydrogelation of an alginate derivative and application to stereolithographic bioprinting using a visible light projector and acid red. *Biomacromolecules* 19, 672–679. doi: 10.1021/acs.biomac.7b01827

Simnick, A. J., Lim, D. W., Chow, D., and Chilkoti, A. (2007). Biomedical and biotechnological applications of elastin-like polypeptides. *Polymer Rev.* 47, 121–154. doi: 10.1080/15583720601109594

Song, C., Wang, L. Y., Ye, G. L., Song, X. P., He, Y. T., and Qiu, X. Z. (2017). Residual ammonium persulfate in nanoparticles has cytotoxic effects on cells through epithelial-mesenchymal transition. *Sci. Rep.* 7:11769. doi: 10.1038/s41598-017-12328-0

Spikes, J. D., Shen, H. R., Kopeckova, P., and Kopecek, J. (1999). Photodynamic crosslinking of proteins. iii. kinetics of the Fmn- and rose bengal-sensitized photooxidation and intermolecular crosslinking of model tyrosine-containing *N*-(2-hydroxypropyl)methacrylamide copolymers. *Photochem. Photobiol.* 70, 130–137. doi: 10.1111/j.1751-1097.1999.tb07980.x

Syedain, Z. H., Bjork, J., Sando, L., and Tranquillo, R. T. (2009). Controlled compaction with ruthenium-catalyzed photochemical cross-linking of fibrin-based engineered connective tissue. *Biomaterials* 30, 6695–6701. doi: 10.1016/j.biomaterials.2009.08.039

Urry, D. W., Parker, T. M., Reid, M. C., and Gowda, D. C. (1991). Biocompatibility of the bioelastic materials, poly(gvgvp) and its gamma-irradiation cross-linked matrix–summary of generic biological test-results. *J. Bioact. Compat. Polym.* 63, 263–282. doi: 10.1177/088391159100600306

Urry, D. W., Trapane, T. L., and Prasad, K. U. (1985). Phase-structure transitions of the elastin polypentapeptide water-system within the framework of composition temperature studies. *Biopolymers* 24, 2345–2356. doi: 10.1002/bip.360241212

Valot, L., Martinez, J., Mehdi, A., and Subra, G. (2019). Chemical insights into bioinks for 3d printing. *Chem. Soc. Rev.* 48, 4049–4086. doi: 10.1039/C7CS00718C

Williams, C. G., Malik, A. N., Kim, T. K., Manson, P. N., and Elisseeff, J. H. (2005). Variable cytocompatibility of six cell lines with photoinitiators used for polymerizing hydrogels and cell encapsulation. *Biomaterials* 26, 1211–1218. doi: 10.1016/j.biomaterials.2004.04.024

Yang, Y. J., Holmberg, A. L., and Olsen, B. D. (2017). Artificially engineered protein polymers. *Annu. Rev. Chem. Biomol. Eng.* 8, 549–575. doi: 10.1146/annurev-chembioeng-060816-101620

Yang, Y. J., Kim, C. S., Choi, B. H., and Cha, H. J. (2015). Mechanically durable and biologically favorable protein hydrogel based on elastic silklike protein derived from sea anemone. *Biomacromolecules* 16, 3819–3826. doi: 10.1021/acs.biomac.5b01130

Zhang, D., Peng, H., Sun, B. C., and Lyu, S. S. (2017). High water content silk protein-based hydrogels with tunable elasticity fabricated via a ru(ii) mediated photochemical cross-linking method. *Fibers Polym.* 18, 1831–1840. doi: 10.1007/s12221-017-7463-6

Supplementary Material

Noncytotoxic dityrosine photocrosslinked polymeric materials with targeted elastic moduli

Camp, Christopher P.[1]; Peterson, Ingrid L.[2,4]; Knoff, David S.[1]; Melcher, Lauren G.[4]; Maxwell, Connor J.[1]; Cohen, Audrey T.[1]; Wertheimer, Anne M.[2,4,*]; Kim, Minkyu[1,3,4,*]

[1]Department of Biomedical Engineering, University of Arizona, Tucson, Arizona, 85721, USA

[2]Applied Biosciences GIDP, University of Arizona, Tucson, Arizona, 85721, USA

[3]Department of Materials Science & Engineering, University of Arizona, Tucson, Arizona, 85721, USA

[4]BIO5 Institute, University of Arizona, Tucson, Arizona, 85719, USA

Supplementary Material

Supplementary Figures

ELP(Tyr):

MGAGVPGAGVPGYGVPGAGVPGAGVPGAGVPGAGVPGYGVPGAGVPGAGVPGAGVP
GAGVPGYGVPGAGVPGAGVPGAGVPGAGVPGYGVPGAGVPGAGVPGAGVPGAGVPG
YGVPGAGVPGAGVPGAGVPGAGVPGYGVPGAGVPGAGVPGAGVPGAGVPGYGVPGA
GVPGAGVPGAGVPGAGVPGYGVPGAGVPGAGVPGAGVPGAGVPGYGVPGAGVPGAG
VPGAGVPGAGVPGYGVPGAGVPGAGVPGAGVPGAGVPGYGVPGAGVPGAGVPGAGV
PGAGVPGYGVPGAGVPGAGVPGAGVPGAGVPGYGVPGAGVPGAGVPGAGVPGAGVP
GYGVPGAGVPGAGVPGAGVPGAGVPGYGVPGAGVPGAGVPGAGVPGAGVPGYGVPG
AGVPGAGVPGAGVPGAGVPGYGVPGAGVPGAGVPGAGVPGAGVPGYGVPGAGVPGA
GVPGAGVPGAGVPGYGVPGAGVPGAGVPGAGVPGAGVPGYGVPGAGVPGAGVPGAG
VPGAGVPGYGVPGAGVPGAGVPGAGVPGAGVPGYGVPGAGVPGAGVPGAGVPGAGV
PGYGVPGAGVPGAGVPGAGVPGAGVPGYGVPGAGVPGAGVPGY

Figure S1. ELP(Tyr) protein sequence.

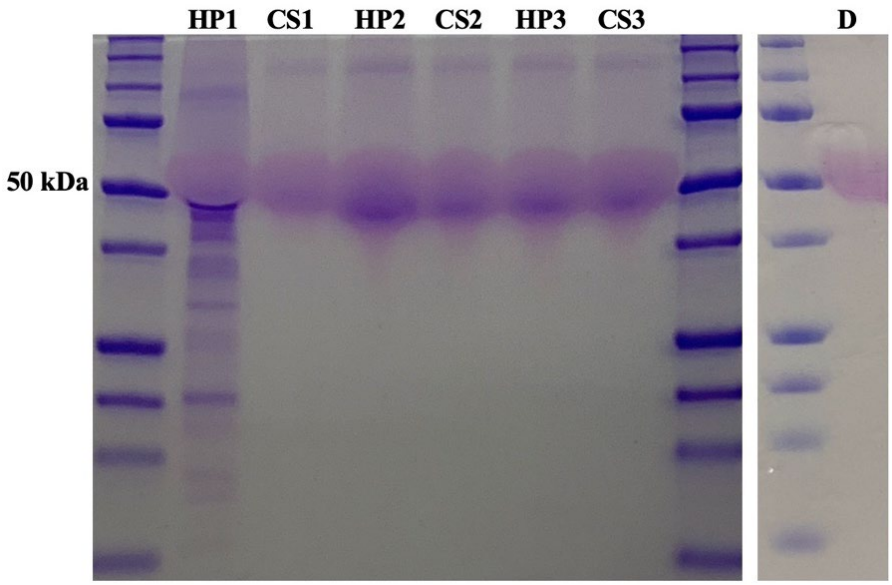

Figure S2. Purity of ELP(Tyr) analyzed via sodium dodecyl sulfate polyacrylamide gel electrophoresis (12% w/v) after the first purification step of inverse transition cycling purification. **HP1:** First resuspended ELP(Tyr) pellet; **CS1:** Soluble ELP(Tyr) fraction after centrifuging the resuspended first ELP(Tyr) pellet at 4°C; **HP2:** Second resuspended ELP(Tyr) pellet obtained by heating CS1 and centrifuging at 40°C; **CS2:** Soluble ELP(Tyr) fraction after centrifuging the resuspended second ELP(Tyr) pellet at 4°C; **HP3:** Third resuspended ELP(Tyr) pellet obtained by heating CS2 and centrifuging at 40°C; **CS3:** Soluble ELP(Tyr) fraction after centrifuging the resuspended third ELP(Tyr) pellet at 4°C. **D:** Dialyzed ELP(Tyr) solution. CS3 samples were dialyzed against deionized water, 7 times every 3+ hours at 4°C and then centrifuged at 4°C. Soluble ELP(Tyr) fractions were lyophilized and used to prepare ELP(Tyr) hydrogels.

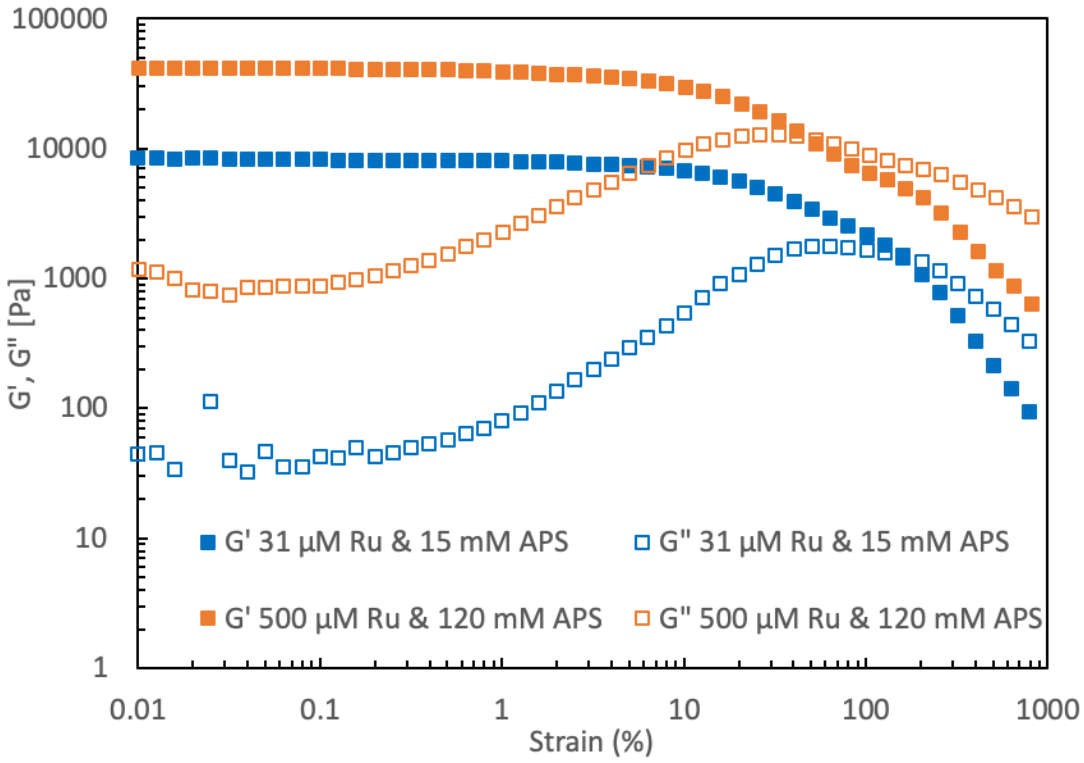

Figure S3. Strain sweep of hydrogels with 31 µM Ru and 15 mM APS, and 500 µM Ru and 120 mM APS. G' values between 0.01 rad/s and 0.1 rad/s were averaged to determine G'.

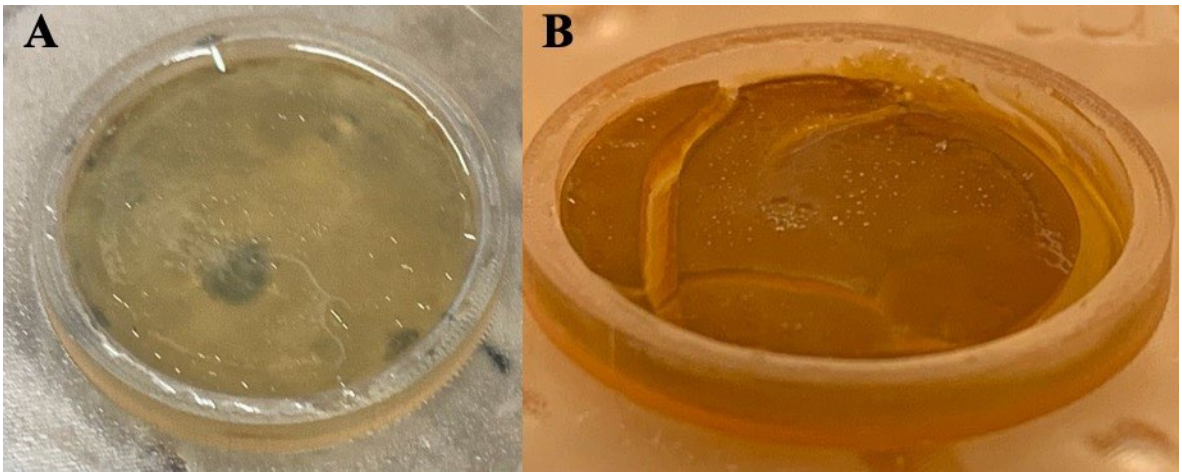

Figure S4. Hydrogels prepared with 10 w/v% ELP(Tyr) that were used to measure G' in Figure 2 or test cytotoxicity in Figure 3. **A:** 30 mM APS and 125 μM Ru hydrogel in 3D printed mold after crosslinking and **B:** 240 mM APS and 1 mM Ru fractured in the mold following crosslinking.

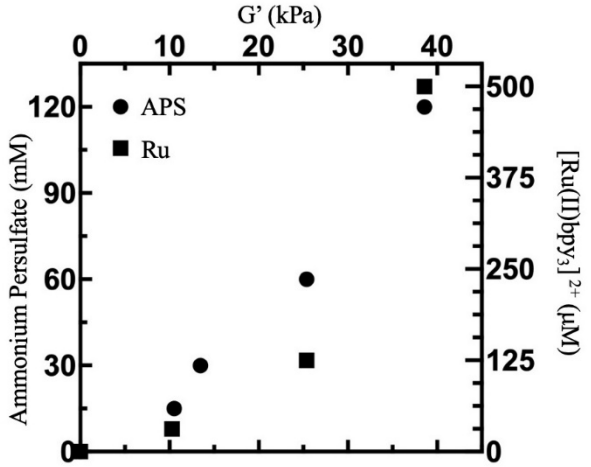

Figure S5. Scatter plot of optimized Ru and APS concentrations to reach a target G'. The points for each G' represent minimal concentrations of each reagent to reach that target G'. For example, to prepare 10 kPa or 25 kPa ELP(Tyr) hydrogels, 31 μM Ru/15 APS and 125 μM Ru/60 mM APS are limiting reagents to target that respective G'. For ~15 kPa, 30 mM APS is limiting, and the minimal Ru concentration should be between 31 μM and 125 μM to avoid

excess. Note that 500 μM Ru and 120 mM APS were the maximum concentrations tested because of hydrogel fracture during photocrosslinking (see Figure S4), thus one or both reagents may not be limiting at ~40 kPa.

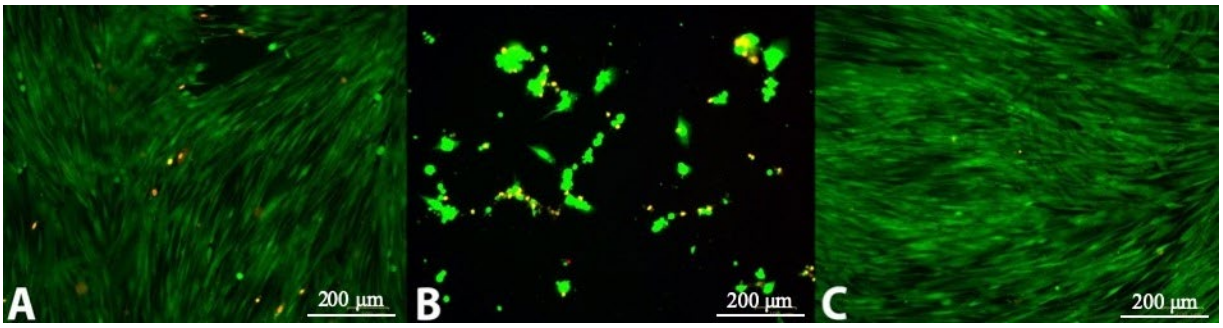

Figure S6. Human fibroblast cytotoxicity/viability assay for ~10 kPa hydrogels prepared using different photocrosslinking formulations. Fibroblasts were seeded at 100,000 cells per well in standard 12 well tissue culture dishes, then treated at 70-80% confluence with 8 mm diameter x 1 mm height hydrogels for 48 hours. Hydrogels were prepared with 10 w/v% ELP(Tyr) and **A:** 31 μM Ru/120 mM APS, **B:** 31 μM Ru/750 mM APS, and **C:** Control well without a hydrogel. Green fluorescence indicates live cells while red indicates dead cells.

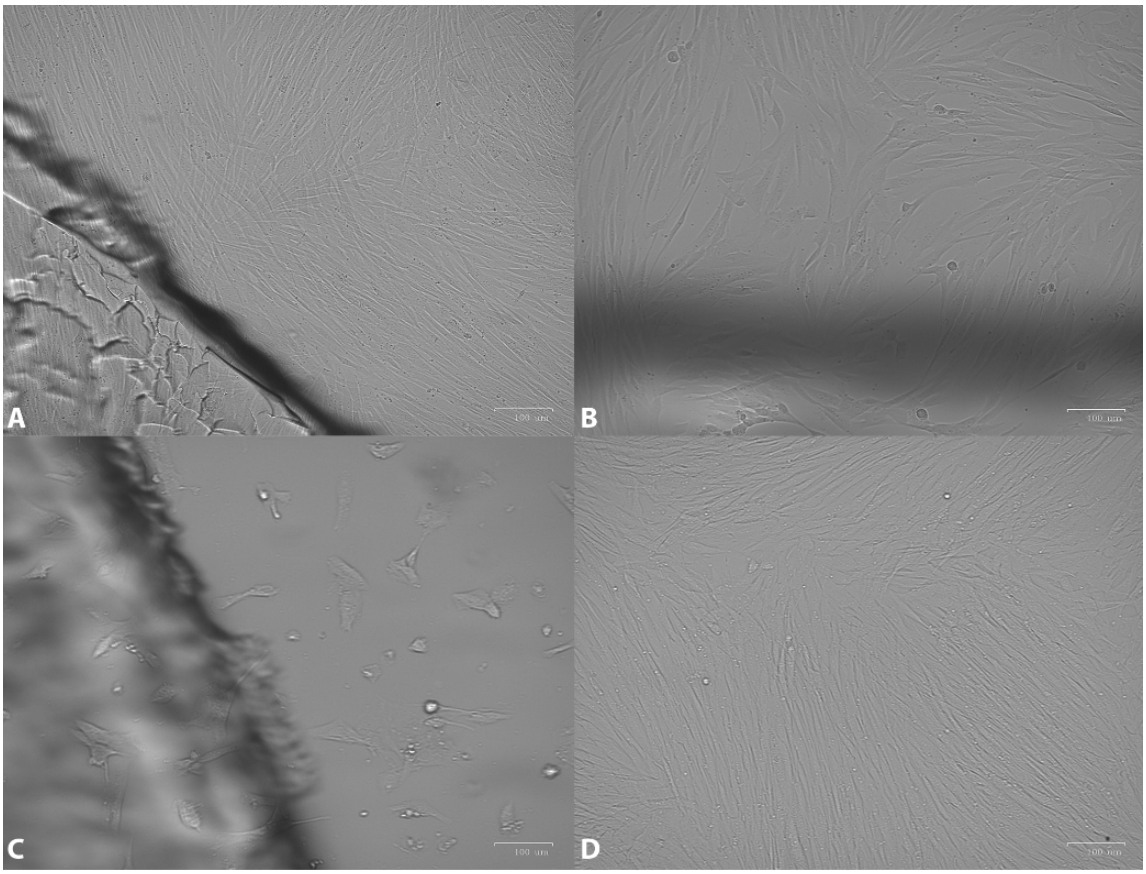

Figure S7. Bright field images of human fibroblasts from the LIVE/DEAD assay (Figure 3) at 48 hours. Fibroblasts were seeded at 125,000 cells per well overnight in standard 12 well dishes then treated at 70-80% confluence with 20 mm diameter x 1 mm height crosslinked hydrogels. **A** 125 μM Ru/15 mM APS; **B** 31 μM Ru/15 mM APS; **C** 31 μM Ru/120 mM APS; **D** Control well with no hydrogel.

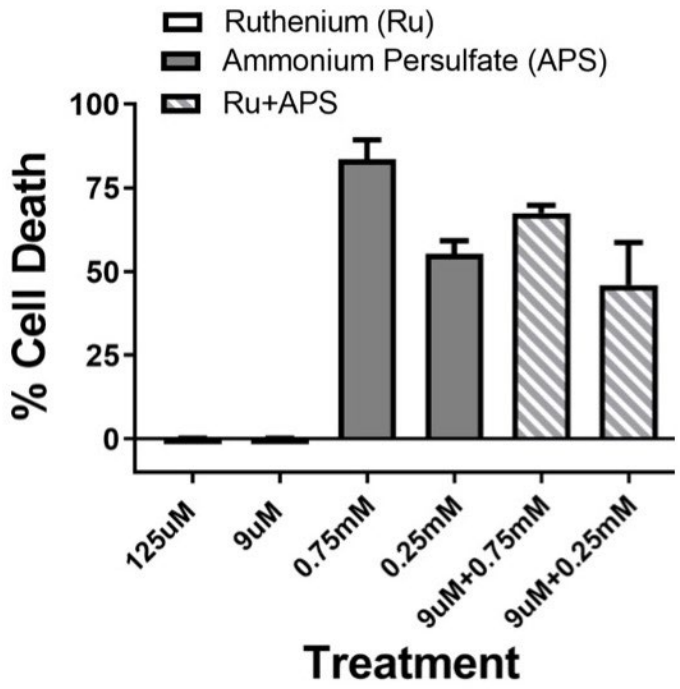

Figure S8. Impact of Ruthenium and Ammonium Persulfate Upon Human Neonatal Fibroblasts. Each compound was introduced to cells in duplicate upon confluence, incubated at 37°C with 5% CO_2 for 24 hours. A standard MTT assay was performed and read at 540 nm. Percent death was calculated based upon untreated cells.

Supplementary Tables

Table S1. 2way ANOVA results determined significant variation for different Ru and APS values. $\alpha = 0.05$.

Source of Variation	% of total variation	P value	P value summary	Significant?
APS + Ru	22.69	<0.0001	****	Yes
APS	40.90	<0.0001	****	Yes
Ru	33.10	<0.0001	****	Yes

ANOVA Table	SS	DF	MS	F (DFn, DFd)	P value
APS + Ru	712.1	6	118.7	F (6, 24) = 27.46	P<0.0001
APS	1284	3	428.0	F (3, 24) = 99.03	P<0.0001
Ru	1039	2	519.5	F (2, 24) = 120.2	P<0.0001
Residual	103.7	24	4.322		

Table S2. Tukey's multiple comparisons test comparing average G' values for hydrogels with constant [Ru] and variable [APS] for Figure 2A. N=3 for each formulation.

Constant Ru	**Mean Diff.**	**95.00% CI of diff.**	**Significant (P<0.05)**	**Summary**	**Adjusted P Value**
31 µM Ru					
15 mM APS vs. 30 mM APS	0.7294	-3.953 to 5.412	No	ns	0.9728
15 mM APS vs. 60 mM APS	-1.226	-5.908 to 3.457	No	ns	0.8873
15 mM APS vs. 120 mM APS	-2.607	-7.290 to 2.075	No	ns	0.4326
30 mM APS vs. 60 mM APS	-1.955	-6.637 to 2.727	No	ns	0.6619
30 mM APS vs. 120 mM APS	-3.337	-8.019 to 1.346	No	ns	0.2286
60 mM APS vs. 120 mM APS	-1.382	-6.064 to 3.301	No	ns	0.8472
125 µM Ru					
15 mM APS vs. 30 mM APS	-3.238	-7.920 to 1.444	No	ns	0.2515
15 mM APS vs. 60 mM APS	-15.15	-19.83 to -10.47	Yes	****	<0.0001

15 mM APS vs. 120 mM APS	-13.51	-18.19 to -8.825	Yes	****	<0.0001
30 mM APS vs. 60 mM APS	-11.91	-16.59 to -7.229	Yes	****	<0.0001
30 mM APS vs. 120 mM APS	-10.27	-14.95 to -5.587	Yes	****	<0.0001
60 mM APS vs. 120 mM APS	1.642	-3.040 to 6.324	No	ns	0.769
500 µM Ru					
15 mM APS vs. 30 mM APS	-2.084	-6.766 to 2.599	No	ns	0.616
15 mM APS vs. 60 mM APS	-11.66	-16.35 to -6.981	Yes	****	<0.0001
15 mM APS vs. 120 mM APS	-28.06	-32.74 to -23.38	Yes	****	<0.0001
30 mM APS vs. 60 mM APS	-9.58	-14.26 to -4.898	Yes	****	<0.0001
30 mM APS vs. 120 mM APS	-25.98	-30.66 to -21.29	Yes	****	<0.0001
60 mM APS vs. 120 mM APS	-16.4	-21.08 to -11.71	Yes	****	<0.0001

Table S3. Tukey's multiple comparisons test comparing average G' values for hydrogels with constant [APS] and variable [Ru] for Figure 2B. N=3 for each crosslinking formulation.

Constant APS	Mean Diff.	95.00% CI of diff.	Significant (P<0.05)	Summary	Adjusted P Value
15 mM APS					
31 μM Ru vs. 125 μM Ru	-2.558	-6.797 to 1.681	No	ns	0.3055
31 μM Ru vs. 500 μM Ru	-2.850	-7.089 to 1.388	No	ns	0.2336
125 μM Ru vs. 500 μM Ru	-0.2923	-4.531 to 3.946	No	ns	0.9838
30 mM APS					
31 μM Ru vs. 125 μM Ru	-6.525	-10.76 to -2.287	Yes	**	0.0022
31 μM Ru vs. 500 μM Ru	-5.663	-9.902 to -1.425	Yes	**	0.0075
125 μM Ru vs. 500 μM Ru	0.8620	-3.377 to 5.101	No	ns	0.8683
60 mM APS					
31 μM Ru vs. 125 μM Ru	-16.48	-20.72 to -12.24	Yes	****	<0.0001
31 μM Ru vs. 500 μM Ru	-13.29	-17.53 to -9.050	Yes	****	<0.0001
125 μM Ru vs. 500 μM Ru	3.194	-1.045 to 7.432	No	ns	0.1658
120 mM APS					
31 μM Ru vs. 125 μM Ru	-13.46	-17.70 to -9.220	Yes	****	<0.0001
31 μM Ru vs. 500 μM Ru	-28.30	-32.54 to -24.06	Yes	****	<0.0001
125 μM Ru vs. 500 μM Ru	-14.84	-19.08 to -10.61	Yes	****	<0.0001

Table S4. Human fibroblast cytotoxicity assay of 8 mm diameter x 1 mm height 10% ELP(Tyr) hydrogels. Various APS and Ru formulations were introduced to 70-80% confluent cells growing in standard 12 well dishes (22.1 mm diameter) with 1 mL media. 100% confluence of monolayer (+++) after 24 hours.

Formulation	8 mm x 1 mm Hydrogel Viability
125 µM Ru 15 mM APS	+++
31 µM Ru 15 mM APS	+++
31 µM Ru 120 mM APS	+++

APPENDIX C

Modulating the Mechanical Strength of Block Copolymer Hydrogels Comprised of Precisely Controlled Protein Polymers

Camp, Christopher P.[1]; Kim, Samuel Y.[1]; Doole, Fathima T.[2]; Knoff, David S.[1]; Kim, Minkyu[1,3,4,*]

[1]Department of Biomedical Engineering, University of Arizona, Tucson, Arizona, 85721, USA

[2]Department of Chemistry & Biochemistry, University of Arizona, Tucson, Arizona, 85721, USA

[3]Department of Materials Science & Engineering, University of Arizona, Tucson, Arizona, 85721, USA

[4]BIO5 Institute, University of Arizona, Tucson, Arizona, 85719, USA

Abstract

Hydrogels can have diverse physicochemical and stimulus-responsive properties based on molecular design parameters of polymer constituents. Compared to homopolymers, block copolymers feature added complexity for use in polymer networks for more intriguing structures and functionalities. However, those complex structures could interfere with the mechanical properties of polymer networks in unknown ways, and a comparison of polymer network mechanical properties between a homopolymer and a block copolymer that was formed as a rearrangement of the homopolymer has not yet been precisely evaluated. Here, we designed a block copolymer as a sequence rearrangement of a protein homopolymer that on its own can form hydrogels with elastic moduli targeted up to 40 kPa, in the range of many soft tissues, by modulating the concentrations of photoinitiators. We found that the block copolymer formed weaker polymeric hydrogels compared to the homopolymer, and we identified a method to overcome the loss of elastic moduli through a polymer mixture of the homopolymer and block copolymer. This serves as a well-controlled study to evaluate the degree to which self-assembled structures in a hydrophobic material forming blocks can alter the mechanical properties of polymeric materials and possible methods to overcome variation of hydrogel mechanical properties caused by interference of self-assembled structures. These findings can be useful in tissue engineering and drug delivery fields where block copolymers need to be integrated or stabilized into a polymer network while the mechanics of the polymer network need to be maintained.

Introduction

Polymers can be crosslinked to form polymeric networks and materials, such as hydrogels, with diverse chemical, mechanical, and stimulus-responsive properties based on monomer sequences, chain lengths, polymer concentrations, and environmental conditions[1-4]. Small changes in any of these factors can lead to large variations in the hydrogel mechanical properties, such as elastic modulus, arising from changes in the numbers of crosslinking sites, inter- and intra-molecular interactions, or entanglements. In healthcare applications, hydrogels are often used in tissue engineering to mimic the environmental conditions of natural extracellular matrices that enable cell survival[5-9]. It is critical for synthetic tissues to closely approximate the elastic moduli of soft tissues, ranging from 1 kPa to over 100 kPa, because cells can differentiate and proliferate differently based on the elasticity of the tissue[10-12]. Careful control of these parameters with conventional polymer synthesis techniques can be difficult because obtaining precisely monodisperse polymer chain lengths and sequences is often challenging.

Artificial protein polymers have gained attention for their precise monodispersed chain lengths and sequences and potential sustainable manufacturing that are permitted by genetic engineering and biosynthesis technologies, as well as self-assembled structures with mechanical or bioactive functionalities[13]. Engineered intrinsically disordered proteins (IDPs) are a class of artificial proteins that lack inherent secondary and higher order structures. However, biosynthetically designed IDPs can self-assemble into dynamic structures (e.g., micelles, cylinders, fibers, vesicles) that often form, disassemble, or change depending on external conditions, such as concentration, pH or temperature[14]. More complex self-assembled structures and biochemical functionalities can be utilized by designing IDP-based block copolymers because different

blocks can have various stimulus-responsive properties, mechanical stiffness, and biochemical activity. For example, one block can contain crosslinking sites to form a polymer network for tissue engineering applications, while the other block can be attached to but not trapped within the polymer network to serve as flexible tethers as attaching sites for peptides, such as signaling, therapeutic, cell recognizing, or antimicrobial, to construct multi-functional scaffolds for tissue engineering, wound dressing, and antimicrobial applications.

Among engineered IDPs, elastin-like polypeptides (ELPs) are extensively studied as research tools, artificial tissues, and drug delivery vehicles[15]. ELPs are composed of the amino acid sequence $(VPGXG)_n$, where X, the guest residue, can be any amino acid except for proline and n is the number of repeats. ELPs will reversibly phase separate above a lower critical solution temperature (LCST), and resolubilize below the LCST[16]. The LCST is a factor of parameters such as chain length, pH, protein concentration, salt concentration, and average polarity, determined by the incorporated guest residues. ELPs are utilized for numerous biotechnological applications (e.g., drug delivery vehicles[16], artificial tissues[17]) because they can utilize cost-efficient purification without conventional chromatography using its LCST behavior called the inverse transition cycling (ITC) method[18], have low immunogenicity, and design flexibility with the guest residue[19]. In addition, the stimulus responsive properties of ELPs can allow for ELP self-assembly into structures such as micelles, cylinders, vesicles, and fibers[14]. ELP block copolymers can generally form more complex structures because each block can be designed to respond differently to external stimuli.

Beyond ELP-based homopolymers, ELP-based block copolymers have formed more intriguing self-assembled structures. ELP-based block copolymer designs have incorporated blocks of

ELPs with different LCSTs, genetically fused blocks of ELP with other stimulus responsive IDPs such as resilin-like polypeptides and silk-like polypeptides, and conjugated ELP blocks with other self-assembled biomolecules such as DNA. The self-assembled structures can be controlled by modulating the mass fractions and hydrophobicity of the blocks, as well as by altering the external conditions such as pH and temperature[14]. The incorporation of complex self-assembled structures into ELP-based block copolymers that can be controlled by external stimuli is exciting for diverse medical applications, such as targeted drug delivery and cancer therapeutics.

ELP block-copolymers can be crosslinked to form polymeric hydrogels that can function as artificial tissues[5]. It is expected that the incorporation of self-assembled structures and biologically active components into the polymer network of artificial tissues can form next generation therapeutics for applications such as wound healing and antimicrobials. Among crosslinking approaches, photocrosslinking is an attractive approach because all components in crosslinking formulations can be completely mixed before light activates the crosslinking process. When controlling the crosslinking time is difficult, there can be clumps of dense and sparse crosslinking regions and therefore an inconsistent elastic modulus across the hydrogel[20]. Furthermore, dityrosine photocrosslinking can be a preferred method because it uses blue light to crosslink rather than UV[21], which can be unsafe when direct application around patients is required.

By incorporating tyrosine as guest residues in ELP, dityrosine photocrosslinking can be utilized to form a polymer network and hydrogels. We previously showed that an ELP homopolymer containing an even distribution of 20% tyrosine and 80% alanine as guest residues (EHP, Figure 1) can form hydrogels via dityrosine photocrosslinking, and the hydrogel elastic modulus could

be targeted up to 40 kPa by modulating the concentrations of the photoinitiators. EHP also contains alanine as guest residues to make EHP more hydrophilic overall and increase the LCST near room temperature (29°C). Despite the ability of EHP hydrogels to target the elastic moduli to match a range of soft tissues, homopolymers with crosslinking sites evenly spaced throughout the polymer strand can have limited functionality besides forming the hydrogel polymer network. Therefore, we decided to rearrange the guest residues in ELP homopolymers to prepare ELP diblock copolymers. However, self-assembled structures formed by block-copolymers could interfere with crosslinking if the crosslinking sites are buried in the structures. A comparison of the mechanical properties between a stimulus-responsive homopolymer and a stimulus-responsive diblock copolymer that was formed as a rearrangement of the homopolymer has not yet been precisely evaluated.

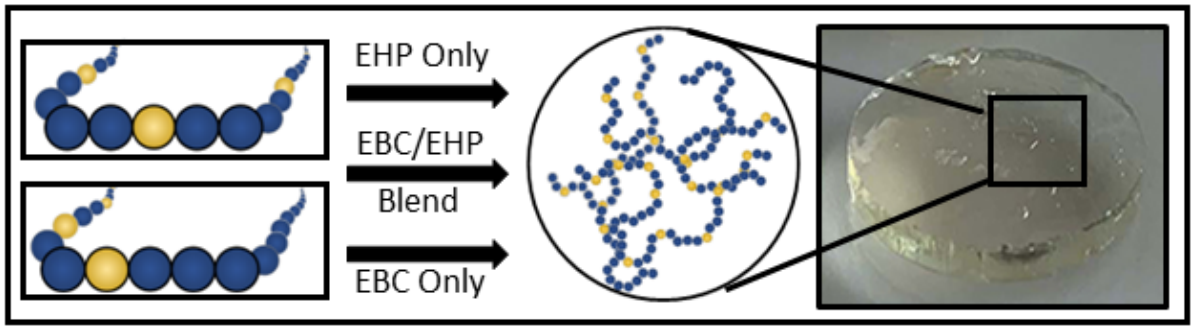

Figure 1. Schematic of EHP and EBC. The polymer network can contain EHP, EBC, or a polymer blend. Blue circles represent the ELP amino acid sequence (VPGAG), while yellow circles represent (VPGYG).

By taking the advantage of the artificial protein technology, we designed an ELP diblock copolymer (EBC, Figure 1) as a precise rearrangement of the sequence of EHP such that all

tyrosine residues and half of the alanine residues were in one block (YB) and the other half of the alanine residues were in the alanine block (AB). The YB is on average more hydrophobic than the AB, therefore the LCST of the YB was expected to be lower than the AB. At temperatures above the LCST of the YB and below the LCST of the AB, we expected EBC could self-assemble into structures, such as micelles, where the YB phase separates and forms the core of a micelle and the AB forms the corona. If the YB is phase-separated in the crosslinking solution, we expect the maximum elastic modulus of EBC hydrogels to be reduced due to tyrosine residues within the structure being blocked from crosslinking, despite having precisely the same chain length, molecular weight, overall chemical composition, and number of potential crosslinking sites compared to EHP. Since a wide range control of mechanical strength is necessary for hydrogels to be used in healthcare, we expect that mixing EBC with EHP can enhance the hydrogel strength since EHP does not form structures and can connect the EBC self-assembled structures as a bridge.

The precisely controlled polymers elucidated the effects of self-assembled structures on hydrogel mechanical properties. We found that EBC can form micelles under specific conditions, and crosslinking of the self-assembled structures lead to weak hydrogels compared to EHP-based hydrogels with the same conditions. Mixing EBC with various concentrations of EHP dramatically increased the elastic modulus of hydrogels, and the polymer blend elastic modulus increased linearly as a function of the mass fraction of EHP. This serves as a well-controlled study to evaluate the degree to which self-assembled structures in a hydrophobic material forming blocks can alter the mechanical properties of polymeric materials and possible methods to overcome that possible loss in mechanical properties for biotechnology applications where

hydrogels and self-assembled structures are critical components, such as drug delivery and tissue engineering.

Results and Discussion

To investigate the targeting of hydrogel elastic moduli to specific values using a block copolymer that forms self-assembled structures, we prepared EBC hydrogels and used rheology to compare their elastic moduli to EHP under the same photocrosslinking conditions. We previously showed that the concentrations of the photoinitiators tris(2,2′-bipyridyl)ruthenium(II) (Ru) and ammonium persulfate (APS) could be modulated to target the elastic modulus of EHP up to 40 kPa. EBC contains the same overall chemical composition, including tyrosine residues used for photocrosslinking, and polymer size, but a different monomer sequence order. To capture significant differences in elastic modulus, we picked photoinitiator concentrations that gave a relatively high elastic modulus for EHP while still having low error due to hydrogel fracturing being more prevalent with higher photoinitiator concentrations[17]. The comparison of elastic moduli between EBC and EHP is shown in Figure 2A, while further characterization of self-assembled structures and temperature responsiveness of EBC, such as dynamic light scattering (DLS) and UV-Visible Spectroscopy (UV-Vis) are shown in Figures 2B-2D.

EBC Characterization and Dityrosine Photocrosslinked Hydrogels

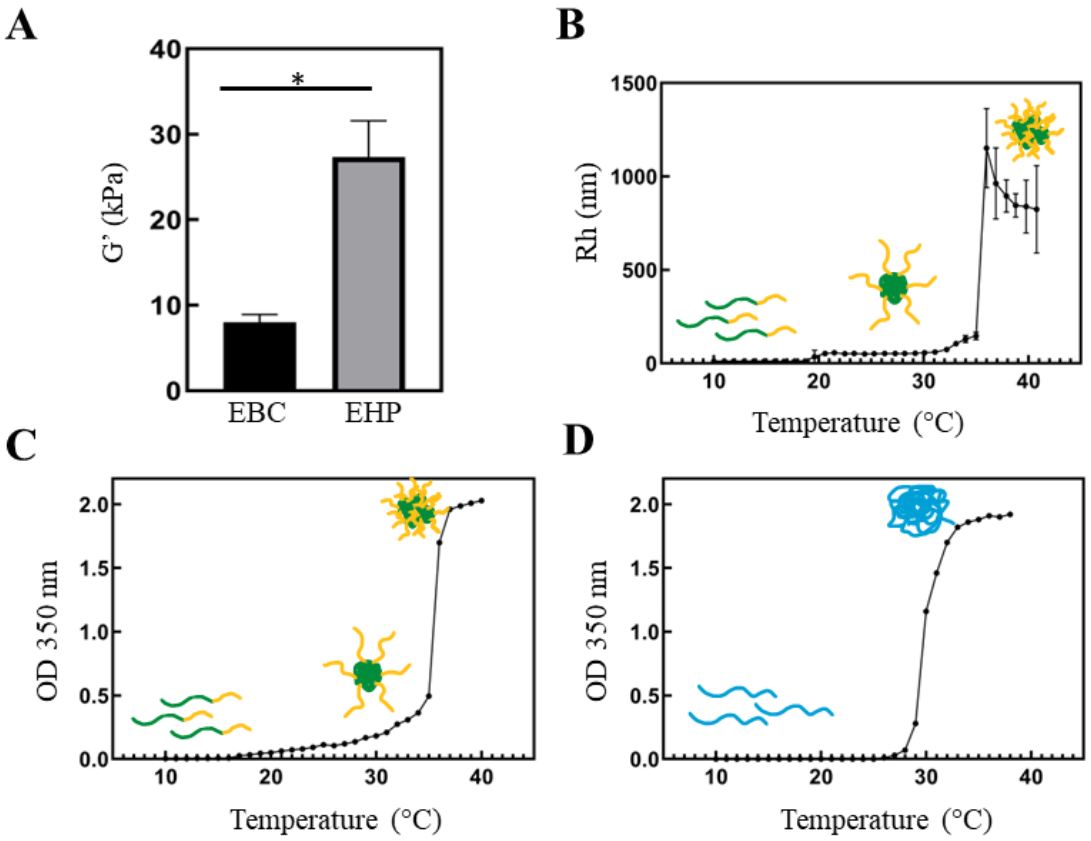

Figure 2. A) Shear elastic modulus of dityrosine photocrosslinked hydrogels using EBC (black bars) and EHP (gray bays). The presented G' measurements were collected from the linear viscoelastic region and averaged for each condition. **B)** Hydrodynamic radius of EBC measured by dynamic light scattering at 1 mg/mL at various temperatures. **C)** UV-Visible Spectroscopy analysis of EBC optical density at 350 nm across various temperatures. **D)** UV-Visible Spectroscopy analysis of EHP optical density at 350 nm across various temperatures. Green represents the tyrosine-incorporated material forming block of EBC. Yellow represents the tether block of EBC without tyrosine. Blue represents EHP.

The hydrogels made from photocrosslinking EBC showed significant differences in elastic moduli compared to EHP (Figure 2A, $p < .05$). The average elastic modulus of EHP hydrogels were reduced by 71% compared to EHP hydrogels. Higher photoinitiator concentrations did not substantially increase the elastic moduli of EBC hydrogels (Figure S2). The material forming block of EBC is more hydrophobic than EHP; therefore, we hypothesized self-assembled structures in the crosslinking solution could be responsible for the lower elastic moduli. Self-assembled structures were characterized via dynamic light scattering (DLS) and UV-Visible spectroscopy (UV-Vis).

DLS analysis of EBC indicated the presence of soluble protein between 10°C and 18°C, with a hydrodynamic radius (Rh) of 11.7 +/- 0.4 nm at 1 mg/mL in PBS (Figure 2B, green and yellow curves). Between 19°C and 30°C, Rh increased to 55 +/- 5.82 nm indicating the presence of micelles. Between 31°C and 35°C, the Rh was to 110 +/- 43 nm, and 841 +/- 98 nm between 36°C and 40°C. Therefore, DLS showed the presence of self-assembled structures above 19°C. The UV-Vis analysis similarly showed the optical density of a 1 mg/mL EBC solution started increasing around 17°C and slowly increased from 17°C to 36°C (Figure 2C). After 36°C a characteristic spike in optical density was observed which is characteristic of the LCST of ELPs. A slow increase in optical density is unusual for typical ELPs, especially homopolymers. The UV-Vis spectrum for EHP is given in Figure 2D, which is more usual for ELPs. The optical density was zero at low temperatures (for which EHP is soluble) until a large spike at 29°C (LCST of EHP) was observed.

While crosslinking of EBC and EHP is performed at 4°C, these analyses require a low EBC concentration of 1 mg/mL. The crosslinking solution has an ELP concentration of 100

mg/mL, which is too high to precisely analyze on DLS or UV-Vis. In addition, the LCST of ELPs is inversely proportional to concentration. Therefore, we hypothesize the dramatic decrease of EBC hydrogel elastic moduli is most likely due to the self-assembled structures forming in the crosslinking formulation, even at 4°C. The self-assembled structures can block tyrosine residues from the photoinitiators, causing fewer dityrosine bonds to form and leading to hydrogels with lower elastic moduli. Altogether, the secondary structures can interfere with crosslinking for the block-copolymer EBC and lead to a lower elastic modulus compared to EHP, even with the polymer size and chemical composition controlled.

The elastic modulus of EBC hydrogels must be able to target the mechanics of natural tissues when the block-copolymers are integrated in artificial tissue hydrogels. Therefore, a method is necessary to incorporate block-copolymers that form self-assembled structures into polymer networks without losing the mechanical properties of the hydrogel to optimize functionality in specific applications. To increase the elastic moduli for EBC hydrogels, we prepared polymer mixtures of EBC with EHP while maintaining 10% w/v total protein in the crosslinking formulation. We expect adding EHP to EBC hydrogels can allow EBC to be incorporated into the polymer network while facilitating a recovery of elastic modulus, as well as an additional parameter to control hydrogel elastic moduli. The elastic moduli of various mixtures are presented in Figure 3.

EBC and EHP Polymer Blend for Dityrosine Photocrosslinked Hydrogels

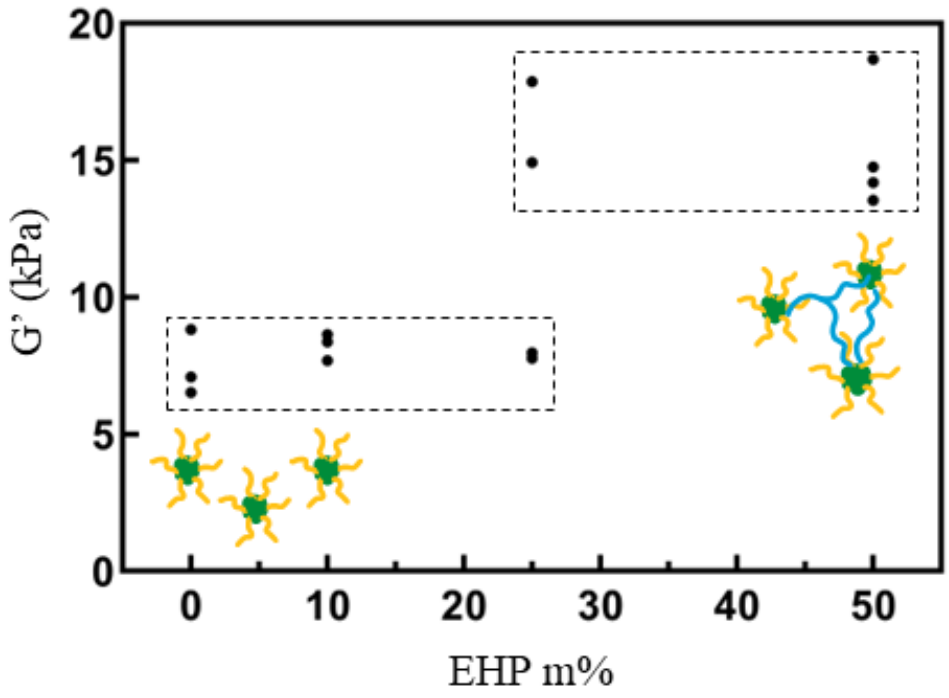

Figure 3. Shear elastic modulus of dityrosine photocrosslinked hydrogels using a mixture of EBC and EHP polymers, given as the mass percent of EHP relative to total mass of polymers. The total protein concentration in each hydrogel was 10 w/v %. The presented G' measurements were collected from the linear viscoelastic region and averaged for each condition. Drawn images represent a proposed model, and dashed boxes represent a general grouping of hydrogels by similar elastic modulus.

When replacing 10 m% of EBC with EHP in EBC hydrogels, the elastic modulus of the polymer did not significantly change (Figure 3, $p>0.05$). However, for 25 m% EHP, half of hydrogels tested had elastic moduli that were about double 0 m% EHP hydrogels, while the other half were not significantly different than 0 m% EHP. The two stronger hydrogels with 25 m% EHP were not significantly different relative to 50 m% EHP ($p>0.05$). Therefore, we hypothesize 25 m%

EHP represents a trigger point where the self-assembled structures can switch, allowing for the structures to be integrated with EHP, forming significantly stronger hydrogels (Figure 3). Utilizing a homopolymer with rearranged monomer sequences allows for controlling the mechanical properties of the hydrogel without altering the overall chemical composition of the chemical network, protein concentration or crosslinking conditions. These data indicate that 25 m% EHP may be enough to double the elastic moduli of EBC hydrogels; however, more testing is required to determine which parameter is responsible for the dramatic change, whether it's small concentration differences or material processing. Methods to recover higher possible elastic moduli can be important in materials or biomedical applications where both the block copolymer design and the elastic modulus of the polymeric material is critical to fit the application.

Conclusions

In prior research we showed a protein homopolymer could be crosslinked using dityrosine photocrosslinking and made to target the elastic moduli of natural tissues by modulating the photoinitiator concentrations. Here, we designed a block copolymer as a precise rearrangement of the homopolymer using genetic engineering and biosynthesis techniques and showed the block copolymer forms self-assembled structures under particular conditions. The block copolymer design can form more intriguing structures for more diverse biotechnological applications, but the hydrogels formed by crosslinking the block copolymer were weaker than the hydrogels formed from the homopolymer. We then identified a method to increase the elastic moduli of the diblock copolymer hydrogels via a polymer blend of both the homopolymer and the block copolymer, where the elastic moduli of hydrogels increased as a function of the

homopolymer mass fraction, possibly due to a change in the polymer network structure. However, more research is required to determine the mechanism of the change in material mechanical properties. This research provides a method to control the elastic moduli of block copolymer hydrogels when self-assembled structures reduce the maximum elastic moduli and make such hydrogels suitable for more tissue engineering and drug delivery applications where stronger polymer networks are required.

Materials and Methods

EHP and EBC Synthesis

The pET-24 a(+) EHP plasmid was kindly provided by the Dr. Harvinder Gill laboratory (Ingrole et al., 2014). The pET-24 a(+) EBC plasmid was purchased from Genscript (Nanjing, China) (Figure S1). For the following steps, both EHP and EBC were synthesized identically with one noted exception. Each plasmid was transformed into BL21(DE3) competent Escherichia coli cells (New England Biolabs, Ipswich, MA), and 1 colony from each kanamycin selection agar plate was amplified in 10 mL lysogeny broth with 50 mg/mL kanamycin. The cultures were shaken in an incubator overnight at 37°C and 220 rpm and 1 mL of overnight culture was added to 1 L terrific broth with kanamycin (24 g yeast extract, 12 g casein, 4 mL glycerol, 2.3 g KH2PO4, 12.5 g K2HPO4, and 50 mg kanamycin) to form the expression culture. The expression culture was incubated at 37°C and shaken at 220 rpm for 48 h, centrifuged at 6,000 x g to harvest cells, then frozen at -80°C for at least 1 h. The cell pellets were resuspended in 50 mL cold phosphate buffer for every 1 L expression culture. The culture was sonicated for 60 minutes, then 16 mL 12.5% polyethyleneimine was added for every 100 mL phosphate buffer. The solution was incubated at 4°C on a rocker for at least 1 h, then centrifuged at 20,000 x g at 4°C for 15 minutes. The supernatant containing the ELP was transferred to a new container and the pellet was discarded. 2 M NaCl was added to EBC cell lysate to lower the effective LCST, and no NaCl was added to EHP lysate. For both EHP and EBC, the lysate was heated in a water bath to 40°C and centrifuged at 40°C for 10 minutes at 8,000 x g. The supernatant was discarded and the pellet containing the ELP was resuspended in 4°C phosphate buffer and the protein was left to dissolve on a rocker at 4°C overnight. The cycle was repeated 5 times, and the ELP was concentrated such that the ELP from 2 L of expression media was contained in 40 mL phosphate

buffer by the end of the 5 cycles. The purity was confirmed via SDS PAGE and the purified protein was dialyzed in 4.5 L deionized water. The water was changed every 3+ hours a total of 7 times. The protein solution was centrifuged at 20,000 x g at 4°C and lyophilized. Lyophilized ELP was stored at -20°C until use.

Photocrosslinked Hydrogels

The photocrosslinking formulation contained 60 mM ammonium persulfate (Sigma-Aldrich, St. Louis, MO), 125 μM tris(2,2′-bipyridyl)ruthenium(II) chloride hexahydrate (Sigma-Aldrich, St. Louis, MO) and a total of 10% w/v ELP, made up of various ratios of EBC to EHP. The photocrosslinking formulation was pipetted into a 20 mm x 2 mm cylindrical well on a 3D printed mold made by a Formlabs FORM 2 printer out of Dental SG resin (Formlabs, Somerville, MA). Gold plated coins were added to the bottom of the wells for preferred surface contact to reduce hydrogels sticking to the mold. The molds containing the crosslinking formulation were irradiated under a 24 W, 460 nm wavelength, 14 x 14 LED array for 10 min at a 10 in distance. The hydrogels were then tested within 2 hrs. via rheology after photocrosslinking.

Rheology

The elastic moduli of the hydrogels were ascertained via small amplitude oscillatory rheology performed on a Discovery Hybrid Rheometer 2 (TA Instruments, New Castle, DE). Rheology was performed as described elsewhere (Camp et al., 2020), except for axial force, which was changed to 0.5 N. Briefly, the reported elastic modulus for each gel was obtained by averaging

G’ values within the linear viscoelastic regions of the strain sweeps. The statistical analyses were performed using Prism 8 software (GraphPad Software Inc., Dotmatics, Boston, MA)

References

(1) Kim, J.; Zhang, G.; Shi, M.; Suo, Z. Fracture, fatigue, and friction of polymers in which entanglements greatly outnumber cross-links. *Science* **2021**, *374* (6564), 212-216. DOI: 10.1126/science.abg6320 From NLM.

(2) Beech, H. K.; Johnson, J. A.; Olsen, B. D. Conformation of Network Strands in Polymer Gels. *ACS Macro Letters* **2023**, 325-330. DOI: 10.1021/acsmacrolett.3c00006.

(3) Lewis, R. M.; Arora, A.; Beech, H. K.; Lee, B.; Lindsay, A. P.; Lodge, T. P.; Dorfman, K. D.; Bates, F. S. Role of Chain Length in the Formation of Frank-Kasper Phases in Diblock Copolymers. *Physical Review Letters* **2018**, *121* (20), 208002. DOI: 10.1103/PhysRevLett.121.208002.

(4) Nguyen, M.; Liu, J. C.; Panitch, A. Physical and Bioactive Properties of Glycosaminoglycan Hydrogels Modulated by Polymer Design Parameters and Polymer Ratio. *Biomacromolecules* **2021**, *22* (10), 4316-4326. DOI: 10.1021/acs.biomac.1c00866.

(5) Wang, H.; Heilshorn, S. C. Adaptable Hydrogel Networks with Reversible Linkages for Tissue Engineering. *Advanced Materials* **2015**, *27* (25), 3717-3736. DOI: 10.1002/adma.201501558.

(6) Kilmer, C. E.; Walimbe, T.; Panitch, A.; Liu, J. C. Incorporation of a Collagen-Binding Chondroitin Sulfate Molecule to a Collagen Type I and II Blend Hydrogel for Cartilage Tissue Engineering. *ACS Biomaterials Science & Engineering* **2022**, *8* (3), 1247-1257. DOI: 10.1021/acsbiomaterials.1c01248.

(7) Li, Y.; Champion, J. A. Photocrosslinked, Tunable Protein Vesicles for Drug Delivery Applications. *Adv Healthc Mater* **2021**, *10* (15), e2001810. DOI: 10.1002/adhm.202001810 From NLM.

(8) Dhankher, A.; Hernandez, M. E.; Howard, H. C.; Champion, J. A. Characterization and Control of Dynamic Rearrangement in a Self-Assembled Antibody Carrier. *Biomacromolecules* **2020**, *21* (4), 1407-1416. DOI: 10.1021/acs.biomac.9b01712.

(9) Hu, X.; Cebe, P.; Weiss, A. S.; Omenetto, F.; Kaplan, D. L. Protein-based composite materials. *Materials Today* **2012**, *15* (5), 208-215. DOI: https://doi.org/10.1016/S1369-7021(12)70091-3.

(10) Engler, A. J.; Sen, S.; Sweeney, H. L.; Discher, D. E. Matrix Elasticity Directs Stem Cell Lineage Specification. *Cell* **2006**, *126* (4), 677-689. DOI: 10.1016/j.cell.2006.06.044.

(11) Guvendiren, M.; Burdick, J. A. Stiffening hydrogels to probe short- and long-term cellular responses to dynamic mechanics. *Nature Communications* **2012**, *3* (1), 792. DOI: 10.1038/ncomms1792.

(12) Chaudhuri, O.; Gu, L.; Klumpers, D.; Darnell, M.; Bencherif, S. A.; Weaver, J. C.; Huebsch, N.; Lee, H.-P.; Lippens, E.; Duda, G. N.; et al. Hydrogels with tunable stress relaxation regulate stem cell fate and activity. *Nature Materials* **2016**, *15* (3), 326-334. DOI: 10.1038/nmat4489.

(13) Yang, Y. J.; Holmberg, A. L.; Olsen, B. D. Artificially Engineered Protein Polymers. *Annual Review of Chemical and Biomolecular Engineering* **2017**, *8* (1), 549-575. DOI: 10.1146/annurev-chembioeng-060816-101620.

(14) Doole, F. T.; Camp, C. P.; Kim, M. Tailoring the formation and stability of self-assembled structures from precisely engineered intrinsically disordered protein polymers: A comprehensive review. *Giant* **2023**, *14*, 100158. DOI: https://doi.org/10.1016/j.giant.2023.100158.

(15) Varanko, A. K.; Su, J. C.; Chilkoti, A. Elastin-Like Polypeptides for Biomedical Applications. *Annual Review of Biomedical Engineering* **2020**, *22* (1), 343-369. DOI: 10.1146/annurev-bioeng-092419-061127.

(16) MacEwan, S. R.; Chilkoti, A. Applications of elastin-like polypeptides in drug delivery. *J Control Release* **2014**, *190*, 314-330. DOI: 10.1016/j.jconrel.2014.06.028 From NLM.

(17) Camp, C. P.; Peterson, I. L.; Knoff, D. S.; Melcher, L. G.; Maxwell, C. J.; Cohen, A. T.; Wertheimer, A. M.; Kim, M. Non-cytotoxic Dityrosine Photocrosslinked Polymeric Materials With Targeted Elastic Moduli. *Frontiers in Chemistry* **2020**, *8*, Original Research. DOI: 10.3389/fchem.2020.00173.

(18) Hassouneh, W.; Christensen, T.; Chilkoti, A. Elastin-Like Polypeptides as a Purification Tag for Recombinant Proteins. *Current Protocols in Protein Science* **2010**, *61* (1). DOI: 10.1002/0471140864.ps0611s61.

(19) Urry, D. W.; Luan, C. H.; Parker, T. M.; Gowda, D. C.; Prasad, K. U.; Reid, M. C.; Safavy, A. Temperature of polypeptide inverse temperature transition depends on mean residue hydrophobicity. *Journal of the American Chemical Society* **1991**, *113* (11), 4346-4348. DOI: 10.1021/ja00011a057.

(20) Kroll, D. M.; Croll, S. G. Influence of crosslinking functionality, temperature and conversion on heterogeneities in polymer networks. *Polymer* **2015**, *79*, 82-90. DOI: https://doi.org/10.1016/j.polymer.2015.10.020.

(21) Fancy, D. A.; Kodadek, T. Chemistry for the analysis of protein–protein interactions: Rapid and efficient cross-linking triggered by long wavelength light. *Proceedings of the National Academy of Sciences* **1999**, *96* (11), 6020-6024. DOI: 10.1073/pnas.96.11.6020.

Supplementary Material

Modulating the Mechanical Strength of Block Copolymer Hydrogels Comprised of Precisely Controlled Protein Polymers

Camp, Christopher P.[1]; Kim, Samuel Y.[1]; Doole, Fathima T.[2]; Knoff, David S.[1]; Kim, Minkyu[1,3,4,*]

[1]Department of Biomedical Engineering, University of Arizona, Tucson, Arizona, 85721, USA

[2]Department of Chemistry & Biochemistry, University of Arizona, Tucson, Arizona, 85721, USA

[3]Department of Materials Science & Engineering, University of Arizona, Tucson, Arizona, 85721, USA

[4]BIO5 Institute, University of Arizona, Tucson, Arizona, 85719, USA

Supplementary Figures

MGAGVPGYGVPGAGVPGAGVPGYGVPGAGVPGAGVPGYGVPGAGVPGAGVPGYGVP

GAGVPGAGVPGYGVPGAGVPGAGVPGYGVPGAGVPGAGVPGYGVPGAGVPGAGVPG

YGVPGAGVPGAGVPGYGVPGAGVPGAGVPGYGVPGAGVPGAGVPGYGVPGAGVPGA

GVPGYGVPGAGVPGAGVPGYGVPGAGVPGAGVPGYGVPGAGVPGAGVPGYGVPGAG

VPGAGVPGYGVPGAGVPGAGVPGYGVPGAGVPGAGVPGYGVPGAGVPGAGVPGYGV

PGAGVPGAGVPGYGVPGAGVPGAGVPGYGVPGAGVPGAGVPGYGVPGAGVPGAGVP

GYGVPGAGVPGAGVPGYGVPGAGVPGPWGAGVPGAGVPGAGVPGAGVPGAGVPGAG

VPGAGVPGAGVPGAGVPGAGVPGAGVPGAGVPGAGVPGAGVPGAGVPGAGVPGAGV

PGAGVPGAGVPGAGVPGAGVPGAGVPGAGVPGAGVPGAGVPGAGVPGAGVPGAGVP

GAGVPGAGVPGAGVPGAGVPGAGVPGAGVPGAGVPGAGVPGAGVPGAGVPGAGVPG

AGVPGAGVPGAGVPGAGVPGAGVPGAGVPGAGVPGAGVPGAGVPAS

Figure S1. Block copolymer (EBC) full protein sequence.

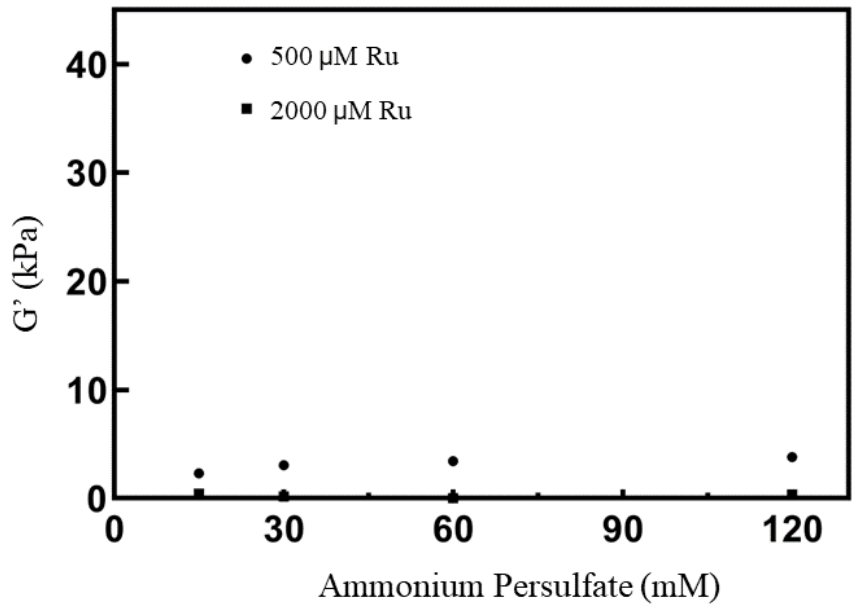

Figure S2. Elastic moduli of EBC hydrogels using higher APS and Ru concentrations